Flow Modelling of a Non Prismatic compound channel By Using C .F .D

A Thesis Submitted in Partial Fulfillment of the Requirements for the Degree of

Master of Technology
in
Civil Engineering

ABINASH MOHANTA

DEPARTMENT OF CIVIL ENGINEERING

NATIONAL INSTITUTE OF TECHNOLOGY, ROURKELA

2014

Flow Modelling of a Non Prismatic compound channel By Using C .F .D

A Thesis Submitted in Partial Fulfillment of the Requirements for the Degree of

Master of Technology
in
Civil Engineering

WITH SPECIALIZATION IN

WATER RESOURCES ENGINEERING

Under the guidance and supervision of

Prof K. K. Khatua & K. C. Patra

Submitted By:

ABINASH MOHANTA

(ROLL NO. 212CE4435)

DEPARTMENT OF CIVIL ENGINEERING

NATIONAL INSTITUTE OF TECHNOLOGY, ROURKELA

2014

National Institute Technology
Rourkela

CERTIFICATE

This is to certify that the thesis entitled "***FLOW MODELLING OF A NON PRISMATIC COMPOUND CHANNEL BY USING C.F.D***" being submitted by **ABINASH MOHANTA** in partial fulfillment of the requirements for the award of *Master of Technology* Degree in *Civil Engineering* with specialization in *Water Resources Engineering* at National Institute of Technology Rourkela, is an authentic work carried out by his under my guidance and supervision.

To the best of my knowledge, the matter embodied in this report has not been submitted to any other university/institute for the award of any degree or diploma.

Dr. Kishanjeet Kumar Khatua
Professor
Department of Civil Engineering

Dr. Kanhu Charan Patra

Place: Rourkela

Date:

ACKNOWLEDGEMENT

A complete research work can never be the work of anyone alone. The contributions of many different people, in their different ways, have made this possible. One page can never suffice to express the sense of gratitude to those whose guidance and assistance was indispensable for the completion of this project.

I would like to express my special appreciation and thanks to my supervisors Professor Dr. Kishanjeet Kumar Khatua and Professor Dr. Kanhu Charan Patra, you both have been tremendous mentors for me. I would like to thank you for encouraging my research and for allowing me to grow as a research scholar. Your advices on both researches as well as on my career have been priceless.

I would also like to thank my committee members, Professor, Nagendra Roy; Head of the Civil Department. And also I am sincerely thankful to Prof. Ramakar Jha, and Prof. A. Kumar for their kind cooperation and necessary advice. I also want to thank you for letting my seminars be an enjoyable moment, and for your brilliant comments and suggestions, thanks to you.

I wish to express my sincere gratitude to Dr. S K Sarangi, Director, NIT, Rourkela for giving me the opportunities and facilities to carry out my research work.

A special words of thanks to Mr. Swayam Bikash Mishra Ph.D. scholar of Production Engineering and Mrs. Bandita Naik, Manaswinee Patnaik, Laxmipriya Mohanty Ph.D. scholar of Civil Engineering Department, for his suggestions, comments and entire support throughout the project work. I express to my special

thanks to my dear friends Monalisa, Ellora, Aparupa, Chita, Bibhuti, Arpan, B. Mohan Kumar for their continuous support, suggestions and love.

Last but not least I would like to thanks to my father Mr. Arjun Chandra Mohanta and mother Mrs. Sabita Mohanta, who taught me the value of hard work by their own example. Thanks a lot for your understanding and constant support, and to my sister Priyanka Mohanta and brother in law Sailendra Mohanta for his encouragement. They rendered me enormous support during the whole tenure of my study at NIT Rourkela. Words cannot express how grateful I am to my Father, Mother, Sister, Brother in law and my little nephew Pragyan for all of the sacrifices that you have made on my behalf. Your prayer for me was that sustained me thus far.

Abinash Mohanta.

ABSTRACT

Flooding situation in river is a complex phenomenon and affects the livelihood and economic condition of the region. The modelling of such flow is primary importance for a river engineers and scientists working in this field. Water surface prediction is an important task in flood risk management. As a result of topography changes along the open channels, designing the converging compound channel is an essential. Fluvial flows are strongly influenced by geometry complexity and large overall uncertainty on every single measurable property, such as velocity distribution on different sectional parameters like width ratio, aspect ratio and hydraulic parameter such as relative depth. The geometry selected for this study is that of a non-prismatic compound channel having converging flood plain. For the research work the parameters, the water depth, incoming discharge of the main channel and floodplains were varied. This total topic represents a practical method to predict lateral depth-averaged velocity distribution in a non-prismatic converging compound channel. Flow structure in non-prismatic compound channel is more complex than straight channels due to 3-Dimentional nature of flow. Continuous variation of channel geometry along the flow path associated with secondary currents makes the depth averaged velocity computation difficult. Design methods based on straight-wide channels incorporate large errors while estimating discharge in converging compound channel.

Then the numerical method is applied to calculate water surface elevation in a non-prismatic compound channel configurations, the results of calculations show good agreement with the experimental data. As numerical hydraulic models can significantly reduce costs associated with the experimental models, an effort has been made through the present investigation to determine the different flow characteristics of a converging compound channel such as velocity distribution, depth averaged velocity distribution, boundary shear etc. In this Thesis a complete

three-dimensional and two phase CFD model for flow distribution in a converging compound channel is investigated. The models using ANSYS – FLUENT, a Computational Fluid Dynamics (CFD) code, are found to give satisfactory results when compared to the newly conducted experimental data under controlled system.

Computational Fluid Dynamics (CFD) is often used to predict flow structures in developing areas of a flow field for the determination of velocity, pressure, shear stresses, effect of turbulence and others. A two phase three-dimensional CFD model along with the Large Eddy Simulation (LES) model is used to solve the turbulence equation. This study aims to validate CFD simulations of free surface flow or open channel flow by using Volume of Fluid (VOF) method by comparing the data observed in hydraulics laboratory of the National Institute of Technology, Rourkela. The finite volume method (FVM) with a dynamic subgrid scale was carried out for five cases of different aspect ratios and convergence condition. The volume of fluid (VOF) method was used to allow the free-surface to deform freely with the underlying turbulence. Within this thesis over-bank flows have been numerically simulated using LES in order to predict accurate open channel flow behavior. The LES results are shown to accurately predict the flow features, specifically the distribution of secondary circulations both for in-bank channels as well as over-bank channels at varying depth and width ratios in symmetrically converging flood plain compound sections.

Key Words:

CFD simulation, Converging floodplain, compound channel, Experimental model, FVM method, LES turbulence model, prismatic and non-prismatic section, Two phase modelling, Velocity profile, VOF method.

TABLE OF CONTENTS

LIST OF ABBREVIATIONS

CFD	Computational Fluid Dynamics
N-S	Navier-Stokes
FVM	Finite Volume Method
FEM	Finite Element Method
FDM	Finite Difference Method
ADV	Acoustic Doppler velocity meter
IDCM	Interactive Divide Channel Method
MDCM	Modified Divide Channel Method
SKM	Shiono Knight Method
ASM	Algebraic Reynolds Stress model
RSM	Reynolds Stress Model
LES	Large Eddy Simulation
LDA	Laser Doppler Anemometer
FVM	Finite Volume Method
VOF	Volume of Fluid
HOL	Height of liquid
DES	Detached eddy simulation
SAS	Scale adaptive simulation
SST	Scale adaptive Simulation Turbulence
RANS	Reynolds Averaged Navier-Stokes
DNS	Direct Numerical Simulation
SGS	Sub Grid Scale

LIST OF TABLES

LIST OF FIGURES AND PHOTOGRAPHS

LIST OF FIGURES AND PHOTOGRAPHS

LIST OF FIGURES AND PHOTOGRAPHS

LIST OF SYMBOLS

A	Cross Sectional Area;
B	Top width of compound channel;
C_r	Courant number;
C_s	Smagorinsky constant;
D	Hydraulic Depth;
Dr	Relative Depth;
$\vec{F}$	Body force;
G	Gaussian filters;
H	Total depth of flow;
P	wetted perimeter;
Q	discharge;
R	hydraulic radius;
S	bed slope of the channel;
S	Slope of the energy gradient line;
S_m	Mass exchange between two phase (water and air);
$\overline{Sij}$	Resolved strain rate tensor;
U_t	Velocity tangent to the wall;
U_b	Bulk Velocity along Stream-line of flow;
$\overline{U}$	Average velocity;
V	Flow Velocity;
b	Main channel width;
c	log-layer constant dependent on wall roughness;

g	acceleration due to gravity;
h	main channel bank full depth;
k	Von Karman constant;
m_{qp}	Mass transfer from phase q to phase p;
m_{pq}	Mass transfer from phase p to phase q;
n	Number of phase;
p	Reynolds averaged pressure;
t	Time;
u	Instantaneous Velocity;
$\bar{u}$	Mean velocity;
u'	Fluctuating Velocity;
u^+	Near wall velocity;
u_*	Friction velocity;
$\vec{v}_m$	Mass average velocity;
$\vec{v}_{dr}$	Drift Velocity;
y	lateral distance along the channel bed;
y^+	Dimensionless distance from the wall;
z	vertical distance from the channel bed;
u, v, w	Velocity components in x, y, z direction;
α	Width Ratio;
α_k	Volume fraction of phase k;

LIST OF SYMBOLS

$\emptyset$	Converging angle;
δ	Aspect Ratio;
θ	Angle between channel bed and horizontal;
μ_t	Turbulent viscosity;
μ	Dynamic Viscosity;
μ_m	Viscosity of the mixture;
ϑ	Kinematic viscosity;
v_R	Eddy viscosity of the residual motion;
ρ	Fluid Density;
ρ_m	Mixture density;
τ_w	Wall shear stress;
τ	Boundary shear stress;
γ	Unit weight of water;
ε	Rate of turbulent kinetic energy dissipation;
ω	specific rate of dissipation;
η	Kolmogorov scale;
Ω	Vorticity;
Δt	Time Step size;
Δl	Grid cell size;

Subscripts

Avg.	Average;
a/act.	Actual;
fp	Flood Plain;
Fr	Froude Number;
h	Hydraulic;
in	Inlet;
Max	Maximum;
mc	Main Channel;
mod.	Modelled;
out	Outlet;
Re	Reynolds Number;
r	Relative;
Sec.	Section;
T	Total;
t	Theoretical;
Vel.	Velocity;
w	Wall;
i, j, k	x, y, z directions respectively;

INTRODUCTION

1.1 RIVER SYSTEM

Rivers play an integral part in the day to day functioning of our planet. Therefore it is important to understand the flow characteristics of rivers in both their in bank and overbank flow condition. An open channel is a passage in which liquid flows with a free surface. An open channel is a passage in which liquid flows with a free surface, open channel flow has uniform atmospheric pressure exerted on its surface and is produced under the action of fluid weight. It is more difficult to analyze open channel flow due to its free surface. Flow is an open channel is essentially governed by Gravity force apart from inertia and viscous forces.

Examples of Open Channel Flow

- The natural drainage of water through the numerous creek and river systems.
- The flow of rainwater in the gutters of our houses.
- The flow in canals, drainage ditches, sewers, and gutters along roads.
- The flow of small rivulets, and sheets of water across fields or parking lots.
- The flow in the chutes of water rides.

An open channel is classified as ***natural*** or ***artificial***.

Natural: Open channels are said to be natural when channels are irregular in shape, alignment and surface roughness. Eg. Streams, rivers, estuaries etc.

Artificial: When the open channels are regular in shape, alignment and uniform surface roughness which are built for some specific purpose, such as irrigation, water supply, water power development etc. are called as artificial open channels.

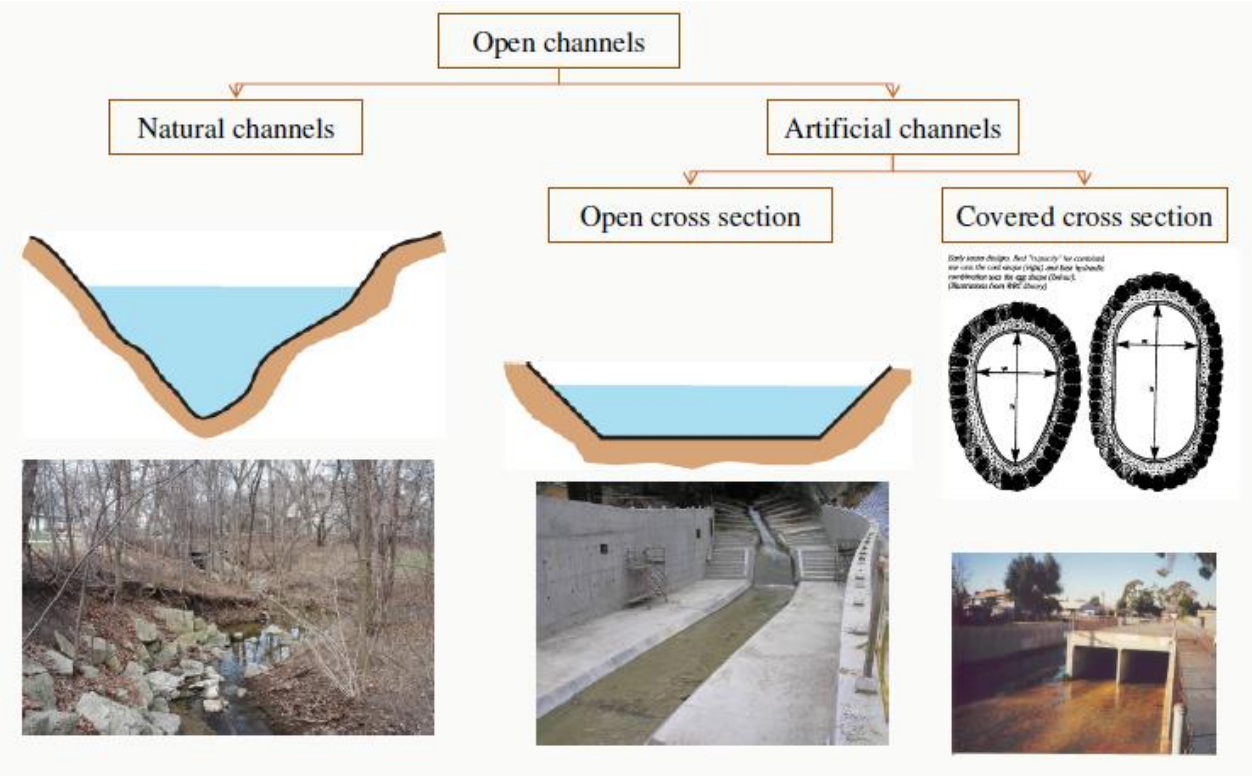

Figure 1.1. Classification of Open channels

The river generally exhibit a two stage geometry

- Deeper main channel.
- Shallow floodplain called compound section.

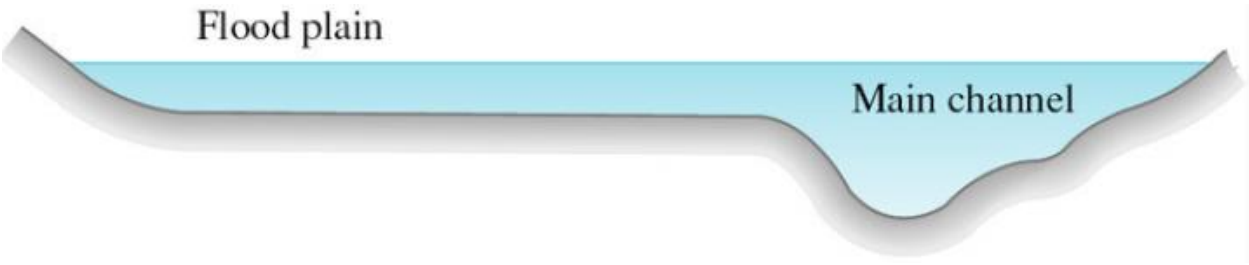

Figure 1.2. Two Stage Geometry of Open Channel

Compound Channel:

When the flow is out of bank, like during flood it is known as compound channel flow.

Generally compound channels are classified as

- *Prismatic compound channel*
- *Non prismatic compound channel*

Figure.1.3. Geometry of a Compound Channel

i. Prismatic compound channels:

A channel is said to be prismatic when the cross section is uniform and the bed slope is constant and having fixed alignment.

Eg. Most of the manmade channels i.e. Rectangular, trapezoidal, circular and parabolic.

ii. Non prismatic compound channels:

A channel is said to be non-prismatic when its cross sectional shape, size and bottom slope are not constant longitudinally.

- Eg. All the natural channels i.e. River, Streams and Estuary. Some examples of non-prismatic channels are flow through culverts, flow through bridge piers, high flow through bridge pier and obstruction, channel junction etc.

Non-prismatic compound channel may be converging and diverging or skewed type.

1.2 RIVER AND FLOODING

Rivers have fascinated scientists and engineers. It is the main source of providing water supply for domestic, irrigation, industrial consumption or transportation and recreation uses. However, the design and organizing these systems require a full perception of mechanics of the flow and sediment transport. River channels do not remain straight for any appreciable distance. Flow separation in open channel expansion has been identified as one of the major problems encountered in many hydraulic structures such as irrigation networks, bridges, flumes, aqueducts, power tunnels and siphons. Eventually, it becomes hard to believe that during flood a gentle river inundate its flood plain thereby causing serious damage to the lives and shelter of the people residing in low-lying areas. Nowadays debate on flooding is gaining momentum due to combining consequences of climate change. From recent times, river engineer's devise solutions by designing flood defenses so as to ensure minimum damage from flooding. Generally river engineer's use hydraulic model to make flood prediction. The hydraulic model incorporates many flow features such as accurate discharge, average velocity, water level profile and shear stress forecast. Prior to producing hydraulic models capable of modeling all these flow features

detailed knowledge on open channel hydrodynamics is required. In this regard, first comes the understanding of geometrical and hydraulic parameters of the river streams. Even the flow properties in rivers vary with the geometrical shape.

1.3 OVERBANK FLOW IN NON-PRISMATIC COMPOUND CHANNEL

In non-prismatic compound channels with converging floodplains, due to further continuous change in floodplain geometry along the flow path, the resulting interactions and momentum exchanges are further increased. This extra momentum exchange is very important parameter and should be taken into account in the overall flow modelling of a river. Super-elevation, secondary flows and their tending to redistribute the mean velocity, permuting the boundary shear stress, bank erosion and shifting, flow separation and bed migration in mobile boundary channels have made the study of the non-prismatic open channels of a high interest in the field of river engineering. In most of the cases, the flows are subcritical in nature. In convergent channel sections, the flow can lead to a continuous reduction of kinetic energy which causes its conversion in part to pressure energy. During this process, energy losses taken place due to changing flow condition in the channel compression. Moreover, the presence of adverse pressure gradient causes flow separation due to the inability of flow to adhere to the boundaries and losses of head taking place due to subsequent formation of eddies. To reduce bed and bank erosion, control of flow separation is required. In the past, to avoid flow separation transition walls were designed. Therefore, it is desirable in hydraulic engineering to investigate structures of open channel expansions to evaluate the velocity distribution, boundary shear distribution, to control flow separation, and to design hydraulic structures properly.

As natural river data during flood are very difficult to obtain, research on such a topic is generally done in laboratory flumes. In a converging compound channel if the flood plain is

contracted, the flow is forced to leave the flood plains and enter to the main channel because of change in cross section area which brings a huge change in mass and momentum transfer.

So the experiments will be conducted to analyze the flow effect due to change in flood plain geometry in terms of converging angle in the Hydraulics and Fluid mechanics Laboratory of Civil Engineering Department of NIT, Rourkela. In the present work, an effort has been made to investigate the velocity profiles for various open-channel geometries using a commercial computational fluid dynamics (CFD) code, namely FLUENT.

1.4 NUMERICAL MODELLING

Computational Fluid Dynamics (CFD) is a computer based numerical analysis tool. The growing interest on the use of CFD based simulation by researchers have been identified in various fields of engineering as numerical hydraulic models can significantly reduce costs associated with the experimental models. The basic principle in the application of CFD is to analyze fluid flow in-detail by solving a system of non-linear governing equations over the region of interest, after applying specified boundary conditions. A step has been taken to do numerical analysis on a non-prismatic compound channel flow having converging floodplains. The work will help to simulate the different flow variables in such type of complex flow geometry. The use of computational fluid dynamics was another integral component for the completion of this project since it was the main tool of simulation. In general, CFD is a means to accurately predict phenomena in applications such as fluid flow, heat transfer, mass transfer, and chemical reactions.

There are a variety of CFD programs available that possess capabilities for modelling multiphase flow. Some common programs include ANSYS and COMSOL, which are both multi physics modelling software packages and FLUENT, which is a fluid-flow-specific software

package. CFD is a popular tool for solving transport problems because of its ability to give results for problems where no correlations or experimental data exist and also to produce results not possible in a laboratory situation. CFD is also useful for design since it can be directly translated to a physical setup and is cost-effective (Bakker et al., 2001).

In the present work, an effort has been made to investigate the velocity profiles for five different sections of a compound channel having converging flood plain by using a computational fluid dynamics (CFD) modeling tool, named as FLUENT. The CFD model developed for a real open-channel was first validated by comparing the velocity profile obtained by the numerical simulation with the actual measurement carried out by experimentation in the same channel using Preston tube. The CFD model has been the used to analyze the effects of flow due to convergence of flood plain width and bed slope, and to study the variations in velocity profiles along the horizontal and vertical directions. The simulated flow field in each case is compared with corresponding laboratory measurements of velocity and water surface elevation. Computational Fluid Dynamics (CFD) is a mathematical tool which is used to model open channel ranging from in-bank to over-bank flows. Different models are used to solve Navier-Stokes equations which are the governing equation for any fluid flow. Finite volume method is applied to discretize the governing equations. The accuracy of computational results mainly depends on the mesh quality and the model used to simulate the flow.

1.5 ADVANTAGES OF NUMERICAL MODELLING

Despite exact results and clear understanding on flow phenomena; experimental approach has some drawbacks such as laborious data collection and data can be collected for limited number of points due to instrument operation limitations; the model is usually not at full scale

and the three dimensional flow behavior or some complex turbulent structure which is the nature of any open channel flow cannot effectively captured through experiments. So in these circumstances, computational approach can be adopted to overcome some of these issues and thus provide a complementary tool. In comparison to experimental studies; computational approach is repeatable, can simulate at full scale; can generate the flow taking all the data points into consideration & moreover can take greatest technical challenge *i.e.;* prediction of turbulence. The complex turbulent structures like secondary flow cells, vortices, Reynolds stresses can be identified by numerical modeling effectively which are quite essential for the study of energy outflow in open channel flows. Many researchers in the recent centuries have numerically modeled open channel flows and has successfully validated with the experimental results.

1.6 OBJECTIVE OF PRESENT STUDY

The present work is aimed to study the distribution of velocity profile in a non-prismatic converging compound channel. The distribution of velocity profile at five different sections along the channel depend on width-depth ratio, relative depth. Out of these parameters width-depth ratio or aspect ratio plays a major role in estimation of velocity distribution in compound channels. Flow in a compound open channel is generally turbulent in nature. The turbulent nature of flow in such channels is three dimensional due to strong secondary lateral flow. It is concluded from literature review that very less work has been done regarding lateral distribution of depth-averaged velocity in non-prismatic compound channel. However lack of qualitative and quantitative experimental data on the depth averaged velocity in non-prismatic compound channels is still a matter of concern. Furthermore, it has been observed from earlier studies that

turbulence flow structure has direct impact in predicting the discharge and resistance in compound channel. The present study aims to collect velocity data from the non-prismatic converging compound channel at different cross section and different depth. Hence, the present study follows an analysis of resistance and discharge in a non-prismatic compound channel flow. The present study focuses on the following aspects:

- To conduct experimentations on non-prismatic compound channels of a converging angle to analyze the nature of change of flow variables throughout the non-prismatic reaches.
- To study the distribution of stream wise depth-averaged velocity at different section for two different flow depth. Also to study its variation at different flow depths for in bank and overbank flow conditions.
- To study, the use of computational fluid dynamics (CFD) to predict the flow characteristics of non-prismatic open channels.
- To quantify the effects of the flow variables such as converging angle, width ratio, depth ratio, aspect ratio etc. for prediction of flow.
- To study the turbulent flow structures of a non-prismatic compound channel flow using Large Eddy Simulation turbulent method.
- The purpose of this project is to choose a computational fluid dynamics (CFD) program that would be utilized to simulate with the experimental convergent channel and to produce results on velocity distribution, boundary shear distribution in non-prismatic channel system.
- Validation and verification of the turbulent flow structure from CFD results such as secondary current, turbulent transport and flow variables such as velocity distribution, boundary shear stress with that of the experimental results.

1.7 ORGANISATION OF THESIS

The thesis consists of six chapters. General *introduction* is given in Chapter 1, *literature survey* is presented in Chapter 2, *experimental work* is described in Chapter 3, *description of numerical parameters* are explained in Chapter 4, *numerical modelling* is described in Chapter 5, Chapter 6 comprises *verification of numerical model* and *discussion of result* and finally the *conclusions* and *references* are presented in Chapter 7.

General view on open channel flow is provided at a glance in the first chapter. Also the chapter introduces river system and flooding in non-prismatic converging compound channel. It also gives the general idea of overbank flow condition in non-prismatic converging compound channel. It gives an overview of numerical modeling in open channel flows.

Chapter 2 contains the detailed literature survey by many renowned researchers that relates to the present work from the beginning till date. The chapter emphasizes on the research carried out on velocity distribution of straight prismatic and non-prismatic compound channels for overbank flow conditions.

The laboratory setup and whole experimental procedure is clearly described in chapter three. This section explains the experimental arrangements and procedure adopted to obtain observation at different points of five different sections in the channel. Also the detailed information about the instrument used for taking observation and geometry of experimental flume is described in this chapter.

The description of numerical model parameter regarding turbulence modelling, governing equation related to turbulence model and finite volume method is briefly described in chapter four. Also this chapter discusses the technique adopted for analyzing the flow variables.

Chapter five presents significant contribution to numerical simulation of the non-prismatic converging compound channel. The numerical model and the software used within this research are also discussed in this chapter. The methodology adopted for performing simulation is clearly discussed in this chapter. This chapter also gives the brief idea about the Two-phase modelling, VOF model, Volume of fraction and LES turbulence model.

Finally, chapter six summarizes the conclusion reached by the present research. In this chapter simulation of numerical modeling is shown. Also in this chapter the validation of longitudinal velocity profile, depth average velocity distribution, streamlines and boundary shear distribution are shown for two different relative depth of flow.

Lastly in chapter seven conclusions are pointed out by simulations and observations of numerical and experimental results. After that scope for the further work is listed out in this chapter.

References that have been made in subsequent chapters are provided at the end of the thesis.

LITERATURE SURVEY

2.1 OVERVIEW

This chapter outlines about the previous research done by other researchers in the field of open channel flow which is relevant to the current work. Distribution of flow velocity in longitudinal and lateral direction is one of the important aspects in open channel flows. It directly relates to several flow features like water profile estimation, shear stress distribution, secondary flow and channel conveyance. The distribution of velocity in open channel flow is generally affected by various factors such as channel geometry, types of channel and patterns of channel, channel roughness and sediment concentration in flow which have critically studied by many renowned researchers. Many approaches are there for predicting stage discharge relationships, velocity distribution and boundary shear distribution on main channel and flood plain perimeter which are mainly applicable to prismatic compound channels. There are many study found in literature related to both prismatic and non-prismatic compound channels flow.

2.2 PREVIOUS EXPERIMENTAL RESEARCH ON VELOCITY DISTRIBUTION IN COMPOUND CHANNEL

Many practical problems in river engineering require accurate prediction of flow in compound channels. Over-bank channels can be characterized by a deep main channel, bounded on one or both sides by a relatively shallow floodplain, which is often hydraulically irregular. Consequently, velocities in the main channel tend to be significantly greater than those on the floodplain. This difference in velocity can lead to large velocity gradients in the region of the interface between the main channel and floodplains.Likewise, local flow conditions determine the erosion and deposition rates of sediment in the main channel and floodplains. Therefore,

accurate prediction of discharge capacity of compound channels is essential for flood mitigation systems.

2.2.1 Prismatic Compound Channel

The flow structure in open channels is highly dependent on the regime of the flow, i.e. laminar or turbulent. It also depends upon existence of vortices at various length scales, acting toward all three directions, typically generated by high shear between fluid layers and its boundaries, as noticed by ***Van Prooijen et al.(2000)*** (Figure 2.1). Such vortices are a form of energy transfer that converts part of the kinetic energy of the flow into heat through viscosity. The common types of vortices that develop in open channel flow are due to surface roughness, the anisotropy of turbulent velocity fluctuations in the y and z directions, leading to secondary flows and high velocity gradients between the main channel and floodplain, explained by ***Shiono & Knight (1990)*** leading to planform vortices at this interface (Figure 2.2). Each of these components is described clearly in the following sections.

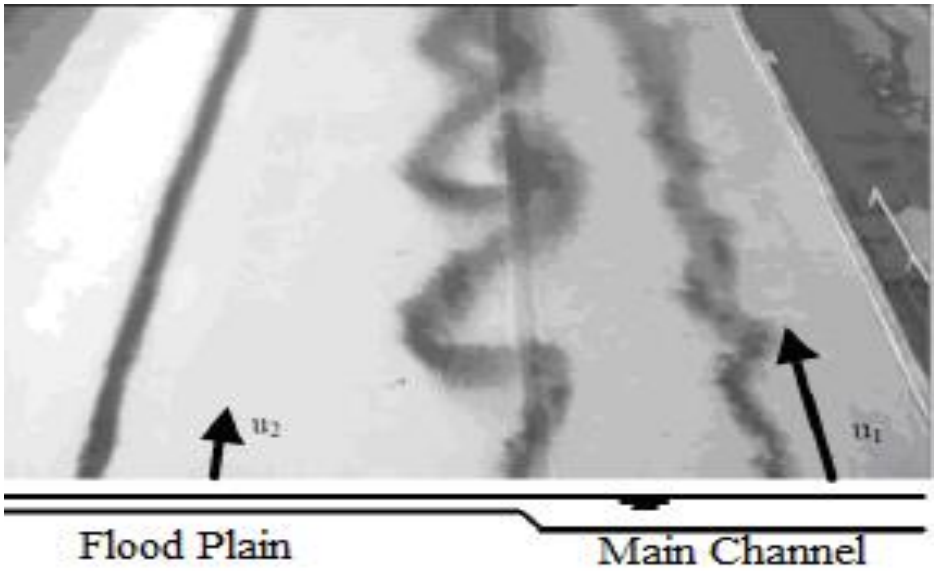

Figure 2.1. Large vortices experimentally observed at the main channel/floodplain interface

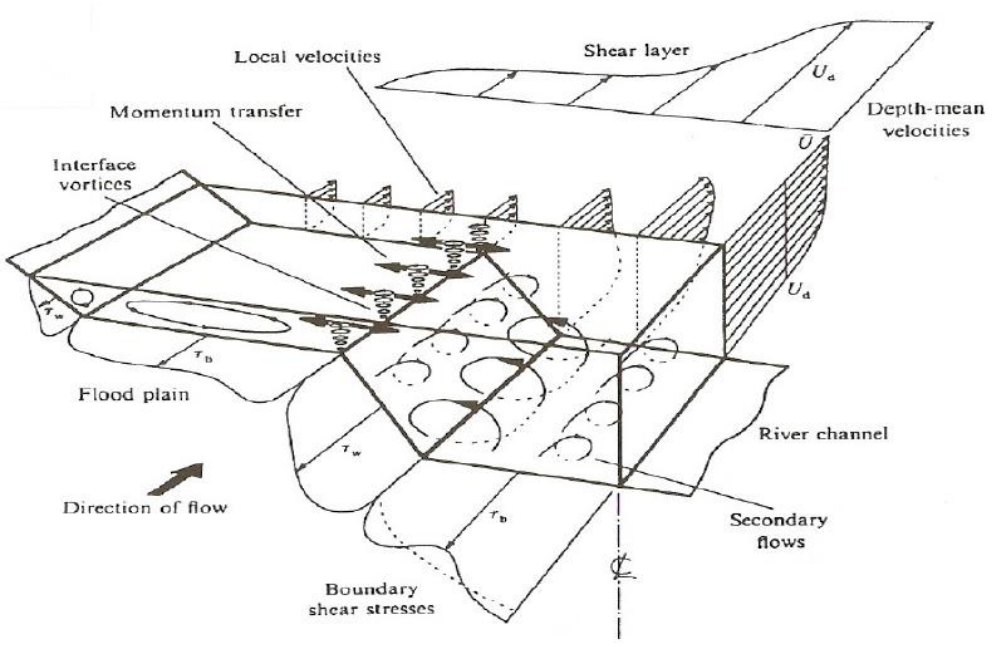

Figure 2.2. Flow structures in a straight two-stage channel (Shiono and Knight, 1990)

Investigation of the interaction between the main channel and the adjoining floodplain was determined by ***Zheleznyakov (1965)***. He also explained the effect of momentum transfer mechanism under laboratory conditions, which was responsible for decreasing the overall rate of discharge for floodplain depths just above the bank full level and also explain that by increasing the depth of floodplain, the phenomenon diminishes.

By introducing an interface shear stress between adjacent compartments parameterized in terms of the velocity difference between main channel and floodplains and the channel dimensions the lateral momentum transfer was described by ***Prinos and Townsend (1984)***.

Myers (1987) has explained that the theoretical considerations of ratios of main channel velocity and discharge to the floodplain values in compound channel which follow a straight line relationship with flow depth and are independent of bed slope but dependent on channel geometry only.

By using fibre-optic laser-Doppler anemometer in steep open-channel flows over smooth and incompletely rough beds the velocity was measured by ***Tominaga & Nezu (1992)*** and discussed about the velocity profile in steep open channel. They explained that the velocity profile is necessary for solving the problems of soil erosion and sediment transport and also observed that, the integral constant used in the log law coincided with the usual value of 5.29 regardless of the Reynolds and Froude number was in subcritical flows, whereas it decreases with an increase of the bed slope in supercritical flows.

By the measurement of stage–discharge relationship and observation of velocity fields in small laboratory two stage channels ***Willetts and Hardwick (1993)*** have found the zones of interaction between the main channel and floodplain flows which was occupied the whole or at least very large portion of the main channel. They have also explained that the water, which approaches the channel by way of floodplain, penetrates to its full depth and there is a dynamic exchange of water between the inner channel and floodplain. This lead to consequent circulation in the channel in the whole section. The energy dissipation mechanism of the trapezoidal section was found to be quite different from the rectangular section and they have suggested for further study in this respect. They have also suggested for further investigation to quantify the influence of floodplain roughness on flow parameters.

For evaluating discharge in straight compound channels, ***Ackers (1992, 1993)*** has proposed a set of empirical equations based on coherence concept considering the momentum transfer between main channels and flood plains.

A model was proposed by ***Shiono and Knight (1999)*** that resolves the depth-averaged flow velocity U(y), as a function of the cross-channel coordinate, to improve the prediction capability.

Bousmar and Zech (1999) have accounted momentum transfer proportional to the product of velocity gradient at the interface and the mass discharge exchanged through the interface between the flood plain and main channels due to turbulence and the resulting averaged flow velocities are determined from a rather complicated set of analytical equations. For estimating discharge in compound channels they have proposed a method named as Exchange Discharge Method.

Some turbulence measurements was carried out by ***Czernuszenko et.al. (2007)*** in an experimental prismatic compound channel in which the surface of the main channel bed was smooth and made of concrete, whereas the flood plains and sloping banks were covered by cement mortar composed with terrazzo. They have measured Instantaneous velocities be means of a three-components by using acoustic Doppler velocity meter (ADV). They have discussed about the results of primary velocity, the distribution of turbulent intensities, Reynolds stresses, autocorrelation functions, turbulent scales, as well as the energy spectra.

Huttoff et al. (2008) have proposed a new method named as Interactive Divided Channel Method (IDCM) which was based on a new parameterization of the interface stress between adjacent flow compartments, typically between the main channel and floodplain of a two stage channel.

Zeng (2010) have studied the accuracy of prediction by analytical model for a lateral depth varying open channel flow.

Khatua and Patra (2012a and 2012b) have presented apparent shear stress and developed a new method named as MDCM to predict the stage discharge relationships in compound channel of higher width ratio.

2.2.2 Non-Prismatic Compound Channel

Schlichting et al. (1955) explained that the pressure increases in the direction of flow and thus the flow decelerates. As a result, the retarded fluid particles cannot penetrate too far into the region of increased pressure. Thus the boundary layer is deflected sideways from the wall, separates from it and moves into the main stream.

James & Brown (1977) carried out research on compound channel where floodplains were skewed. They worked on three different skew angle of 7.2°, 11.0° and 24.0° and concluded that resistance to the flow increased with the skew angle and also explained the flow on the expanding floodplain accelerated while the flow on the converging floodplain decelerated.

Johnson et al. (1987a) explained that, like a typical jet flow, a stalled region develops near one wall while the flow becomes attached to the other wall if a density current with large densimetric Froude number travels in a diffuser with certain range of half angle.

Johnson & Stefan (1988) and Johnson et.al. (1989) performed a comprehensive study of separated undercurrent in diffusers. They concluded that whether or not a density current remains attached to both the walls or separated from one, depends strongly not only on the diffuser angle but also on the inflow densimetric Froude number.

Johnson et.al. (1989) investigated on attached flow in diffuser with small divergence angle. He concluded that for a diffuser half angle of less than 5^o, the density current remains attached to both walls in a diffuser with horizontal bottom. He also concluded that if the densimetric Froude number is less than 2.0, the density current does not separate from the wall at diffuser half angle as large as 40^o.

Further skewed channel experiments were done at the Flood Channel Facility (FCF) by researchers ***Elliott & Sellin (1990)***, with three different skew angle of 2.1°, 5.1° and 9.2°.

Elliott (1990) carried out further work at the Flood Channel Facility in the UK as part of the Series- A experiments on straight channels. He carried out detailed measurements of velocity, boundary shear stress and direction of flow.

The reduced conveyance of a skewed compound channel was confirmed by ***Jasem (1990)*** by compared it with a prismatic channel of similar cross-section.

Ervine and Jasem (1995) concluded that the velocity in the main channel is approximately constant or decreases slightly downstream. It causes a process of substitution occurs along the channel, due to the cross-over flow whereby the flow enters the main channel from the right floodplain must produce analogous removal of fluid from the main channel onto the left floodplain.

Bousmar (2002) and Bousmar et al. (2004a) analyzed the experiments on converging compound channels with symmetrically narrowing floodplains and explained about the geometrical momentum transfer and the associated additional head loss due to symmetrically narrowing floodplains. They also estimated the additional head loss due to the mass transfer.

Bousmar et al. (2004b) also executed an additional investigations by using digital imaging to record surface velocities and horizontal turbulent structures that generally develop in prismatic channels.

Proust (2005) and Proust et al. (2006) investigated the flow analysis of a non-prismatic compound channel with asymmetric geometry with rushed convergence. They also found that a larger mass transfer and total head loss occurs at higher convergence angle as 22°.

Bahram Rezaei (2006) analyzed the experimental results of non-prismatic compound channels with converging floodplains. Due to change in floodplain geometry they found that the flow interaction of main channel and flood plain increases which causes large exchanges of momentum.

Chlebek (2009) has carried out a new experimental work on skewed channel and produced much more detailed data sets than the previously existing ones.

Rezaei and Knight (2009) developed a method for compound channels with non-prismatic floodplains by modifying the SKM method named as Modified SKM. In this the convergence effects were accounted by substituting the energy line slope (Se) with the channel bed slope (S0x).

J.Chlebek, Bousmar et.al. (2010) have explained the comparison of overbank flow conditions in skewed and converging/diverging channels. They observed that head losses increased due to the mass and momentum transfer and increased velocity gradient increased due to the expand of floodplains. They also observed the differences in the flow forcing from one subsection to another, velocity and bed shear stress measurements and significant differences in the flow distribution between main channel and floodplains.

Proust et al. (2010) estimated the energy losses in straight, skewed, divergent, and convergent compound channels by using first law of thermodynamics. They also concluded that the slope of energy line equals the head loss gradient at the total cross-section, yet the gradient of head loss differs with slope of energy line in the main channel or the floodplain.

Rezaei and Knight (2011) investigated the discharge distributions along three non-prismatic compound channel configurations for different converging angles. They also found that the discharge evolution seems linear for lower water depths; whereas non- linear for higher water

depths and in the second half of the converging length the mass transfer is higher than that in the first half of the converging reach i.e. velocity increases significantly in the second half of the converging length.

2.3 OVERVIEW OF NUMERICAL MODELLING ON OPEN CHANNEL FLOW

The features characterized in open channel flow result from the complex interaction between the fluid and a number of mechanism including shear stress along the channel bed and walls, friction, gravity and turbulence. As numerical hydraulic models can significantly reduce costs associated with the experimental models, therefore in recent decades the use of numerical modelling has been rapidly expanded. With widely spread in computer application, interest has risen in applying more techniques providing more accurate results. In other fluid flow fields such as aeronautics and thermodynamics the implementation of more complex models has represented the advances in computer technology and 3D models are now commonly used. However in open channel flow this conversion has not occurred as rapidly than other sector of engineering and most hydraulics models are either 1D or 2D with very few application of 3D models. In this work the application of Computational Fluid Dynamics (CFD) package to open channel flow has been considered. The software includes various models to solve general fluid flow problems. Across the globe various numerical models such as standard k-ε model, non-linear k-ε model, k-ω model, algebraic Reynolds stress model (ASM), Reynolds stress model (RSM) and large eddy simulation (LES) have been implemented to simulate the complex secondary structure in open channel flow. The standard k- ε model is an isotropic turbulence closure but fails to reproduce the secondary flows. Although nonlinear k- ε model can simulate secondary currents successfully in a compound channel, it cannot accurately capture some of the turbulence structures. Reynolds stress model (RSM) is very effective in computing the time-averaged quantities and requires

much less computing cost. RSM computes Reynolds stresses by directly solving Reynolds stress transport equation but its application to open channel is still limited due to the complexity of the model. Large eddy simulation (LES) solves spatially-averaged Navier-Stokes equation. Large eddies are directly resolved, but eddies smaller than mesh are modelled. Though LES is computationally expensive to be used for industrial application but can efficiently model nearly all eddy sizes. The work of previous researchers regarding the advancements in numerical modelling of open channel flow has been listed below.

Cokljat & Younis and Basara & Cokljat (1995) proposed the RSM (Reynolds Stress Model) for numerical simulations of free surface flows in a rectangular channel and in a compound channel and found good agreement between predicted and measured data.

Thomas and Williams (1995) described about Large Eddy Simulation of steady uniform flow in a symmetric compound channel of trapezoidal cross-section at a Reynolds number of 430,000. The complex interaction between the main channel and the flood plains was found out by simulation and they have predicted the bed stress distribution, velocity distribution, and the secondary circulation across the floodplain. The results were compared with experimental data from the SERC Flood Channel Facility at Hydraulics Research Ltd, Wallingford, England.

Salvetti et al. (1997) has conducted LES simulation at a relatively large Reynolds number for producing results of bed shear, secondary motion and vortices and then simulate with experimental results.

Rameshwaran P, Naden PS. (2003) analyzed three dimensional nature of flow in compound channels.

Ahmed Kassem, Jasim Imran and Jamil A. Khan (2003) analyzed from the three-dimensional modeling of negatively buoyant flow in a diverging channel with a sloping bottom.

He modified the k-ϵ turbulence model for the buoyancy effect and Boussinesq approximation for the Reynolds-averaged equations in diverging channels.

Lu et al. (2004) applied a three-dimensional numerical model to simulate secondary flows, the distribution of bed shear stress, the longitudinal and transversal changes of water depth and the distribution of velocity components at a 180° bend using the standard k-ϵ turbulence model.

Bodnar and Prihoda (2006) presented a numerical simulation of the turbulent free-surface flow by using the k-ϵ turbulence model and analyzed the nature of non-linearity of water surface slope at a sharp bend.

Sugiyama H., Hitomi D., Saito T. (2006) used turbulence model consists of transport equations for turbulent energy and dissipation, in conjunction with an algebraic stress model based on the Reynolds stress transport equations. They have shown that the fluctuating vertical velocity approaches zero near the free surface. In addition, the compound meandering open channel was clarified somewhat based on the calculated results. As a result of the analysis, the present algebraic Reynolds stress model is shown to be able to reasonably predict the turbulent flow in a compound meandering open channel.

Booij (2003) and VanBalen et al. (2008) modelled the flow pattern at a mildly-curved 180º bend and assessed the secondary flow structure using large eddy simulation (LES).

Jing, Guo and Zhang (2009) simulated a three-dimensional (3D) Reynolds stress model (RSM) for compound meandering channel flows. The velocity fields, wall shear stresses, and Reynolds stresses are calculated for a range of input conditions. Good agreement between the

simulated results and measurements indicates that RSM can successfully predict the complicated flow phenomenon.

Cater and Williams (2008) reported a detailed Large Eddy Simulation of turbulent flow in a long compound open channel with one floodplain. The Reynolds number is approximately 42,000 and the free surface was treated as fully deformable. The results are in agreement with experimental measurements and support the use of high spatial resolution and a large box length in contrast with a previous simulation of the same geometry. A secondary flow is identified at the internal corner that persists and increases the bed stress on the floodplain.

B. K. Gandhi, H.K. Verma and Boby Abraham (2010) determined the velocity profiles in both the directions under different real flow conditions, as ideal flow conditions rarely exist in the field. 'Fluent', a commercial computational fluid dynamics (CFD) code, has been used to numerically model various situations. He investigated the effects of bed slope, upstream bend and a convergence / divergence of channel width of velocity profile.

Balen et.al. (2010) performed LES for a curved open-channel flow over topography. It was found that, notwithstanding the coarse method of representing the dune forms, the qualitative agreement of the experimental results and the LES results is rather good. Moreover, it is found that in the bend the structure of the Reynolds stress tensor shows a tendency toward isotropy which enhances the performance of isotropic eddy viscosity closure models of turbulence.

Esteve et.al., (2010) simulated the turbulent flow structures in a compound meandering channel by Large Eddy Simulations (LES) using the experimental configuration of Muto and Shiono (1998). The Large Eddy Simulation is performed with the in-house code LESOCC2. The

predicted stream wise velocities and secondary current vectors as well as turbulent intensity are in good agreement with the LDA measurements.

Ansari et.al., (2011) determined the distribution of the bed and side wall shear stresses in trapezoidal channels and analyzed the impact of the variation of the slant angles of the side walls, aspect ratio and composite roughness on the shear stress distribution. The results show a significant contribution on secondary currents and overall shear stress at the boundaries.

Rasool Ghobadian and Kamran Mohammodi (2011) simulated the subcritical flow pattern in 180° uniform and convergent open-channel bends using SSIIM 3-D model with maximum bed shear stress. He observed at the end of the convergent bend, bed shear stress show higher values than those in the same region in the channel with a uniform bend.

Khazaee & M. Mohammadiun (2012) investigated three-dimensional and two phase CFD model for flow distribution in an open channel. He carried out the finite volume method (FVM) with a dynamic Sub grid-scale for seven cases of different aspect ratios, different inclination angles or slopes and convergence divergence condition.

Omid Seyedashraf, Ali Akbar Akhtari& Milad Khatib Shahidi (2012) concluded that the standard k-ε model has the capability of capturing specific flow features in open channel bends more precisely. Comparing the location of the minimum velocity occurrences in an ordinary sharp open channel bend, the minimum velocity occurs near the inner bank and inside the separation zone along the meandering.

Anthony G. Dixon (2012) simulated Computational fluid dynamics (CFD) software with fluid flow interactions between phases and he analyzed and improved it. He included use of CFD to simulate an experiment on multiphase flow to compare results on flow regime and pressure drop.

Larocque, Imran, Chaudhry (2013) presented 3D numerical simulation of a dam-break flow using LES and k- ε turbulence model with tracking of free surface by volume-of-fluid model. Results are compared with published experimental data on dam-break flow through a partial breach as well as with results obtained by others using a shallow water model. The results show that both the LES and the k –ε modelling satisfactorily reproduce the temporal variation of the measured bottom pressure. However, the LES model captures better the free surface and velocity variation with time.

Ramamurthy et al. (2013) simulated three-dimensional flow pattern in a sharp bend by using two numerical codes along with different turbulent models, and by comparing the numerical results with experimental results validated the models, and claimed that RSM turbulence model has a better agreement with experimental results.

From literature survey, it was found that very limited work on velocity distribution, boundary shear stress have been reported for compound channel with non-prismatic flood plain. Although adequate literature is available on numerical studies that make use of different turbulence models for modeling non-prismatic compound channels but the literature lacks substantial experimental works for non-prismatic compound channels.

EXPERIMENTAL SETUP AND PROCEDURE

3.1. GENERAL

Evaluation of discharge capacity in a non-prismatic compound channel is a complicated process due to variations in geometry, channel alignments and flow conditions. The evaluation of discharge capacity is directly dependent on accurate prediction of velocity distribution in the compound channel. Velocity distribution is never uniform across a compound channel cross-section. It is higher in deeper main channel than the shallower floodplain, as in compound channels the shallow floodplains offer more resistance to flow than the deep main channel. Variation of velocity leads to lateral momentum transfer between the main channel and the adjoining shallow floodplains. The present research work utilises the flume facility available in the Fluid Mechanics and Hydraulic Engineering Laboratory of the Civil Engineering Department at the National Institute of Technology, Rourkela, India. The basic objective behind these experiments is to conceive better understanding on the variation of velocity distribution. The following section provides a brief overview of details of hydraulic and geometric parameters of the present non-prismatic converging compound channel, experimental arrangements, measuring equipments and procedure used in the experimentation process.

3.2 EXPERIMENTAL ARRANGEMENTS

3.2.1 Geometry Setup

Experiments are conducted in a non-prismatic compound channels having symmetrically converging flood plains with varying cross section built inside a concrete flume measuring 15m×0.9m×0.5m in the hydraulic engineering laboratory of the National Institute of Technology

Rourkela, India. The channel has the width ratio (α) as $1 \leq \alpha \leq 1.8$ and the aspect ratio(δ) of 5. The converging angle of the channel is 13.39°.Converging length of the channel is 0.84 m. The channel is made up of cement concrete. Details of experimental parameters for converging compound channel is shown in Table 3.1.

Table 3.1. Details of Experimental parameters for Converging Compound Channel

Sl. No	Item Description	Converging compound channel
1	Geometry of main channel	Rectangular
2	Geometry of flood plain	Converging
3	Main channel width(b)	0.5m
4	Bank full depth of main channel	0.1m
5	Top width of compound channel (B_1) before convergence	0.9m
6	Top width of compound channel (B_2) after convergence	0.5m
7	Converging length of the channel	0.84m
8	Slope of the channel	0.0017
9	Width ratio(α) = Ratio of top width (B) to main channel width (b)	$1 \leq \alpha \leq 1.8$
10	Aspect Ratio (δ)=Ratio of main channel width(B) to main channel height	5
11	Angle of convergence of flood plain (Ø)	13.39°
12	Flume size	15 m×.9 m×0.5 m
13	Position of experimental section 1	After 12m distance from start of the channel or 0.05m before converging part
14	Position of experimental section 2	0.1 m forward from sec 1. Or 0.05m forward from start of converging part
15	Position of experimental section 3	Middle of converging part Or 0.42m forward from start of convergence
16	Position of experimental section 4	0.05m before end of converging part.
17	Position of experimental section 5	0.05m after end of converging part Or 0.1m forward from section 4.

3.2.2 Experimental Procedure

Water is supplied through a Centrifugal pumps (15 HP) discharging into a RCC overhead tank (Figure3.3). In the downstream end there is a measuring tank (Figure 3.8) followed by a sump which feeds back water to the overhead tank through pumping thus completing recirculation path. Water is supplied to the flume from an underground sump via an overhead tank by centrifugal pump and returns back to the sump after flowing through the compound channel and a downstream volumetric tank fitted with closure valves for calibration purpose. Water enters the channel bell mouth section (Figure 3.4) via an upstream rectangular notch specifically built to measure discharge. An adjustable vertical gate along with flow straighteners is provided in the upstream section sufficiently ahead of rectangular notch to reduce turbulence and velocity of approach in the flow near the notch section. At the downstream end another adjustable tail gate (Figure3.7) is provided to control the flow depth and maintain a uniform flow in the channel. A movable bridge (Figure3.6) is provided across the flume for both span wise and stream wise movements over the channel area so that each location on the plan of converging compound channel could be accessed for taking measurements. Figure.3.1 shows the schematic diagram of experimental setup of the open channel flow.

The parameters of the channel are aspect ratio of main channel (δ), width ratio (α). Experimentation is taken place in the compound channel by taking two different relative depth (Dr) value i.e. 0.2Dr, 0.3Dr in different position and depth. Experimentations are taking place at various depth and position longitudinally in five different sections. Where first section is taken before start of converging area, second, third and fourth sections are taken inside the convergence area and fifth section is situated after the end of converging area. In section 1 width

ratio(α) is more which is equal to 1.8 where in section 5 width ratio is less and the value is 1 as there is no flood plain. From section 1 to section 5 width ratio decreases which lies between 1.8 to 1. It means after section 1 flood plain converges towards longitudinal direction. Figure.3.2 show the plan view of five different experimental sections of the channel.

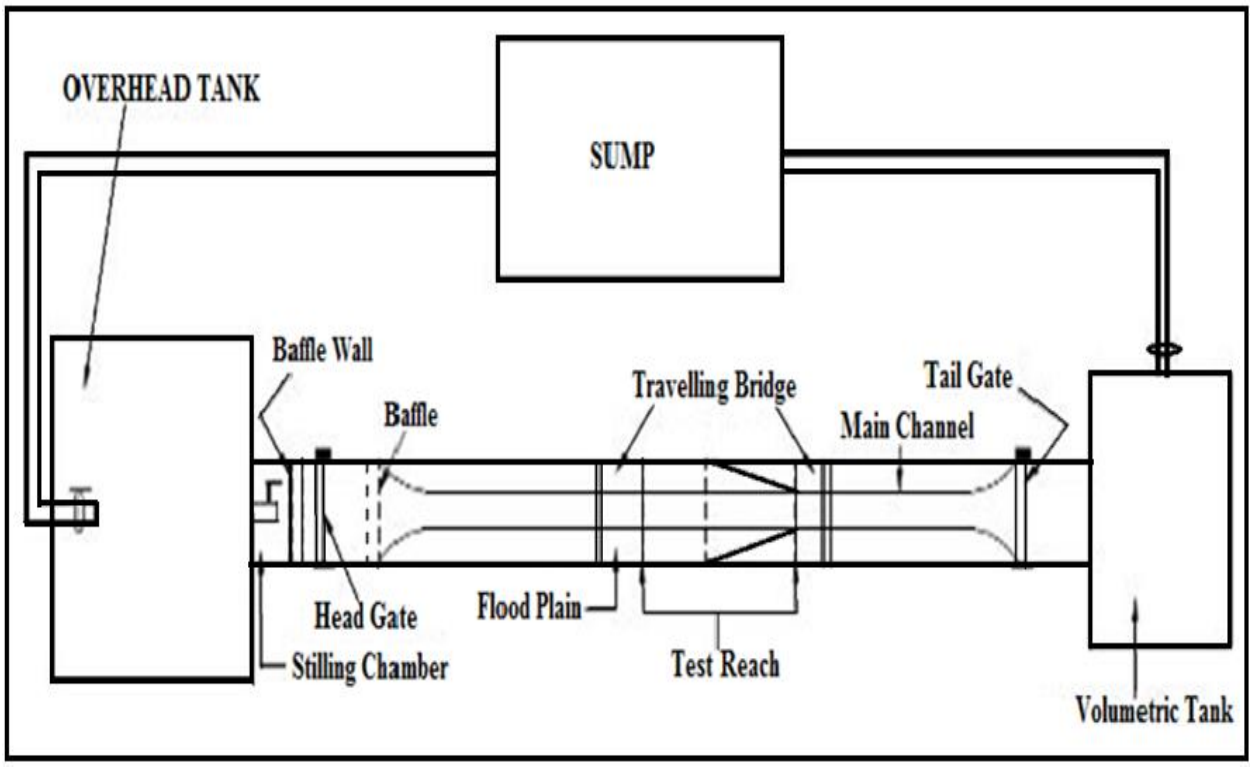

Figure. 3.1. Plan view of experimental setup of the channel

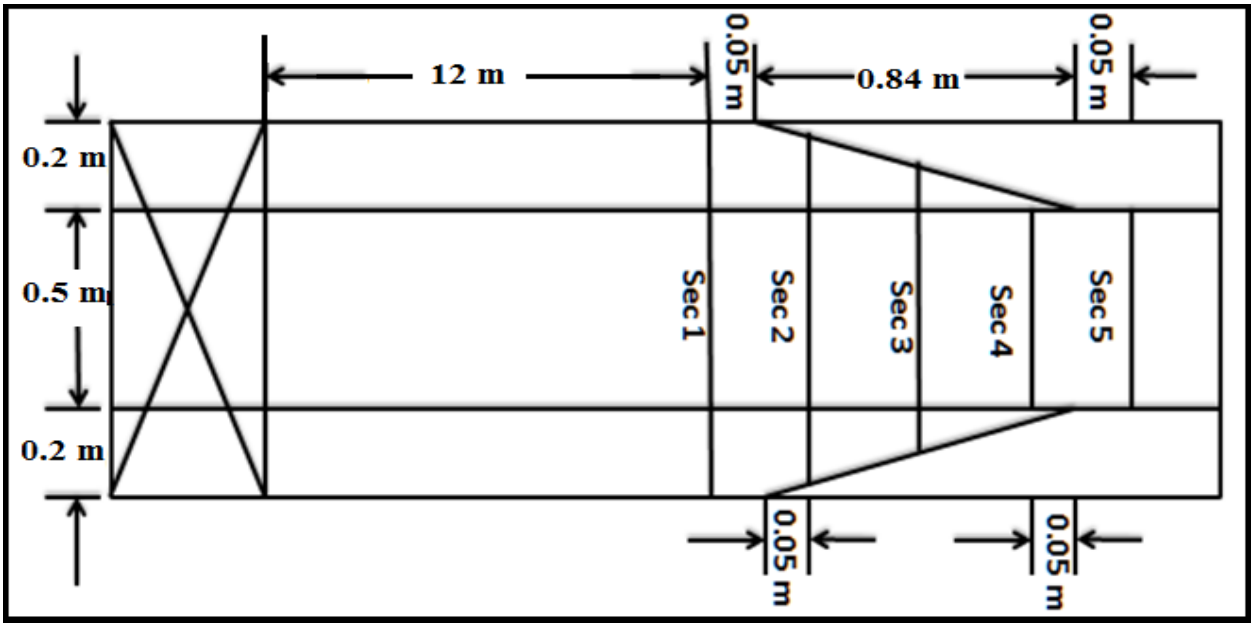

Figure. 3.2. Plan view of five different experimental sections

Figure 3.3. Front view of RCC Overhead Tank

Figure 3.4. Photo of Inlet mouth section

Figure 3.5. Photo of Non Prismatic Converging Comound Channel.

Figure 3.6. Photo of movable bridge used for Experimentation.

Figure 3.7. Photo of Tailgate at down stream

Figure 3.8. Photo of Volumetric tank

NUMERICAL MODELLING

4.1 DESCRIPTION OF NUMERICAL MODEL PARAMETERS

In this study, Fluent, a Computational Fluid Dynamics simulation tool is used for model verification which is based on the three-dimensional form of Navier-Stokes equations. Computational Fluid Dynamics (CFD), is a branch of fluid mechanics that uses numerical methods and algorithms to solve and analyze problems that involve fluid flows. Computers are used to perform the calculations required to simulate the interaction of liquids and gases with surfaces defined by boundary conditions. With high-speed supercomputers, better solutions can be achieved. Ongoing research yields software that improves the accuracy and speed of complex simulation scenarios such as transonic or turbulent flows. It has started around 1960 and with the process of improvement in computer processor speed, CFD simulation is now showing astounding accuracy. The CFD based simulation relies on combined numerical accuracy, modeling precision and computational cost.

Generally CFD uses a finite volume method (FVM). Fluent can use both structured and unstructured grids. In free-surface modeling e.g. VOF (Ferziger and Peric 2002) and height of liquid (HOL) or LES, the governing equations are discretized in both space and time which generally requires transient simulation. Here Large Eddy Simulation model is used for turbulence modeling. The LES equations are discretized in both space and time. In this study the algorithms adopted to solve the coupling between pressure and velocity field is PISO, the pressure implicit splitting of operators use in Fluent (Issa 1986). A noniterative solution method PISO is used to calculate the transient problem as it helps to converge the problems faster. When the residuals of the discretized transport equation reach a value of 0.001 or when the solution do

not change with further iterations, the numerical solution is converged. To promote the convergence of the solution

the changing variables are controlled during the calculations. For the simulations with an unsteady solver, the difference in the mass flow rates at the velocity inlet and pressure outlet is monitored to be less than 0.01% in the final solution. Furthermost, a number of extra time steps are added to verify the steadiness of the flow field in the final solution.

4.2 TURBULENCE MODELLING

"Turbulence is an irregular motion which in general makes its appearance in fluids, gaseous or liquid, when they flow past solid surfaces or even when neighbouring streams of the same fluid flow past or over one another." ***GI Taylor and von Karman, 1937***

"Turbulent fluid motion is an irregular condition of flow in which the various quantities show a random variation with time and space coordinates, so that statistically distinct average values can be discerned." ***Hinze, 1959***

The flow in a compound channel is turbulent in nature. Channel Shape or geometry and gravity force is mainly responsible for the turbulent flow. Turbulent flow is a flow regime characterized by chaotic and stochastic property changes. This includes low momentum diffusion, high momentum convection, and rapid variation of pressure and velocity in space and time. Turbulence occurs when the inertia forces in the fluid become significant compared to viscous forces, and is characterized by a high Reynolds Number. Generally turbulence is a random three dimensional time-dependent eddying motion with many large scales eddies. The three dimensional nature of turbulent flows are decomposed into two different parts i.e. mean part and fluctuation part, which is well known as Reynolds decomposition. The spatial character

of turbulence reveal the eddies with wide range scales. In turbulence, separated fluid particles are brought close together by eddying motion which causes the effective exchange of heat, mass and momentum. The turbulence in compound channel is quite complex and the flow structure involved in it creates uncertainty in prediction of flow variables. Particularly in converging compound channels, turbulent structures are generalized by large shear layers generated by difference of velocity between main channel and converging floodplain. This large shear layer region creates vortices both longitudinal as well as vertical direction. The anisotropy and inhomogeneity of turbulent structure causes secondary current, which creates the velocity dip and affects the flow variables. Hence in this study an effort is made to recognize the effect of the turbulence in symmetrical compound open channel with converging flood plain. Incorporating turbulence, CFD considers the instantaneous velocity that consisting of an average velocity component and a fluctuating velocity component given as

Instantaneous velocity = mean velocity + fluctuating velocity given as

$$u = \bar{u} + u' \tag{4.1}$$

The Navier-Stokes momentum equation is taken as:

$$\frac{\partial \rho u_i u_j}{\partial x_j} = -\frac{\partial p}{\partial x_i} + \frac{\partial}{\partial x_j}\left(\mu \frac{\partial u_i}{\partial x_j}\right) \tag{4.2}$$

By substituting $\bar{u} + u'$ for u in equation (4.2) and averaging the term we get:

$$\frac{\overline{\partial u}}{\partial x} = \frac{\overline{\partial(\bar{u}+u')}}{\partial x} = \frac{\partial \bar{u}}{\partial x} \tag{4.3}$$

For non-linear function the equation (1) becomes

$$\frac{\partial(uu)}{\partial x} = \frac{\partial(\overline{u}\overline{u})}{\partial x} + \frac{\partial \overline{u'u'}}{\partial x} \tag{4.4}$$

Now the Navier-Stokes equations become:

$$\frac{\partial \overline{u_j}}{\partial x_j} = 0 \tag{4.5}$$

$$\frac{\partial \rho \overline{u_i u_j}}{\partial x_j} = -\frac{\partial \overline{p}}{\partial x_i} + \frac{\partial}{\partial x_j}\left(\mu \frac{\partial \overline{u_i}}{\partial x_j}\right) - \frac{\partial \rho(u_i' u_j')}{\partial x_j} \tag{4.6}$$

The term $\frac{\partial \rho\left(u_i' u_j'\right)}{\partial x_j}$ is known as the "Reynolds stress". Due to closure problem of both the equations 4.5 and 4.6 we have to come up with ways of replacing the extra terms with other terms that were known or devising ways of calculating these terms. A first attempt at closing the equations is:

$$\frac{\partial}{\partial x_j}\left(\mu \frac{\partial \overline{u_i}}{\partial x_j}\right) = \frac{\partial \rho\left(u_i' u_j'\right)}{\partial x_j} \tag{4.7}$$

In equation (4.7) both terms represent a diffusion of energy. The term $\frac{\partial}{\partial x_j}\left(\mu \frac{\partial \overline{u_i}}{\partial x_j}\right)$ represents diffusion of energy through viscosity and the other term $\frac{\partial \rho\left(u_i' u_j'\right)}{\partial x_j}$ represents the diffusion through turbulence. By defining $\mu_t$as turbulent viscosity, equation (4.6) becomes:

$$\frac{\partial \rho \overline{u_i u_j}}{\partial x_j} = -\frac{\partial \overline{p}}{\partial x_i} + \frac{\partial}{\partial x_j}\left((\mu + \mu_t)\frac{\partial \overline{u_i}}{\partial x_j}\right) \tag{4.8}$$

To enable the effects of turbulence to be predicted, a large amount of CFD research has concentrated on methods which make use of turbulence models. Turbulence models have been specifically developed to account for the effects of turbulence without recourse to a prohibitively fine mesh and direct numerical simulation. Most turbulence models are statistical turbulence model, as mentioned below.

4.2.1 Turbulence Models

- Algebraic (zero-equation) model.
- k-ε, RNG k-ε model.
- Shear stress transport model.
- K-ω model.
- Reynolds stress transport model (second moment closure).
- K-ω Reynolds stress.
- Detached eddy simulation (DES) turbulence model.
- SST scale adaptive simulation (SAS) turbulence model.
- Smagorinsky large eddy simulation model (LES).
- Scalable wall functions.
- Automatic near-wall treatment including integration to the wall.
- User-defined turbulent wall functions and heat transfer.

4.3 GOVERNING EQUATION

The governing equation used here is based on conservation of mass, momentum and energy. The C.F.D package namely Fluent was employed to solve the governing equations, which uses Finite Volume Method (FVM) to solve the equations. FVM involves

discretization and integration of the governing equations over the control volume. The numerical method FVM was based on the integral conservation which is applied for solving the partial difference i.e. Navier-Stokes equation then calculate the values of the variables, averaged across the volume. The integration of the equations over each control volume results in a balance equation.

The conservation law is enforced on small control volumes which is defined by computational mesh. The set of balance equations then discretized with respect to a set of discretization schemes and is solved by using the initial and boundary conditions.

The governing Reynolds Averaged Navier-Stokes and continuity equations are stated as:

$$\frac{\partial(\rho)}{\partial t} + \frac{\partial(\rho u_i)}{\partial x_i} = S_m \quad \textbf{(4.9)}$$

$$\frac{\partial(\rho u_i)}{\partial t} + \frac{\partial(\rho u_i u_j)}{\partial x_j} = -\frac{\partial p}{\partial x_i} + \frac{\partial}{\partial x_j}\mu\left[\frac{\partial u_i}{\partial x_j} + \frac{\partial u_j}{\partial x_i}\right] + \frac{\partial(-\rho\overline{u_i' u_j'})}{\partial x_j} \quad \textbf{(4.10)}$$

Where t=time, u_i=i-th component of the Reynolds-averaged velocity, x_i=i-th axis, ρ=water density, p= Reynolds averaged pressure, g=acceleration due to gravity, μ=viscosity (here it is equal to zero), S_m=mass exchange between two phase (water and air).

Here for unsteady solver the time-averaged values of velocities and other solution variables are taken instead of instantaneous values. The term $\left(-\rho\overline{u_i' u_j'}\right)$ is called as Reynolds Stress. To link the mean rate of deformation with Reynolds stresses, Boussinesq hypothesis is used:

$$-\rho u_i' u_j' = \mu_t\left(\frac{\partial u_i}{\partial x_j} + \frac{\partial u_j}{\partial x_i}\right) \quad \textbf{(4.11)}$$

Where μ_t=the turbulent viscosity

5.1 METHODOLOGY

The process of the numerical simulation of fluid flow using the above equation generally involves four different steps and the details are given below.

(a) *Problem identification*

1. Defining the modelling goals

2. Identifying the domain to model

(b) *Pre-Processing*

1. Creating a solid model to represent the domain (Geometry Setup)

2. Design and create the mesh (grid)

(c) *Solver*

1. Set up the physics

- Defining the condition of flow (e.g. turbulent, laminar etc.)
- Specification of appropriate boundary condition and temporal condition.

2. Using different numerical schemes to discretize the governing equations.

3. Controlling the convergence by iterating the equation till accuracy is achieved

4. Compute Solution by Solver Setting.

- Initialization
- Solution Control
- Monitoring Solution

(d) ***Post processing***

1. Visualizing and examining the results

2. X-Y Plots

3. Contour Draw

5.2 PREPROCESSING

In this initial step all the necessary information which defines the problem is assigned by the user. This consists of geometry, the properties of the computational grid, various models to be used, and the number of Eulerian phases, the time step and the numerical schemes.

5.2.1 Creation Geometry

The first step in CFD analysis is the explanation and creation of computational geometry of the fluid flow region. A consistent frame of reference for coordinate axis was adopted for creation of geometry. Here in coordinate system, x axis corresponded the stream wise direction of fluid flow. Y axis aligned with the lateral direction which indicates the width of channel bed and Z axis represented the vertical component or aligned with depth of water in the channel. The origin was placed at the upstream boundary and coincided with the base of the centre line of the channel. The water flowed along the positive direction of the x-axis.

The simulation was done on a non-prismatic compound channel which was having converging flood plain. The setup of the compound channel is shown in Figure 5.1 and the cross-section of channel geometry is shown in Figure 5.2.

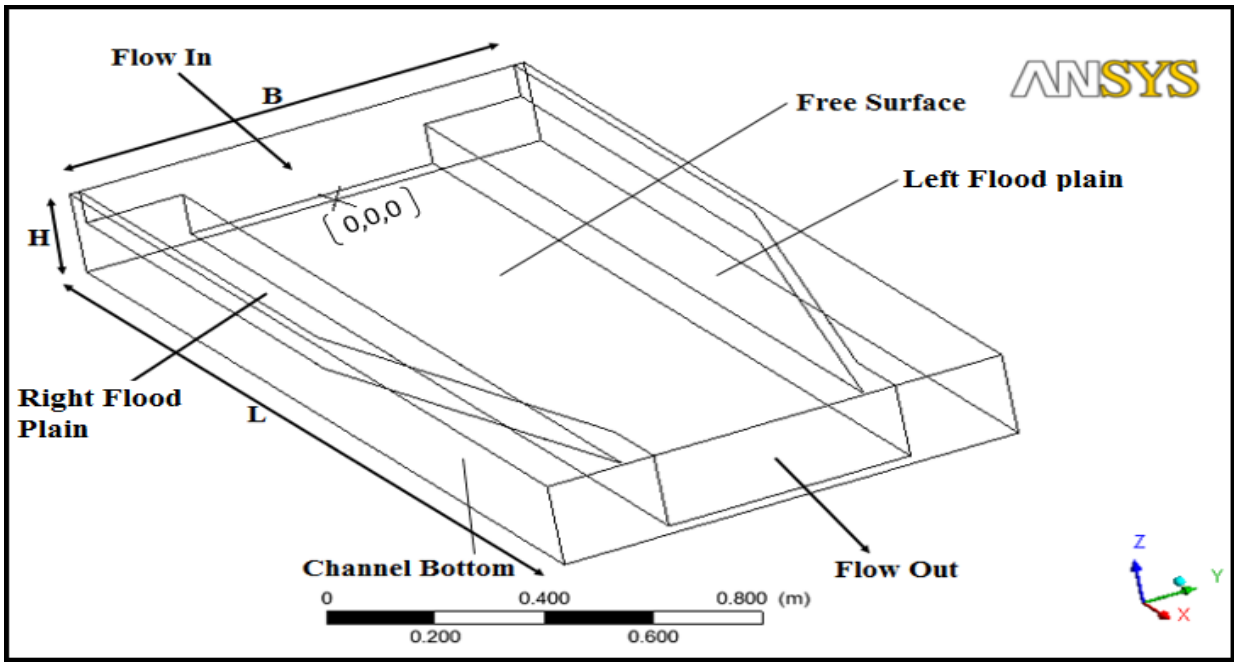

Figure 5.1. Geometry Setup of a Non-Prismatic Compound Channel

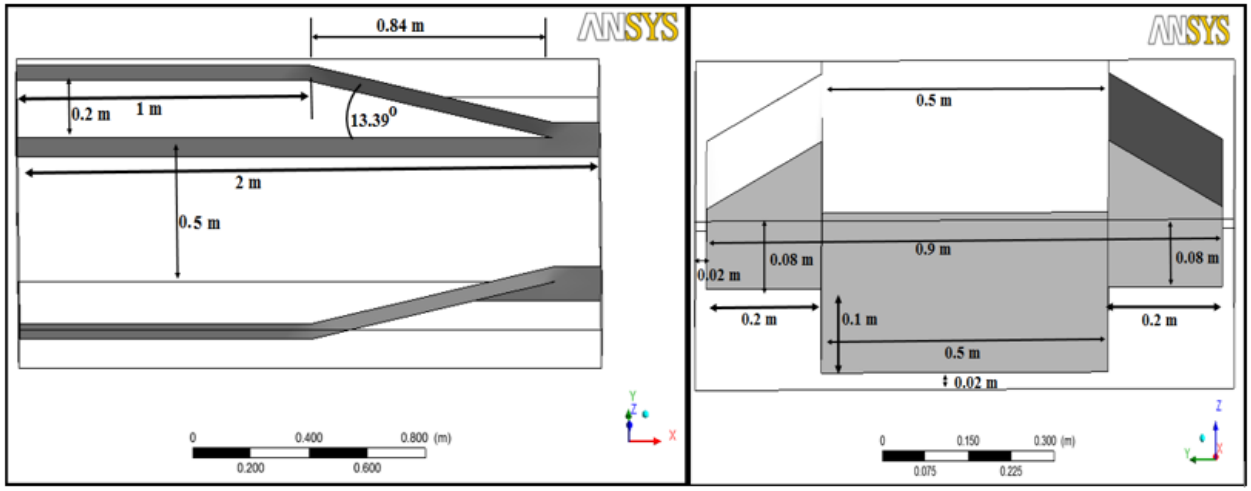

Figure 5.2. Cross sectional geometry of the non-prismatic compound channel

As can be seen from the Figure 5.2, the channel geometries were 0.15 m height, 0.9 m width and 2m length. In the non-prismatic compound channel, the width of main channel was 0.5m and main channel height was 0.1m. The width of both left and right flood plain of the prismatic part was 0.2m. The length of the prismatic section was 1m. After the prismatic section i.e. after 1m the width of flood plain gradually decreases towards outlet of the channel i.e. flood

plain converges with a converging angle of 13.39°. The converging length of the channel was 0.84m. In addition the fact that the channel is symmetric has been exploited by utilizing a symmetry plane along the centre of the channel such that the flow in half of the channel geometry is modelled. The computational geometry (half sectional geometry) is indicated in Figure 5.3.

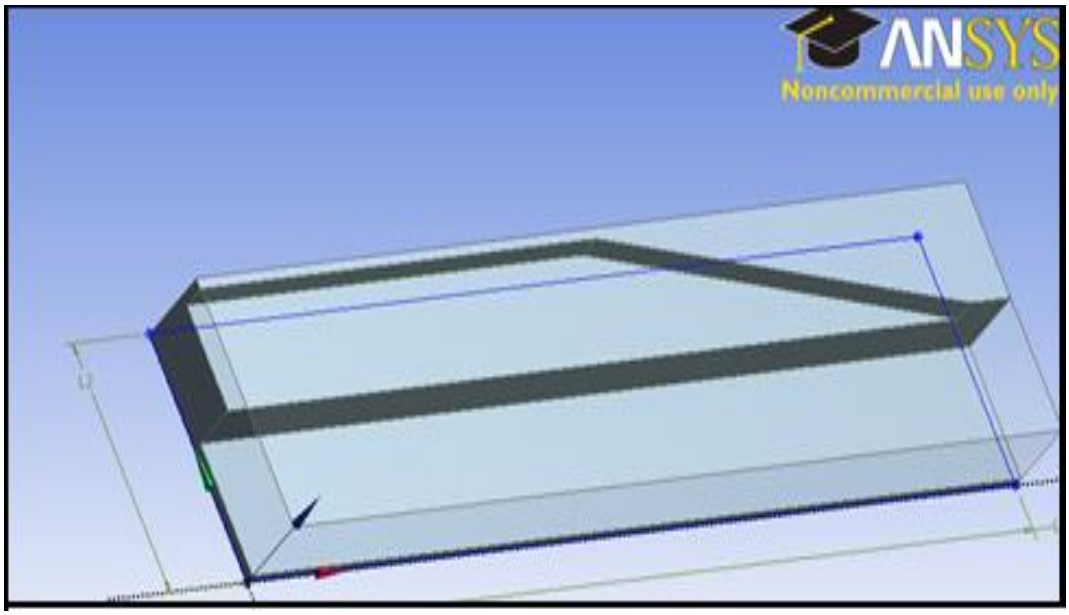

Figure 5.3. The half Sectional Geometry of a non-prismatic compound channel.

During the model construction, an additional consideration is to identify any entity of the geometry which need to be identified for future reference as to identify a particular domain for conduct some analysis and for applying boundary condition upon a particular domain. Figure 5.4 shows the geometrical entities used in a non-prismatic compound channel and Figure 5.5 shows the geometrical entities used in the half sectional channel of a non-prismatic compound channel.

For identify the domain six different surfaces are generated.

- Inlet
- Outlet
- Free Surface
- Side Wall
- Channel Bottom
- Centre line

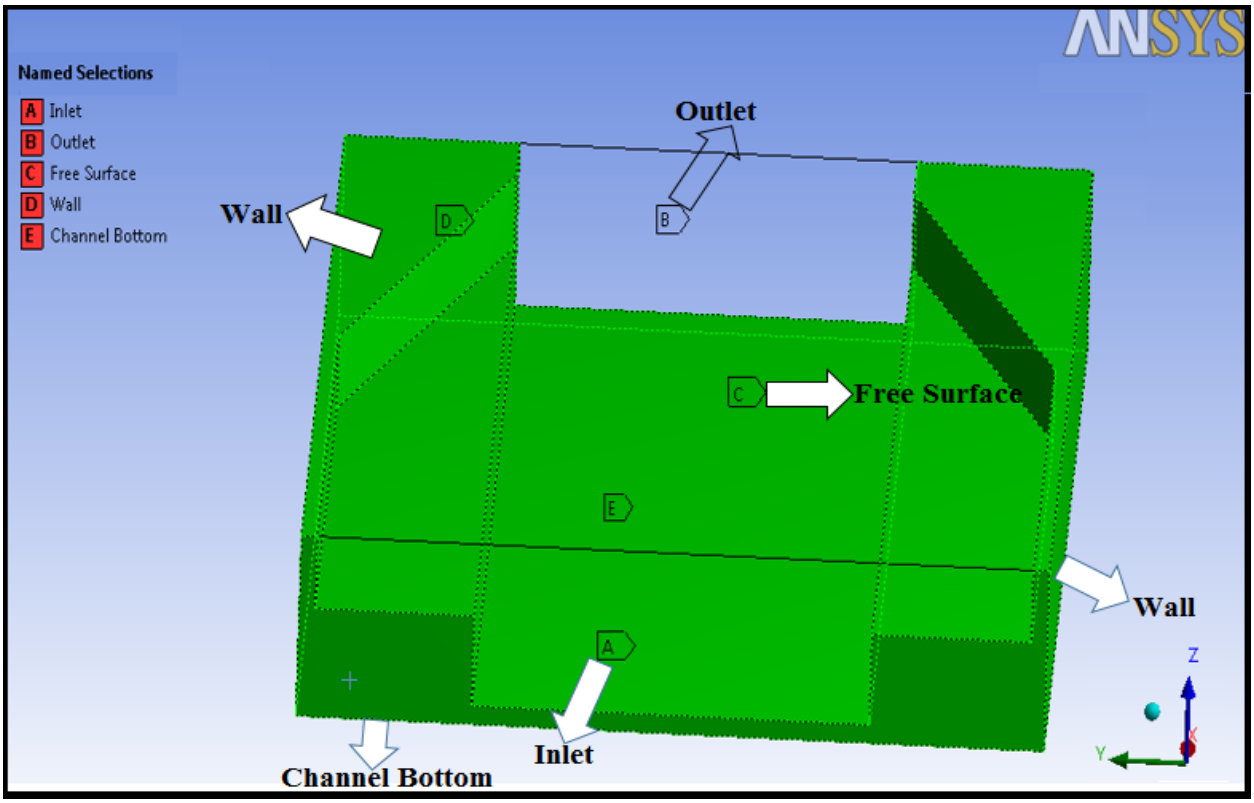

Figure 5.4 Different Geometrical entities used in a non-prismatic compound channel

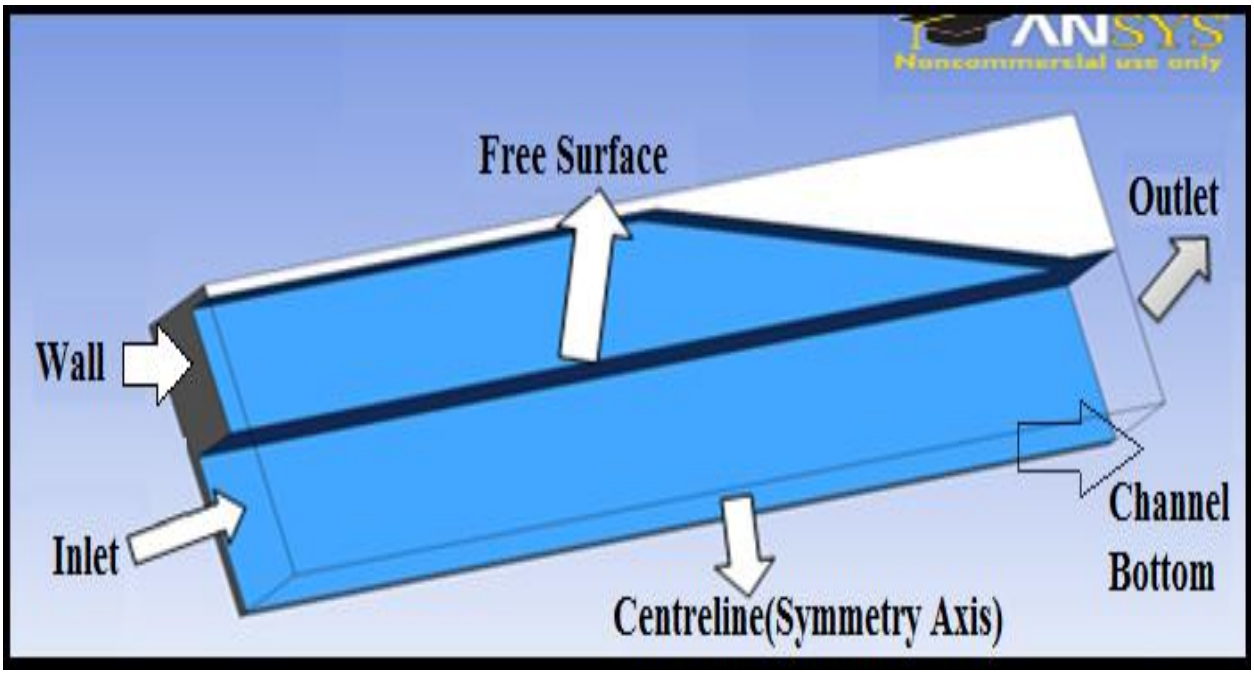

Figure 5.5 Geometrical entities used for different domains of channel half section

5.2.2 MESH GENERATION

Second and very most important step in numerical analysis is setting up the grid associated with the construction of geometry. The Navier-Stokes Equations are non-linear partial differential equations, which consider the whole fluid domain as a continuum. In order to simplify the problem the equations are simplified as simple flows have been directly solved at very low Reynolds numbers. The simplification can be made using what is called discretization. Construction of mesh involves discretizing or subdividing the geometry into the cells or elements at which the variables will be computed numerically. By using the Cartesian co-ordinate system, the fluid flow governing equations i.e. momentum equation, continuity equation are solved based on the discretization of domain. The CFD analysis needs a spatial discretization scheme and time marching scheme. Meshing divides the continuum into finite number of nodes. Generally the domains are discretized by three different ways i.e. Finite element, Finite Volume and Finite

Difference Method. Finite element method is based on dividing the domain into elements. In finite element method the numerical solutions are obtained by integrating the shape function and weighted factor in an appropriate domain. This method is suitable for both structured and unstructured mesh. But the Finite Volume method divides the domain into finite number of volumes. Finite volume method solves the discretization equation in the center of the cell and calculates some specified variables. The values of quantities, such as pressure, density and velocity that are present in the equations to be solved are stored at the center of each volume. The flux into a region is calculated as the sum of the fluxes at the boundaries of that region. As the values of quantities are stored at nodes but not at boundaries this method requires some interpolation at nodes. Generally finite Volume method is suitable for unstructured domain. Whereas finite Difference method is based on approximation of Taylor's series. This method is more suitable for regular domain.

For transient problems an appropriate time step needs to be specified. To capture the required features of fluid flow with in a domain, the time step should be sufficiently small but not too much small which may cause waste of computational power and time. Spatial and time discretization are linked, as evident in the Courant number.

5.2.2.1 Courant Number

A criterion often used to determine time step size is known as Courant number. The Courant number stops the time step from being large enough for information to travel entirely through one cell during one iteration. For explicit time stepping schemes Courant number should not be greater than 1. For implicit time stepping schemes this number may be higher than 1. The Courant number is defined as:

$$C_r = \frac{\overline{U}\Delta t}{\Delta l} \quad \textbf{(5.1)}$$

Where C_r is the Courant number, $\overline{U}$ is the average velocity, Δt is the maximum time step size and Δl is the largest grid cell size along the direction of flow.

A mesh consists of too few nodes cause quick solution of simulation but not a very accurate one. However a very dense mesh of nodes cause excess computational time and memory. For CFD analysis more nodes are required in some areas of interest, such as near wall and wake regions, in order to capture the large variation of fluid properties. Thus, structure of grid lines causes further wastage of computer storage due to further refinement of mesh. In this study, the flow domain is discretized using structured grid and body-fitted coordinates.

It must be noted that the running time is low and it is obtained by grid-independent results. The grid structure must be fine enough, especially near the wall boundaries (in order to consider the viscous flow), nearer to converge (the rapid changes area) and at free surface. In this numerical simulation, various computational trials are conducted with different number of grid cells. It is concluded that the results are almost independent from the grid size and running time is optimal. The detailed meshing of the flow domain with two views are shown in Figure 5.6.

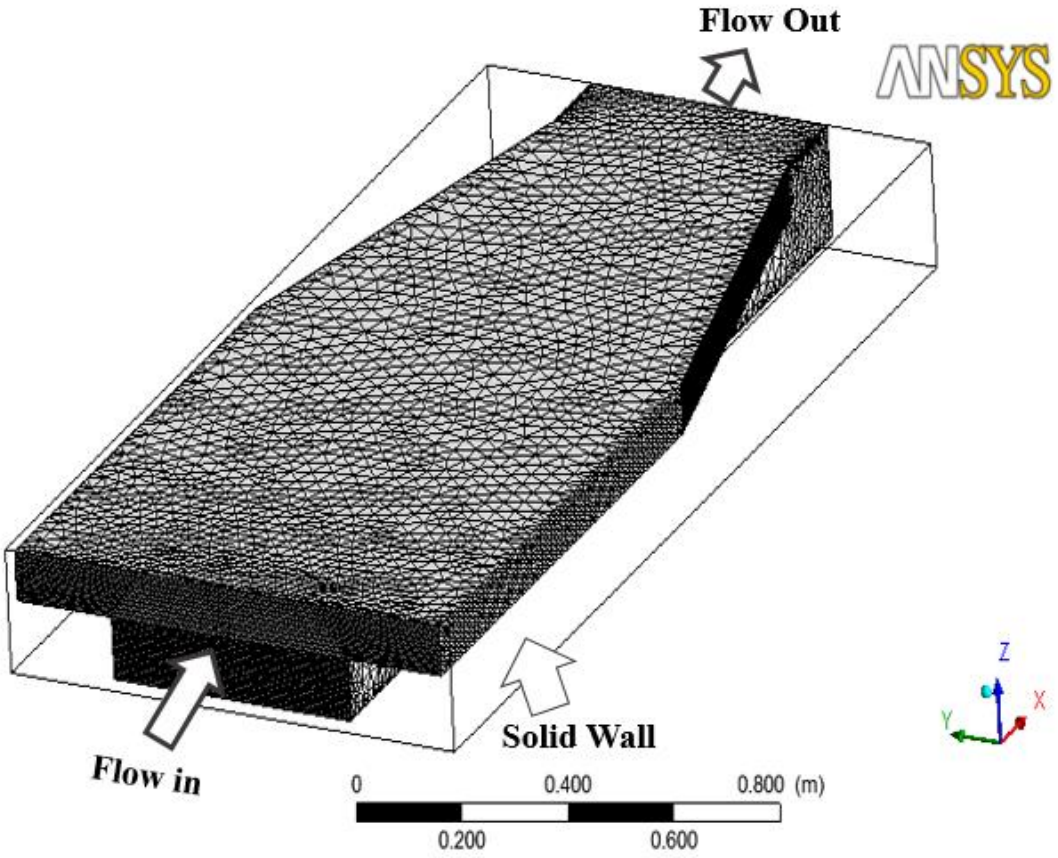

Figure 5.6. A Schematic view of the Grid used in the Numerical Model

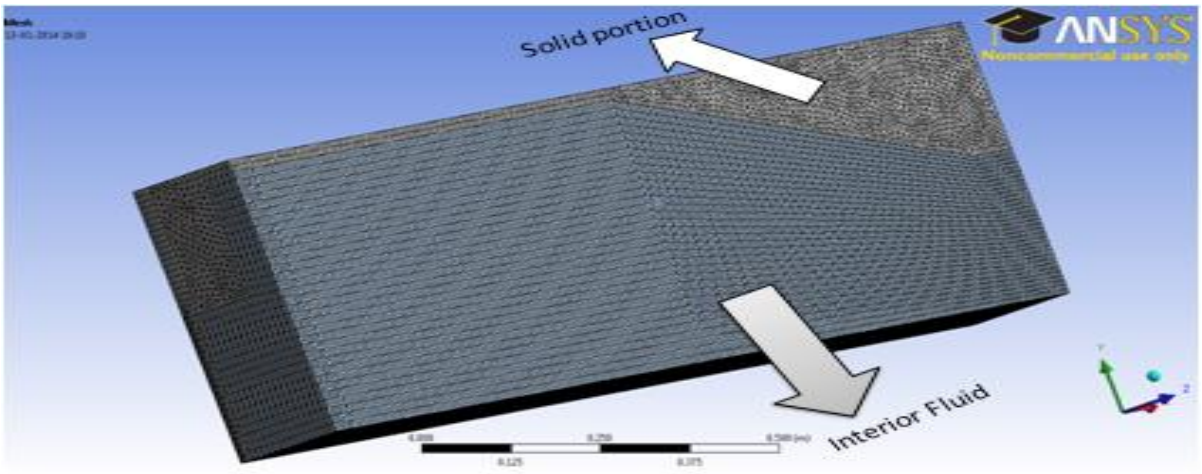

Figure 5.7. A Schematic view of the Grid used in the Numerical Model for channel half Symmetric section

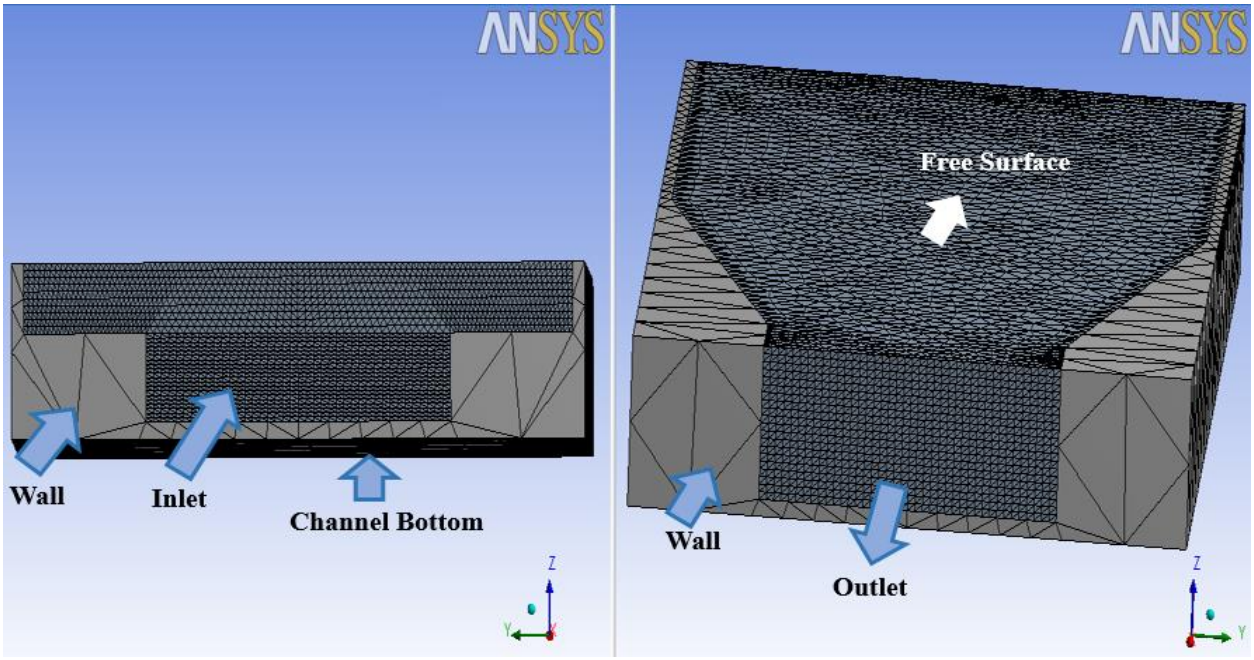

Figure 5.8. Meshing of Inlet, Outlet and free surface of a non-prismatic compound channel

5.3 SOLVER SETTING

The numerical scheme that CFD codes adopt is the finite volume method. The differential transport equations are integrated over each computational cell, and the Gauss and Leibnitz theorems are applied in this method. This consists of various models used for analysis, the initial and boundary conditions, the number of Eulerian phases, the properties of the materials, the physical and chemical phenomena involved. At last, the set of algebraic equations is solved by iteration process and the cell-centre values of the flow variables are calculated.

5.3.1 TWO PHASE MODELING EQUATIONS

A large number of flows encountered in nature are known as a mixture of phases. Solid, liquid and gas are three physical phase of matter. But the concept of phase in a multiphase flow system is applied in a wider way. In multiphase fluid flow, a phase is described as a particular class of material that has a certain inertial response and interaction with the fluid flow and the potential field in which it is immersed. Currently there are two approaches for the numerical calculation of multiphase flows: the Euler-Lagrange approach and the Euler-Euler approach.

5.3.1.1 Euler-Lagrange Approach

In Ansys Fluent, the Lagrangian discrete phase model follows the Euler-Lagrange approach. The fluid phase is treated as a continuum by solving the Navier-Stokes equations, while the dispersed phase is solved by tracking a large number of particles, bubbles or droplets through the calculated flow field. The dispersed phase can exchange the momentum, mass, and energy within the fluid phase.

5.3.1.2 Euler-Euler approach

In the Euler-Euler approach, the different phases are treated as interpenetrating continua. Since the volume of a phase cannot be occupied by the other phases, the volume of fraction concept is introduced. These volume fractions are assumed to be continuous functions of space and time and their sum is equal to one.

There are three different approaches in Euler-Euler multiphase models i.e. the volume of fluid (VOF) model, the mixture model, and the Eulerian model. The VOF model is a surface-tracking technique which is applied for a fixed Eulerian mesh. It is used for two or more immiscible fluids where the position of the interface between the fluids is of interest. In the VOF model, a single set of momentum equation is shared by the fluids, and the volume fraction of

each of the fluids in computational cell is followed throughout the domain. Whereas the mixture model is designed for two or more phases (fluid or particulate) and it solves for the mixture momentum equation and suggests relative velocities to describe the dispersed phases. But in the Eulerian model, the phases are treated as interpenetrating continua.

5.3.2 VOLUME OF FLUID (VOF) MODEL

The VOF formulation in ANSYS FLUENT is generally used to compute a time dependent Solution. In VOF model, while solving a momentum equation for each phase the interface must be tracked as an Eulerian variation in which the secondary phase is not dispersed within the primary phase but rather there is an interface between the phases. The volume of fluid (VOF) method is a computational tool for the analysis of free surface flows (Hirt and Nichols 1981). The interface between the phases is accomplished by the solution of a continuity equation for the volume fraction of one (or more) of the phases. For the q^{th} phase, this equation has the following form (Rahimzadeh et al. 2012):

$$\frac{\partial \alpha_q}{\partial t} + \nabla \cdot \left(\vartheta \cdot \alpha_q\right) = 0 \qquad \textbf{(5.2)}$$

Where $\propto_q$ is the volume fraction of the q^{th} phase. In each control volume, the volume fractions of all phases sum up to unity. The following three conditions are possible for each cell:

If $\propto_q$ = 0, the cell is empty.

If $\propto_q$ = 1, the cell is full.

If 0 <$\propto_q$< 1, the cell contains the interface between the q^{th} phase and one or more other phases. In each cell the average properties are computed according to the volume fraction of each phase. VOF method was developed to trace the moving free surface of the incompressible viscous flow.

5.3.2.1 Volume Fraction Equation

For the volume fraction of one (or more) of the phases the tracking of the interface(s) between the phases is accomplished by the solution of a continuity equation. For the q^{th} phase the volume fraction equation is defined as:

$$\frac{1}{\rho_q}\left[\frac{\partial}{\partial t}\left(\alpha_q \rho_q\right) + \nabla \cdot \left(\alpha_q \rho_q \vec{\vartheta_q}\right) = S_{\alpha_q} + \sum_{p=1}^{n}\left(m_{pq} - m_{qp}\right)\right] \quad \textbf{(5.3)}$$

Where $m_{qp}$is indicates the mass transfer from phase q to phase p.

m_{pq} is indicates the mass transfer from phase p to phase q.

Here S_{α_q},the source term is equal to zero. But sometimes a constant or a user defined mass source is specify for each phase.

The volume fraction equation will not be solved for the primary phase. The primary phase volume fraction will be computed based on:

$$\sum_{p=1}^{n} \alpha_q = 1 \quad \textbf{(5.4)}$$

5.3.2.2 Material Properties

By the presence of the component phases, the properties appearing in the transport equations are determined in each control volume. In a two-phase modelling, if the phases are represented by the subscripts 1 and 2, and the mixture density in each cell is given by:

$$\rho = \alpha_2 \rho_2 + (1 - \alpha_2)\rho_1 \quad \textbf{(5.5)}$$

In general, for n phase system, the volume-fraction-averaged density takes on the following form:

$$\rho = \sum \alpha_q \rho_q \quad \textbf{(5.6)}$$

All other properties (e.g., viscosity) are also computed in this way.

5.3.2.3 Momentum Equation

A single momentum equation is solved throughout the domain and the resulting velocity field is shared among the phases. The momentum equation is dependent on the volume fractions of all phases through the properties ρ andμ and the equation is given as.

$$\frac{\partial}{\partial t}(\rho\vec{v}) + \nabla\cdot(\rho\vec{v}\vec{v}) = -\nabla p + \nabla\cdot[\mu(\nabla\vec{v} + \nabla\vec{v}^T)] + \rho\vec{g} + \vec{F} \quad \textbf{(5.7)}$$

In shared-fields approximation when large velocity differences exist between the phases, the accuracy of the velocities computed near the interface is undesirably affected.

5.3.3 MIXTURE MODEL

The mixture model is a simplified multiphase model. The mixture model allows to select granular phases and calculates all properties of the granular phases. Generally it is applied for liquid-solid flows.

5.3.3.1 Continuity Equation

$$\frac{\partial}{\partial t}(\rho_m) + \nabla\cdot(\rho_m\vec{v}_m) = 0 \quad \textbf{(5.8)}$$

Where $\vec{v}_m$is the mass average velocity.

$$\overrightarrow{v_m} = \frac{\sum_{k=1}^{n}\alpha_k\rho_k\vec{v}_k}{\rho_m} \quad \textbf{(5.9)}$$

And $\rho_m$is the mixture density.

$$\rho_m = \sum_{k=1}^{n}\alpha_k\rho_k \quad \textbf{(5.10)}$$

α_k is the volume fraction of phase k.

5.3.3.2 Momentum Equation

The momentum equation for the mixture can be obtained by summing the individual momentum equations for all phases. It can be expressed as:

$$\frac{\partial}{\partial t}(\rho_m \vec{v}_m) + \nabla \cdot (\rho_m \vec{v}_m \vec{v}_m) = -\nabla p + \nabla \cdot \left[\mu_m \left(\nabla \vec{v}_m + \nabla \vec{v}_m^{\,T}\right)\right] + \rho_m \vec{g} + \vec{F} + \nabla \cdot \left(\sum_{k=1}^{n} \alpha_k \rho_k \vec{v}_{dr,k} \vec{v}_{dr,k}\right) \quad \textbf{(5.11)}$$

Where n is the number of phase, $\vec{F}$ is the body force and μ_m is the viscosity of the mixture and defined as

$$\mu_m = \sum \alpha_k \mu_k \quad \textbf{(5.12)}$$

$\vec{v}_{dr,k}$ is the drift velocity for secondary phase k.

Where $$\vec{v}_{dr,k} = \vec{v}_k - \vec{v}_m \quad \textbf{(5.13)}$$

5.3.3.3 Volume Fraction Equation for Secondary Phase:

From the continuity equation for secondary phase p, the volume fraction equation p can be obtained as:

$$\frac{\partial}{\partial t}(\alpha_p \rho_p) + \nabla \cdot (\alpha_p \rho_p \vec{v}_m) = -\nabla (\alpha_p \rho_p \vec{v}_{dr,p}) + \sum_{q=1}^{n} m_{qp} - m_{pq} \quad \textbf{(5.14)}$$

5.3.4 SOLVING FOR TURBULENCE

5.3.4.1 Used Large Eddy Simulation Turbulence Model

Large eddy simulation model is an intermediate approach to DNS and RANS turbulence model. LES relies on a spatial filter, rather than a time averaging process. Turbulent flows have generally wide range of length and time scales. To distinguish eddies that are going to be calculated from those that are going to be modelled, a filtering function (eg. Gaussian, Box cutoff, Fourier) is used. The large scale motions are generally more energetic than the small

ones. Large eddies depend highly on boundary conditions which determine the basic feature of flow. Large scale eddy causes the transfer of momentum and heat. The concept of Large Eddy Simulation (LES) is adopted for accuracy in turbulence nature. The LES model directly resolves the large eddies present in turbulent flows and models the smaller scale eddies. This model captures larger scale motion, as well as it covers the effects of small scales of eddies by using sub-grid scale (SGS) model. In this technique direct calculation is used to resolve the eddies that are larger than the size of the finite volume cell, while a simple model is used to model the more universal nature of the small scale eddies that are smaller than the mesh size. By seeing advantages of the LES method, it is adopted for the simulation.

Generally LES uses a spatial average instead of time-averaging sceam. Here the velocity component is split into a resolved component $\bar{U}$ and an unresolved component u′. The governing equations employed for LES are obtained by filtering the time-dependent Navier-Stokes equations in either wave number (Fourier) space or configuration (physical) space. The instantaneous velocity variable u can be written as:

$$u = \bar{U} + u' \tag{5.15}$$

Where u' is the unresolved part and $\bar{U}$ is the large scale part defined through volume averaging as:

$$\bar{U}(x_j, t) = \int_{vol} G(x_i - x_i')u(x_j', t)dx_i' \tag{5.16}$$

Where $G(x_i - x_i')$ is the Gaussian filter.

The non-filtered Navier-Stokes equation is:

$$\frac{\partial(\rho u_i)}{\partial t} + \frac{\partial(\rho u_i u_j)}{\partial x_j} = -\frac{\partial p}{\partial x_j} + \mu \frac{\partial^2 u_i}{\partial x_i x_j} \tag{5.17}$$

After performing the volume averaging and neglecting density functions, the filtered Navier-Stokes Equations become

$$\frac{\partial(\rho\overline{U_i})}{\partial t} + \frac{\partial(\rho\overline{u_i u_j})}{\partial x_j} = -\frac{\partial \bar{p}}{\partial x_j} + \mu\frac{\partial^2 \overline{u_i}}{\partial x_i x_j} \quad \textbf{(5.18)}$$

The Non-linear transport term in equation (15) can be explained as:

$$\overline{U_i U_j} = \overline{(\bar{U}_i + u_i')(\bar{U}_j + u_j')}$$

$$= \overline{\bar{U}_i \bar{U}_j} + \overline{\bar{U}_i u_j'} + \overline{\bar{U}_j u_i'} + \overline{u_i' u_j'} \quad \textbf{(5.19)}$$

(I) (II) (III) (IV)

In time averaging the term II &III vanish but not in volume averaging.

Introducing the residual stress or subgrid scale (SGS) stresses defined as τ_{ij} and expressed as

$$\tau_{ij} = \overline{u_i u_j} - \overline{U_i U_j} \quad \textbf{(5.20)}$$

Now equation (15) can be written as:

$$\frac{\partial(\rho\overline{U_i})}{\partial t} + \frac{\partial(\rho\overline{U_i U_j})}{\partial x_j} = -\frac{\partial \bar{p}}{\partial x_j} + \mu\frac{\partial^2 \overline{U_i}}{\partial x_i x_j} - \frac{\partial(\rho\tau_{ij})}{\partial x_j} \quad \textbf{(5.21)}$$

Equation (18) is the basis of the LES turbulence model.

Various LES techniques are totally dependent upon the SGS (Sub Grid Scale) model used.

5.3.4.2 Sub-Grid Scale Model

The non-linear transport of energy generates ever smaller scales like a cascade process until it reaches the viscous dissipation range or the size of Kolmogorov scales. The energy drain from resolved large scales to the unresolved small scales properly and the interaction between the resolved and unresolved sub-grid scales in LES is an essential task. The most popular class of SGS turbulence model is the Eddy-Viscosity type Smagorinsky Model (Smagorinsky 1963).

5.3.4.3 Smagorinsky Model

In this study Smagorinsky model is used to carry out the simulation. LES is modelled most simply by an eddy viscosity model and the SGS stress tensor,τ_{ij}, aids in providing model closure for the LES. In these models the SGS stress tensor is related to the resolved strain rate tensor $\overline{S_{ij}}$ through a scalar eddy viscosity coefficient. The SGS stress tensor is written as:

$$\tau_{ij}^{R} = 2\rho v_R \overline{S_{ij}} + \frac{1}{3}\delta_{ij}\tau_{kk}^{R} \qquad \textbf{(5.22)}$$

Where $\overline{S_{ij}}$ is defined as:

$$\overline{S_{ij}} = \left(\frac{\partial \overline{v_i}}{\partial x_j}\right) + \frac{\partial \overline{v_j}}{\partial x_i} \qquad \textbf{(5.23)}$$

Where the eddy viscosity of the residual motion, $v_R = C_s^2 l^2 \left(2\overline{S_{ij}S_{ij}}\right)^{1/2}$ **(5.24)**

Where C_s is the Smagorinsky constant.

5.3.5 SETUP PHYSICS

For a given computational domain, boundary conditions are imposed which can sometimes over specify or under-specify the problem. Usually, after imposing boundary conditions in non-physical domain may lead to failure of the solution to converge. It is therefore important, to understand the meaning of well-posed boundary conditions. The boundary conditions implemented for this study are shown in Fig 4.2.4. Subsequently these conditions are discussed in the follows:

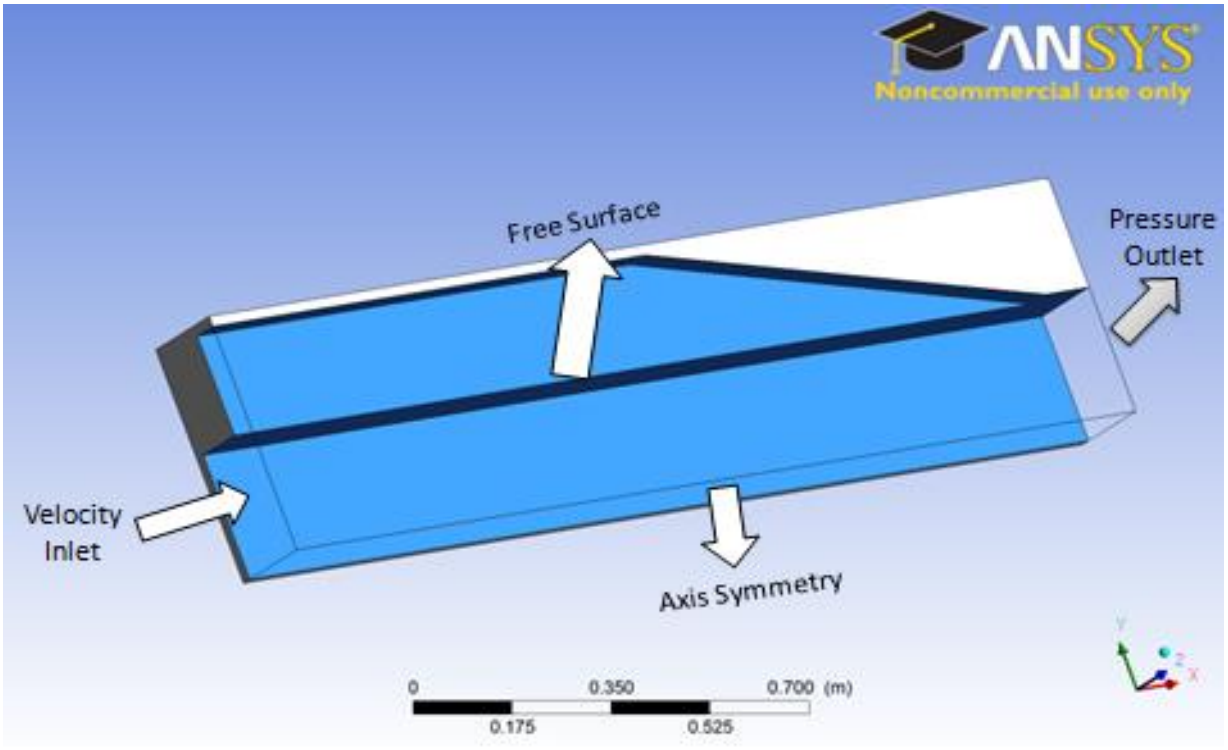

Figure 5.9. A Schematic Diagram of converging compound channel with boundary conditions

5.3.5.1 Inlet and Outlet Boundary Condition

All of the channels reported were performed with translational periodic boundaries in the stream wise direction of the flow which allow the values on the inlet and outlet boundaries to coincide. Further the pressure gradient was specified across the domain to drive the flow. To initialize the flow, a mean velocity is specified over the whole inlet plane upon which velocity fluctuations are imposed. The inlet mean velocities are derived from the experimental average values. The mean velocity was specified over the whole inlet plane and is computed by $U_{in} = {}^{Q}/_{A}$, where Q is the flow discharge of the channel and A is the cross sectional area of the inlet. In order to simplify slope changes and specify the pressure gradient the channel geometries were all created flat. The effects of gravity and channel slope implemented via a resolved gravity vector. Here the angle θ represents the angle between the bed of the channel and the horizontal, the gravity vector is resolved in x, y and z components as :

$$(\rho g \sin\theta, 0, -\rho g \cos\theta) \qquad \textbf{(5.25)}$$

Where θ = angle between bed surface to horizontal axis and tan θ=slope of the channel. Here, the x component causes the direction responsible for flow of water along the channel and the z component is responsible for creating the hydrostatic pressure upon the channel bed. From the simulation, "z" component of the gravity vector ($-\rho g \cos\theta$) is found to be responsible for the convergence problem of the solver.

5.3.5.2 Wall

The channel walls i.e. side walls and bottom are represented as non-slip walls. A no-slip boundary condition is the most common boundary condition implemented at the wall and prescribes that the fluid next to the wall assumes the velocity at the wall, which is zero i.e.

$$U = V = W = 0 \quad \textbf{(5.26)}$$

5.3.5.3 Free-Surface

For top free surface generally symmetry boundary condition is used. This specifies that the shear stress at the wall is zero and the stream wise and lateral velocities of the fluid near the wall are not retarded by wall friction effects as with a no-slip boundary condition. This condition follows that, no flow of scalar flux occurs across the boundary. Thus, there is neither convective flux nor diffusive flux across the top surface. In implementing this condition normal velocities are set to zero and values of all other properties outside the domain are equated to their values at the nearest node just inside the domain. Here the experimental bulk velocity of the flow is initially approximated as:

U = 0.569 m/s, V = 0, W= 0 and $\frac{\partial u}{\partial x} = 0$, for relative depth (Dr) =0.3

And

U=0.51 m/s, V=0, W=0 and $\frac{\partial u}{\partial x} = 0$, for Relative depth (Dr) =0.2

5.3.6 NEAR WALL MODELLING

Nearer to a no-slip wall, there are strong gradients in the dependent variables. Generally at boundary layer regions, rapid variation of flow variables occurs i.e. in viscous layer. Also in

boundary layer viscous effects on the transport processes are large. Further transition from viscous to buffer layer produces large variation within the flow features. Therefore, it is essential to imitate these changes in the discretization process to carry out simulation process successfully. Hence, near wall modeling is done to include these changes in flow features for this study. The representation of these processes within a numerical simulation raises the problems about the viscous effects at the wall and how to resolve the rapid variation of flow variables, which occurs within the boundary layer region. Experimental and numerical analysis have shown that the near-wall region can be subdivided into two layers. The flow will be stationary at the wall itself and therefore there will be a narrow boundary layer of laminar flow which is call as "viscous sublayer". At viscous sublayer, molecular viscosity plays a dominant role in momentum and energy transfer problem. Further away from the wall there is mixing process takes place and produces turbulence, is known as the "logarithmic layer". Finally, there exists a region between the viscous sublayer and the logarithmic layer which is called as the "buffer layer". At buffer layer the effects of molecular viscosity and turbulence are of equally significance. The Figure 5.10 exemplifies these subdivisions of velocity profile as the near-wall region, buffer and outer region of the flow.

Wall functions are the most popular technique to account wall effects. The mesh node next to the wall is placed in the turbulent boundary layer and a model of flow in that region is used for defining wall function. At that point the sets values of velocity, pressure and turbulent quantities are replaced the solution with the Navier-Stokes Equation. In CFX the wall-function approach is an extension of the method derived by Launder and Spalding (1974). The logarithmic nature of the velocity profile in open channels is well known as "log- law of the wall". Assuming that the logarithmic profile practically approximates the velocity distribution

near the wall and numerically computes the fluid shear stress as a function of the velocity at a given distance from the wall. This is known as "wall function". The Figure 5.11 illustrates wall functions. In the log-law region, the near wall tangential velocity is related to the wall shear stress τ_w by means of a logarithmic relation.

$$u^+ = \frac{U_t}{u_*} = \frac{1}{k} ln(y^+) + C \quad \textbf{(5.27)}$$

Where $y^+ = \frac{\rho \Delta y u_*}{\mu}$ **(5.28)**

$$u_* = \left(\frac{\tau_w}{\rho}\right)^{1/2} \quad \textbf{(5.29)}$$

Here $u^+$is the near wall velocity, u_* is the friction velocity, U_t is the known velocity tangent to the wall at a distance of Δy from the wall, y^+ is the dimensionless distance from the wall, τ_w is the wall shear stress, k is the von Kármán constant and c is a log-layer constant dependent on wall roughness. The execution of a wall function eliminates the need for very fine meshes at the time of discretization process nearer to the wall, which resolve the flow down to the wall.

However, when performing LES method, an extremely fine grids are required to resolve the viscous sub-layer down to a wall at normal distance y^+, where, $y^+ = (u_* y)/v$, y = depth at a point. Therefore LES directly computes the variables down to the wall without the application of a wall function. Even though LES does not replace the N-S equations with a wall function near the wall, it uses a wall-function approximation to make an estimate of u_* at the wall. This is accurate for numerically simulated open channel flows and involves fitting a log-law to the mean velocity profile and calculating a shear velocity from it. Thomas and Williams (1995a) adopt this method and draw comparison between $u^+$and y^+ for experiment, LES and Equation 5.27, for which all are comparable. Nezu and Rodi (1986) show a wall-function approximation to be

satisfactory for wide channels, and Gavrilakis (1992) suggest that the logarithmic profile (based on local shear velocity) found for turbulent flow in a square duct exhibits a logarithmic region similar to Equation 5.27. The profile for the channel simulated in Thomas and Williams (1995a) was considered intermediate between square duct and open channel.

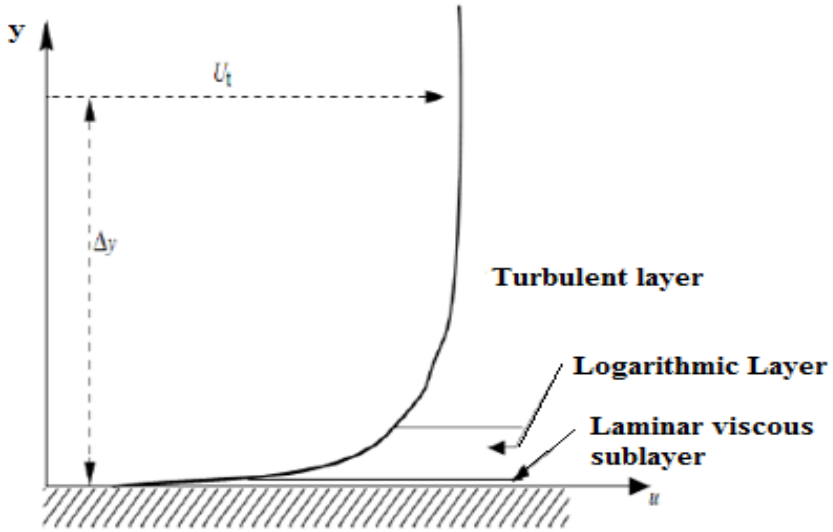

Figure 5.10. The subdivisions of the near-wall region.

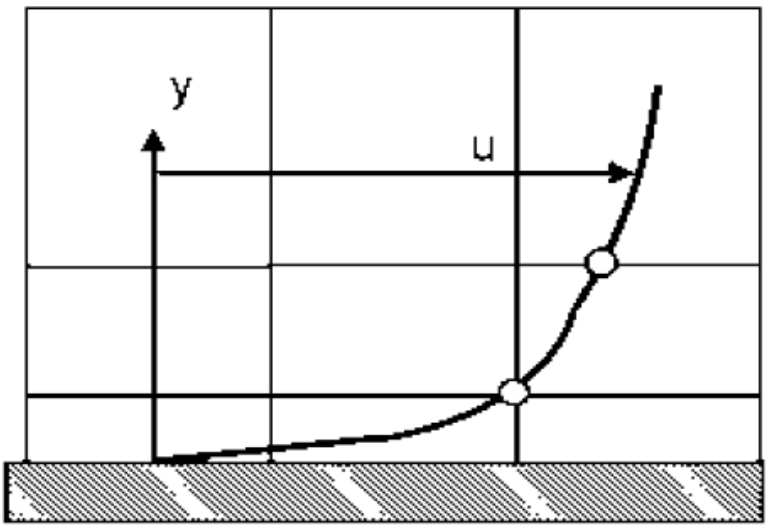

Figure 5.11 Wall functions used to resolve boundary layer.

VALIDATION AND VERIFICATION OF RESULTS

6.1. OVERVIEW

6.1.1 EXPERIMENTAL RESULTS

The experimental results concerning the distribution of velocity along the compound channel section, boundary shear along the wetted perimeter and flow has been presented in this chapter. Analysis is also done for depth averaged velocity and longitudinal velocity distribution in the converging compound channel with two different flow depth i.e. relative depth (Dr). Where Relative Depth (Dr) $= \frac{\text{Total depth } of\ water(H) - Height\ of\ main\ channel(h)}{\text{Total depth } of\ water(H)}$. Analysis of results is done for distribution of boundary shear stress in a non-prismatic converging compound channel and shear force results are derived accordingly for the relative depth (Dr) of 0.2. In this study, various flow variables are studied in a converging compound channel with five different sections, which are discussed separately below. The positions of different experimental five sections are clearly shown in Fig 6.1. Positions of five different sections are decided to analyze the effect of convergence of the flood plain in a non-prismatic compound channel. To see the effect of turbulence and boundary shear and to compare these effects two sections are taken outside the converging part. One is section 1 which is situated before the converging part and other section is taken after the converging part (section 5).Other three different sections are taken inside the convergence area. Section 2 is located just after the start of convergence and section 4 is taken just before end of convergence. Section 3 is situated in the middle of the converging part of the channel. Velocity measurements were carried out in the compound channel transition with the 55% compression of flood plain. The upstream flow conditions were subcritical and the Froude number range was from 0.45 to 0.573. The variation of flow rate was from 0.033 m^3 /s to

0.05 m^3/s. The Reynolds number Re varied from 32,129 to 52,085 representing the turbulent flow regime. The data obtained from Pitot tube measurements of the velocity were analyzed and velocity profiles were drawn. And then experimental analyzed results were compared and validated with numerical analyzed or CFD simulated results. The overall summary of experimental runs for the converging compound channel is given in Table-6.1.

Table 6.1. Hydraulic parameters for the experimental runs

Relative Depth $(Dr) = \frac{H-h}{H}$ **= 0.3**	**Position**	**Distance from upstream**	**Width Ratio** $\left(\alpha = \frac{B}{b}\right)$	**Discharge (Q)**	**Velocity(V)**	**Froude No.** (Fr=$\frac{V}{\sqrt{gD}}$)	**Reynolds No.** (Re=$\frac{UR}{10^{-6}}$)
	Sec 1	**11.95 m**	**1.8**	**0.050**	**0.5646**	**0.573**	**42403.22**
	Sec 2	**12.05 m**	**1.75**	**0.049**	**0.5654**	**0.571**	**42547.45**
	Sec 3	**12.42 m**	**1.4**	**0.047**	**0.5912**	**0.562**	**47572.41**
	Sec 4	**12.79 m**	**1.05**	**0.041**	**0.6130**	**0.547**	**52085.25**
	Sec 5	**12.89 m**	**1**	**0.039**	**0.6127**	**0.545**	**52033.34**
Relative Depth $(Dr) = \frac{H-h}{H}$ **= 0.2**	**Sec 1**	**11.95 m**	**1.8**	**0.0372**	**0.506**	**0.566**	**32293.5**
	Sec 2	**12.05 m**	**1.75**	**0.0362**	**0.505**	**0.564**	**32129.97**
	Sec 3	**12.42 m**	**1.4**	**0.0347**	**0.533**	**0.559**	**36799.38**
	Sec 4	**12.79 m**	**1.05**	**0.0331**	**0.573**	**0.550**	**43918.81**
	Sec 5	**12.89 m**	**1**	**0.0330**	**0.580**	**0.549**	**45311.63**

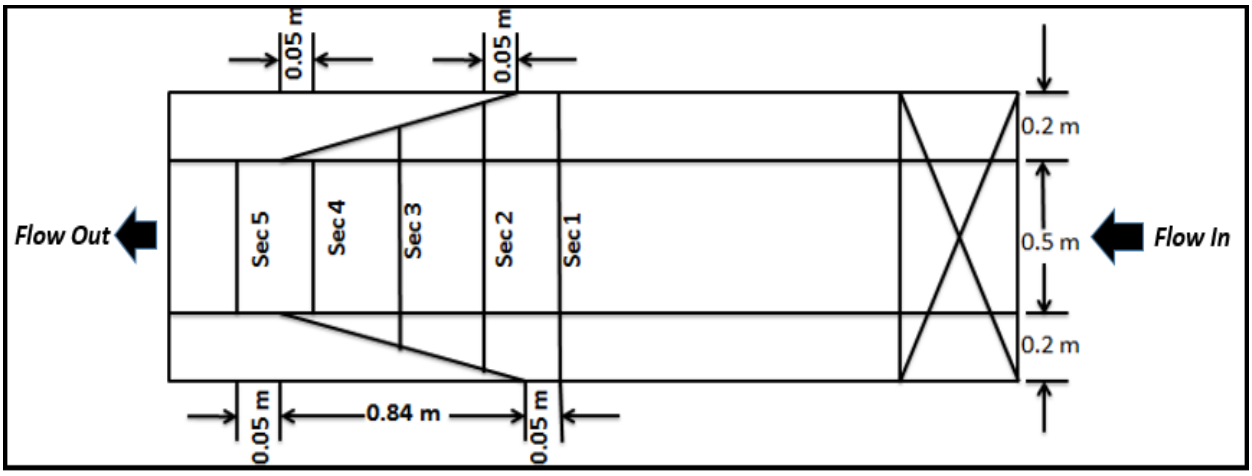

Figure 6.1. Position of Five Different Experimental Section

6.1.2 NUMERICAL ANALYSIS RESULTS

Generally, experimental and theoretical analysis are the main tools for finding out the solution of open channel flow problems to meet the needs of field requirements. In recent times CFD techniques are being used extensively to solve the flow problems. In this study, a few simulations were carried out by using the commercial code namely ANSYS to simulate the present experimental investigation. Simulation was carried out to predict the velocity distribution, streamlines along the channel and boundary shear stress distribution along the channel bed. Here Large Eddy Simulation model is used for turbulence modeling. The LES equations are discretized in both space and time. In this study the algorithms adopted to solve the coupling between pressure and velocity field is PISO which is the pressure implicit splitting operators use in Fluent (Issa 1986). A non-iterative solution method PISO is used to calculate the transient problem as it helps to converge the problems faster. Here the advection property is discretized with bounded central difference scheme and transient terms are discretized with Second order scheme. Courant number (Cr) is controlled between 0 - 0.5 and the transient time step size is taken as 0.0001 s. After that, the equation is iterated over and over till desirable level

of accuracy of 10-3 of residual value is achieved. When the residuals of the discretized transport equation reach a value of 0.001 or when the solution do not change with further iterations, the numerical solution is converged. To promote the convergence of the solution the changing variables are controlled during the calculations. For the simulations with an unsteady solver, the difference in the mass flow rates at the velocity inlet and pressure outlet is monitored to be less than 0.01% in the final solution. Furthermost, a number of extra time steps are added to verify the steadiness of the flow field in the final solution.

The numerically simulated results are compared with the experimental results. Here mean bulk velocity is calculated using the formulation:

$$U_b = \frac{\int udA}{A} \qquad \textbf{(6.1)}$$

Where, U_b = Bulk Velocity along Stream-line of flow. U = streamline velocity at any point, A = Cross-section area of the channel. The composite Manning‘s friction factor is calculated from Manning's equation.

In this study, various flow variables are studied in a converging compound channel with five different experimental sections for two different flow depths, which are discussed separately below. CFD simulation was carried out for two relative depth (Dr) of flow i.e. Dr=0.3 and 0.2.The positions of five different sections where the simulation results were studied are clearly shown in Figure 6.2. Positions of five different sections are decided to analyse the effect of convergence of the flood plain in a non-prismatic compound channel.

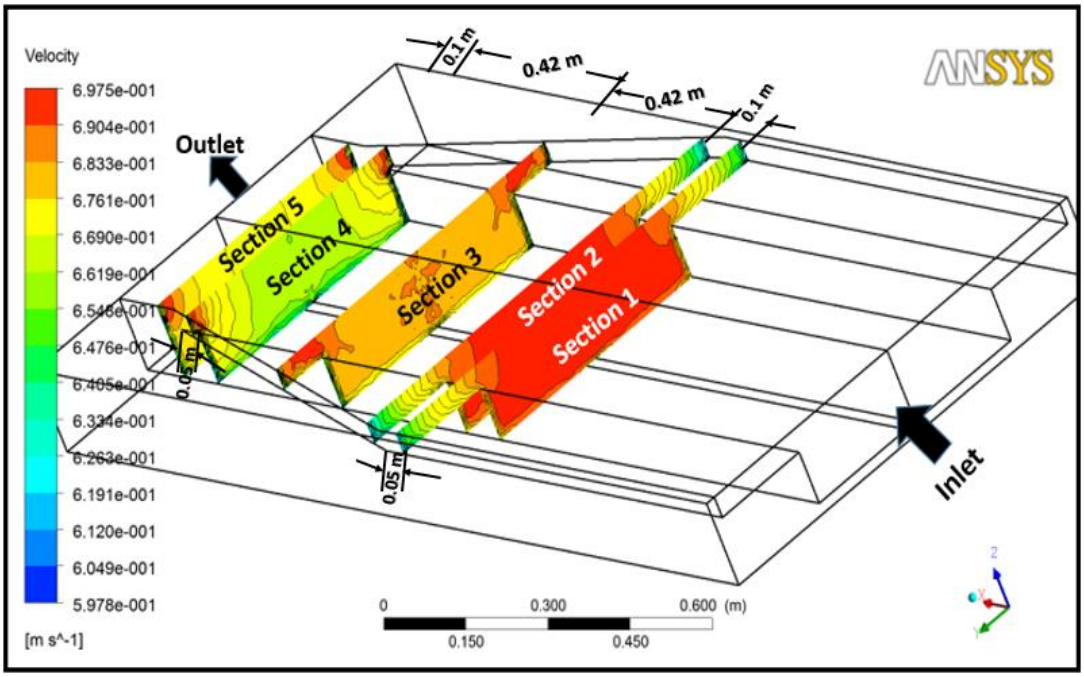

Figure 6.2. Velocity contour of five different experimental sections

6.2. LONGITUDINAL VELOCITY DISTRIBUTION IN CHANNEL DEPTH

To compare the effect of convergence and to analyse the secondary flow structure in between the channel, velocity is measured at different positions experimentally by using Pitot tube, a velocity measuring instrument. In the experiments, the local velocities are measured at nodes located at different depths and widths in each section. As flood plain width decreases gradually the vertical distributions of the velocity with the logarithmic law at five different sections are shown for validation of experimental results with CFD simulation. In all of the sections, the vertical velocity distributions obey the logarithmic distribution law, except near the interface zone. The results showed that the velocity gradient at interface zone decreases by taking depth ratio (Dr) =0.3 and 0.2. If the roughness ratio also increased on the floodplain, the velocity gradient at interface zone will be increased. Towards a longitudinal direction in a non-

prismatic channel, at interface zone the velocity gradient decreases gradually by taking the constant depth ratio 0.2 or 0.3. In all of the tests, the velocity gradient after the end of convergence reach was much higher than the other reach in a non-prismatic channel.

Here the local velocities were also measured across the entire cross section, laterally every 50 mm and vertically at 0.2h, 0.4h, 0.6h, 0.8h, 0.9h level where "h" is the height of water for a particular section in the channel at five selected sections, at the beginning before convergence (section1) and end after convergence (section 5) and at three sections (section 2, 3 and 4) inside the converging flume portion. In this experiment section 3 is situated at middle of the convergence part of the flume. The different position of experimentation of a particular section is shown in Figure 6.3. The velocity distributions at five measurement cross-sections for convergence angle of $\emptyset = 13.39°$ and Dr =0.3 and 0.2 are shown in Fig. 6.4 and 6.5 accordingly. Here, Figure 6.4 and 6.5 are clearly shown that the CFD analysed results are validated the experimental results. The velocity distributions were then integrated over the flow depth to calculate the discharge and the depth-averaged velocity.

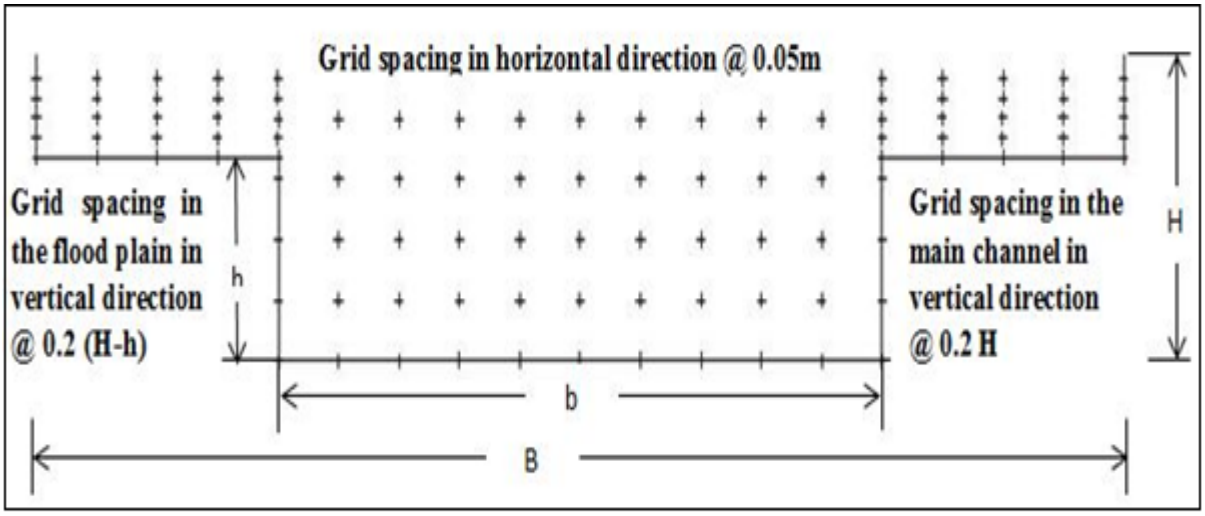

Figure 6.3. Different Position of experimentation of a particular section

The distribution of longitudinal and transverse velocity components is given on Figure 6.2.2 and 6.2.3 for 5 cross-sections (section 1 through section 5) of the 0.84 m length narrowing case having converging angle 13.39^{o}, for relative depth Dr = 0.3 and 0.2. This shows clearly the effects of the contraction : (1) the velocity increases along the channel, as the cross-section area decreases; (2) the flow on the floodplain causes a transverse component towards the main-channel, corresponding to the water forced to leave the floodplain; (3) as a result, due to the inflow of slower water from the floodplain, there is slight decrease of the longitudinal velocity component in the main-channel, near the interface zone and (4) the transverse component of the velocity, above the bank level, develops until the main-channel centre line.

6.2.1. Validation of Numerical results with Experimentation for Relative Depth (Dr) =0.3

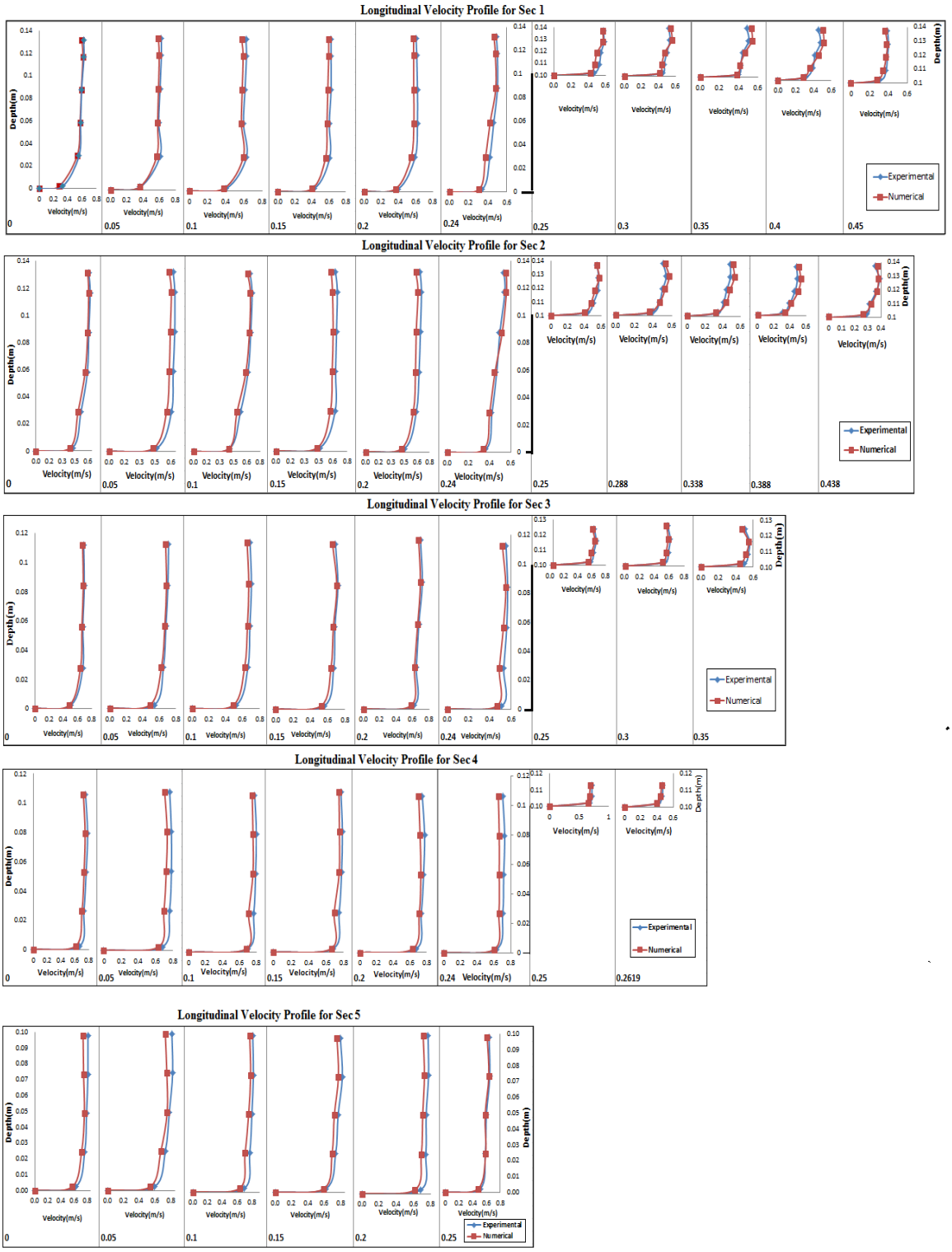

Figure 6.4. Longitudinal Velocity Profile of five different sections for Dr 0.3

6.2.2. Validation of Numerical simulation with experimentation for Relative Depth (Dr) =0.2

Longitudinal velocity profile of Section 1

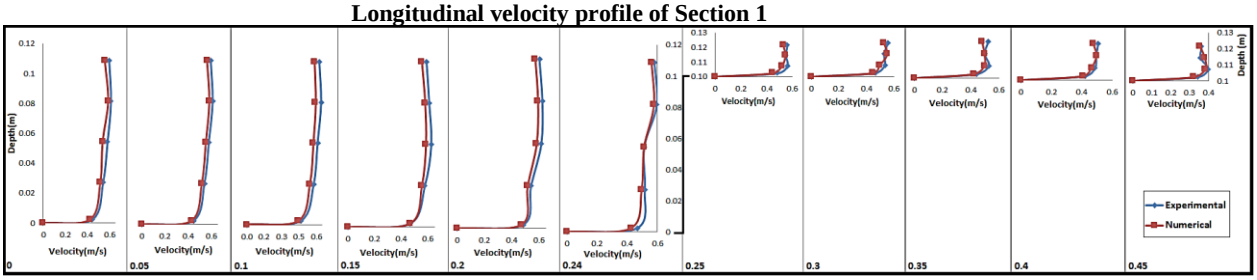

Longitudinal velocity profile of Section 2

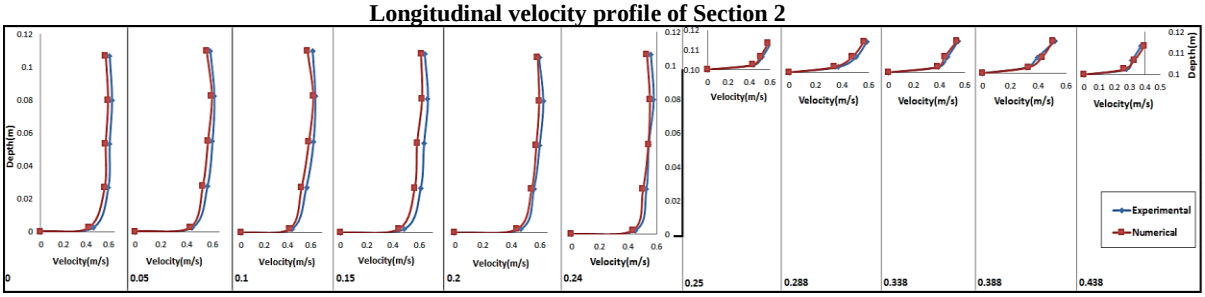

Longitudinal velocity profile of Section 3

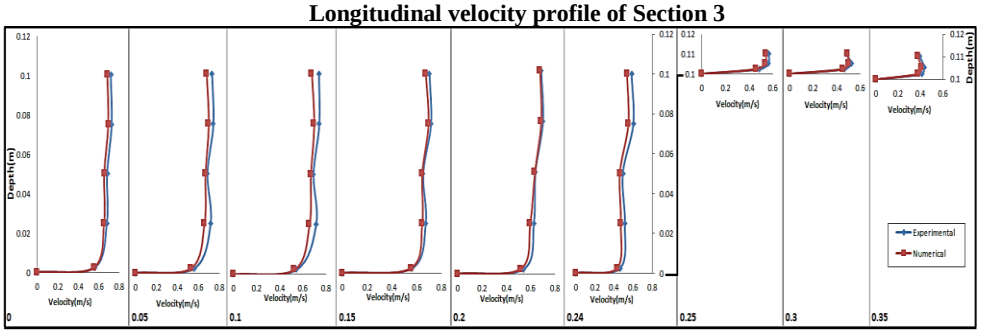

Longitudinal velocity profile of Section 4

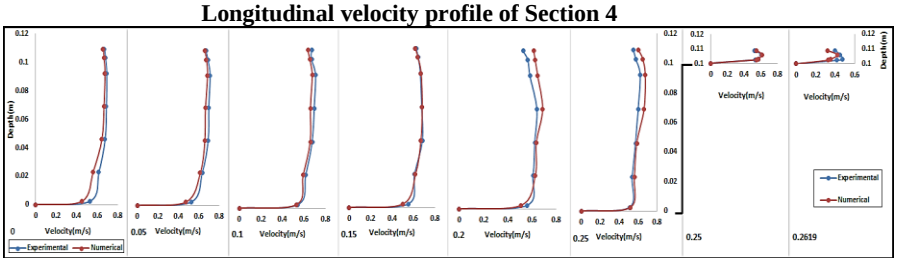

Longitudinal velocity profile of Section 5

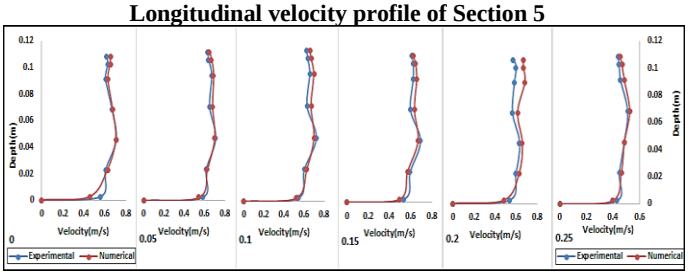

Figure 6.5. Longitudinal Velocity Profile of five different sections for Dr 0.2

6.3 DEPTH AVERAGE VELOCITY DISTRIBUTION FOR DIFFERENT CHANNEL DEPTH

6.3.1 Experimental Results

The depth-averaged velocity distribution in a cross section was measured at different experimental sections along the flume (Figure 6.1). Point depth-averaged velocity measurements were made laterally each 50 mm at a depth of $0.4H$ from the bed in the main channel and $0.4(H-h)$ on the floodplains. The experimental results of these measurements for convergence angle of $\theta = 13.39°$ and two different relative depths of 0.3 and 0.2 are shown in Figure 6.6 and 6.7. Here Figure 6.6 shows the comparison of depth average velocity of relative depth 0.3 at five different sections along the converging compound channel flume and Figure 6.7 indicates the comparison of depth average velocity of relative depth 0.2 at particular five different sections along the experimental flume.

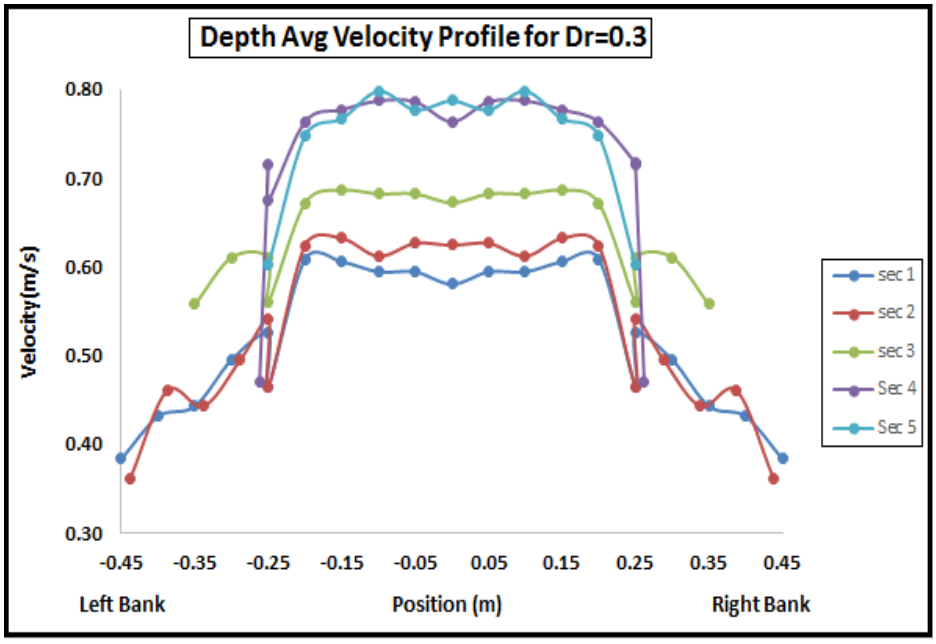

Figure 6.6. Comparison of Depth Average Velocity Profile for Dr 0.3

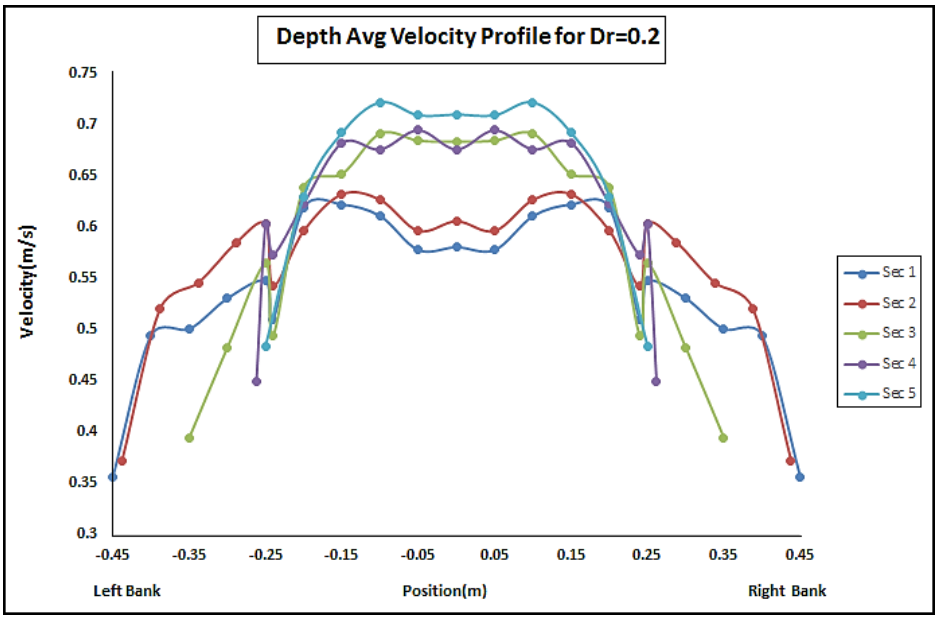

Figure 6.7. Comparison of Depth Average Velocity Profile for Dr 0.2

6.3.2 Numerical Validation

Lateral depth-averaged velocity distributions are calculated and compared with the CFD results for two different relative depth 0.3 and 0.2. Figure 6.8 through 6.12 shows comparison of numerical analyzed depth average velocity profile results with experimental calculated depth average velocity profile results of section 1 to section 5 accordingly for relative depth of 0.3 of the particular flume and Figure 6.13 through 6.17 shows the validation of depth average velocity profile for relative depth of 0.2 of section 1 to 5 accordingly by using experimental method and CFD simulation. As shown in these Figures, in the non-prismatic converging compound channel with the same angle of convergence, decreasing the width ratio leads to an increase in the difference between the mean velocity in the main channel and floodplain. When the floodplain

width decreases, the velocity has to increase in the downstream part of the floodplain, while another part of the discharge is transferred to the main-channel.

6.3.2.1 Validation of Numerical Results for Relative Depth of 0.3

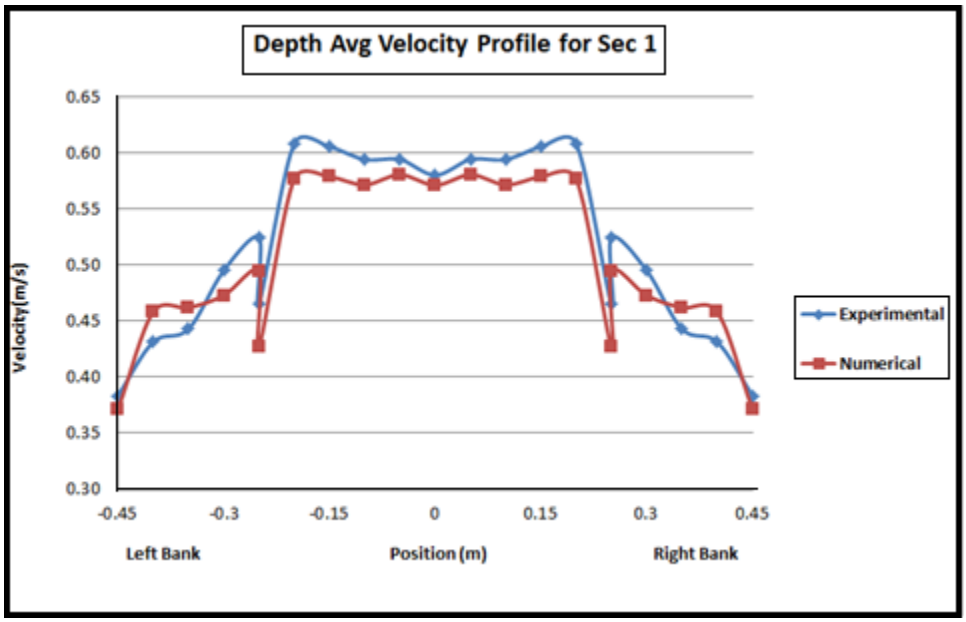

Figure 6.8. Comparison of Depth Average Velocity profile of Section 1

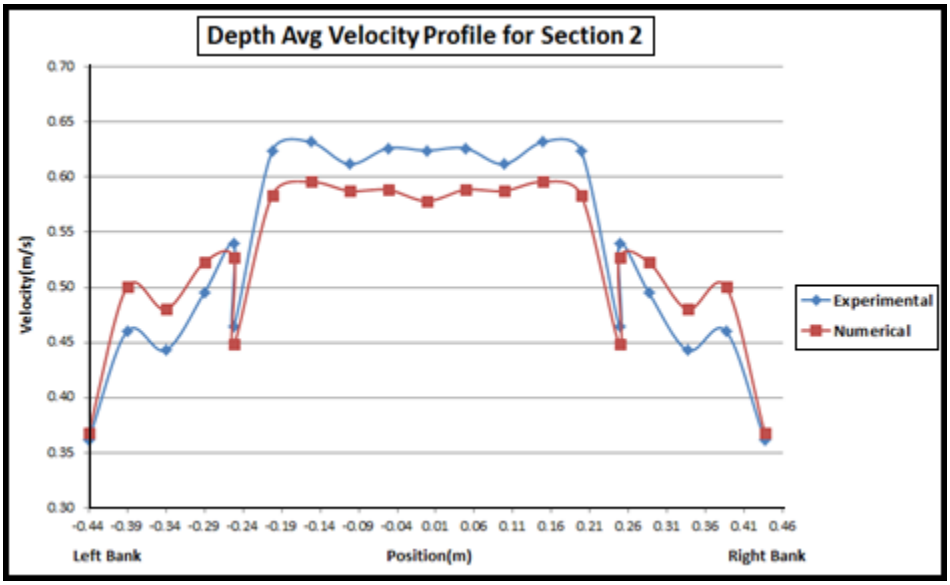

Figure 6.9. Comparison of Depth Average Velocity Profile of Section 2

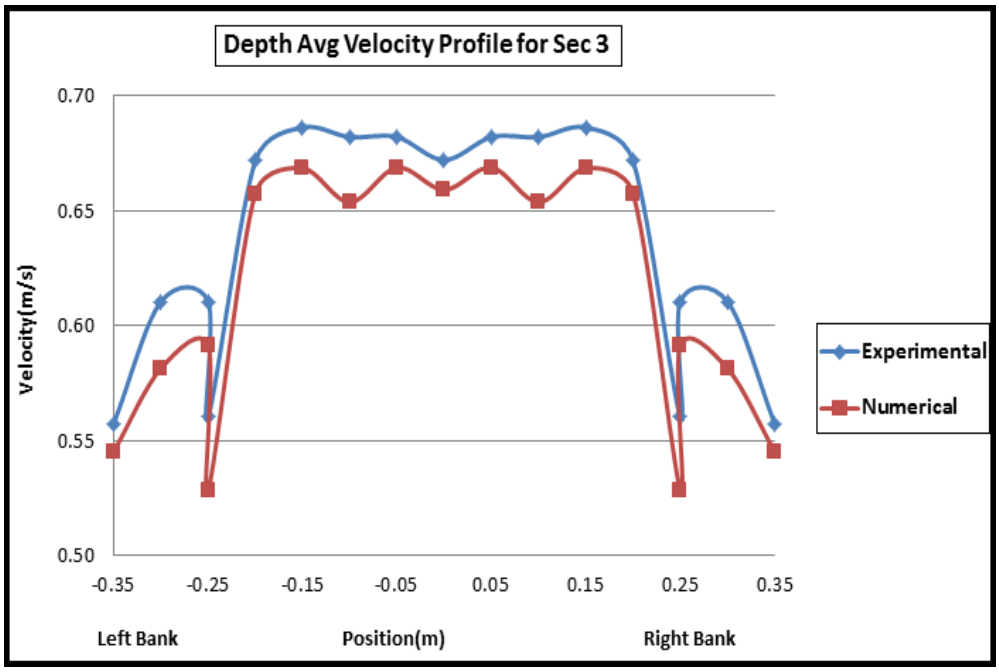

Figure 6.10. Comparison of Depth Average Velocity Profile of Section 3

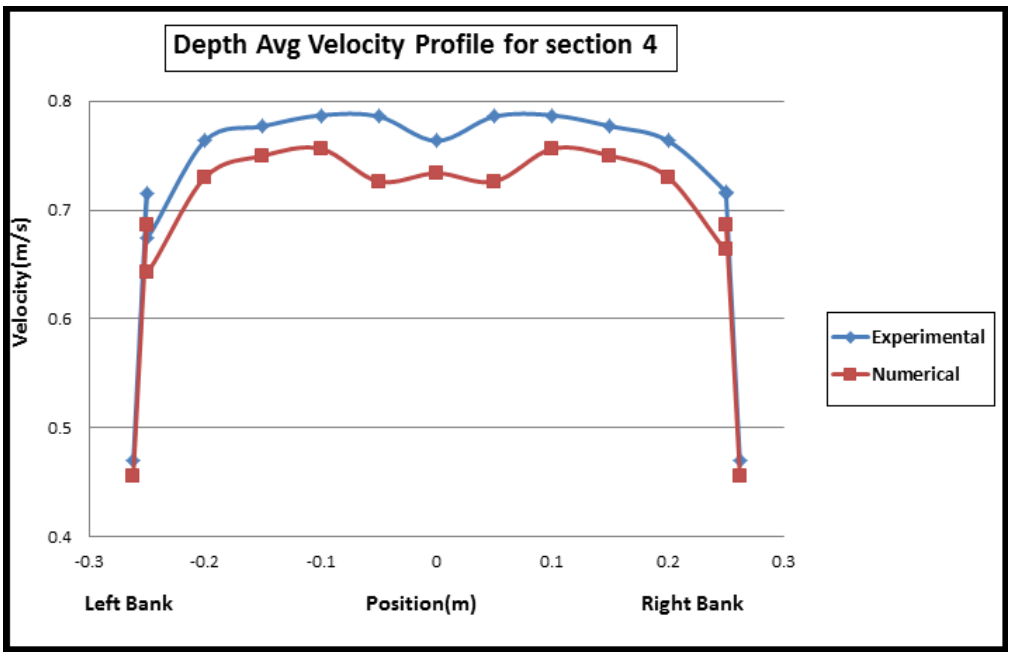

Figure 6.11. Comparison of Depth Average Velocity Profile of Section 4

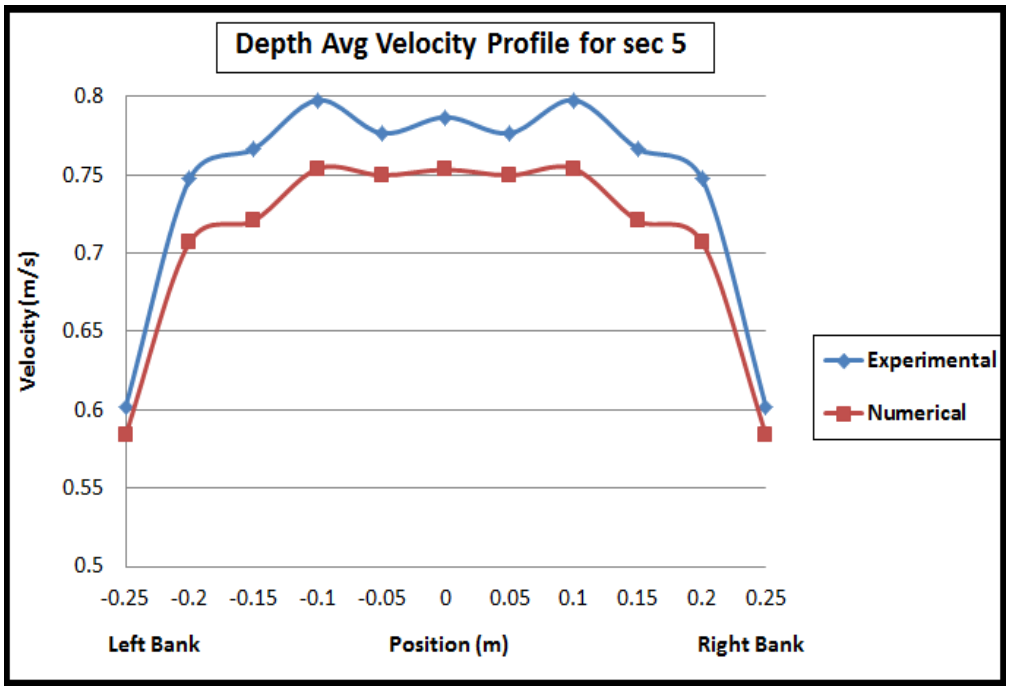

Figure 6.12. Comparison of Depth Average Velocity Profile of Section 5

6.3.2.2 Validation of Numerical Results for Relative Depth of 0.2

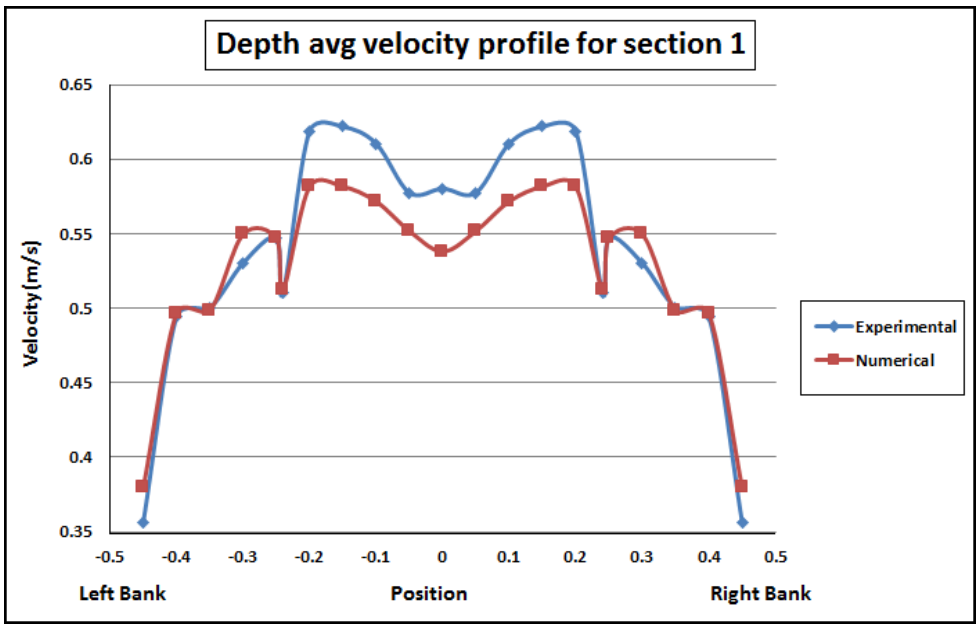

Figure 6.13. Comparison of Depth Average Velocity Profile of Section 1

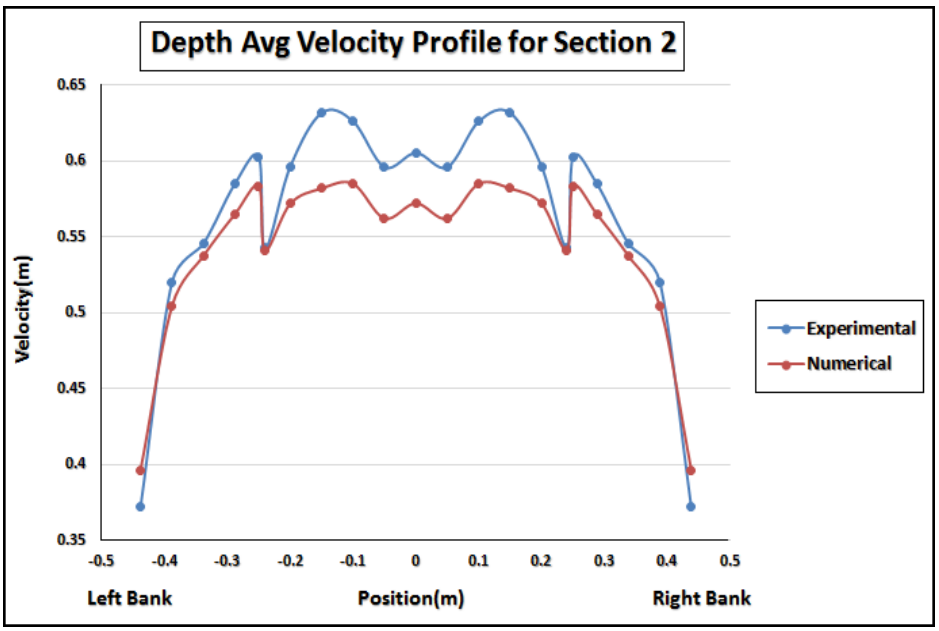

Figure 6.14. Comparison of Depth Average Velocity Profile of Section 2

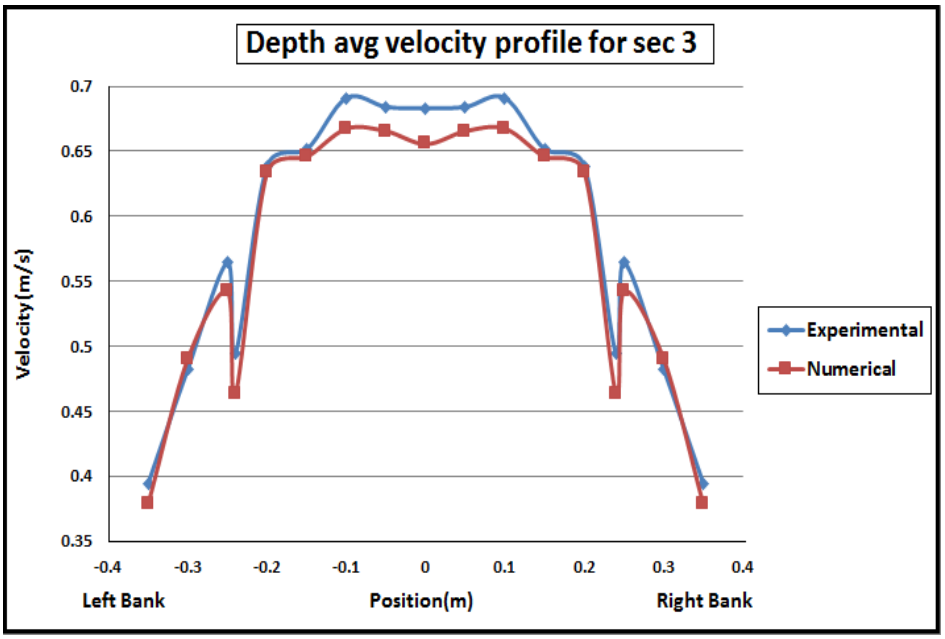

Figure 6.15. Comparison of Depth Average Velocity Profile of Section 3

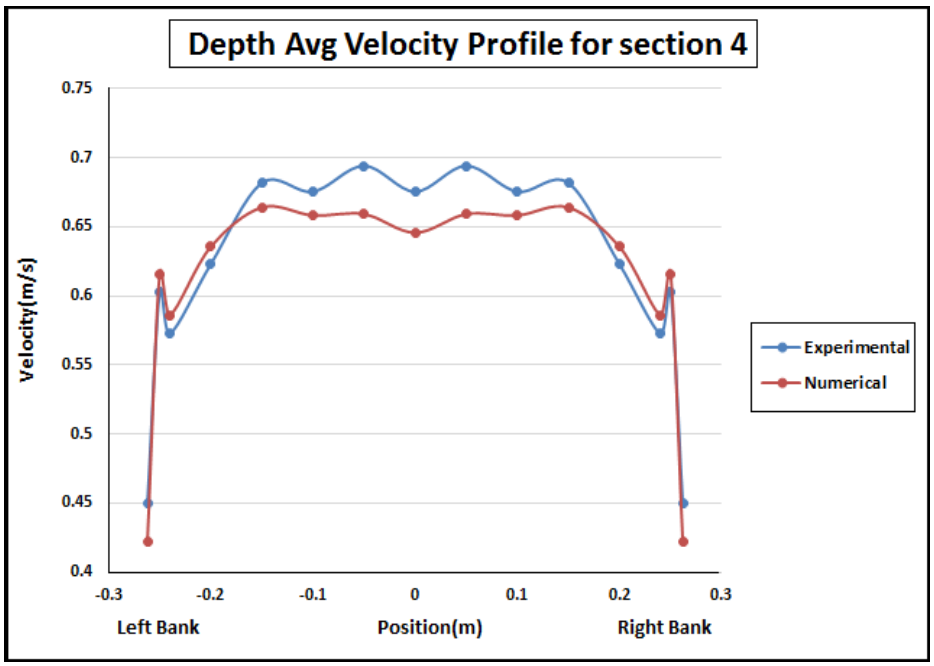

Figure 6.16. Comparison of Depth Average Velocity Profile of Section 4

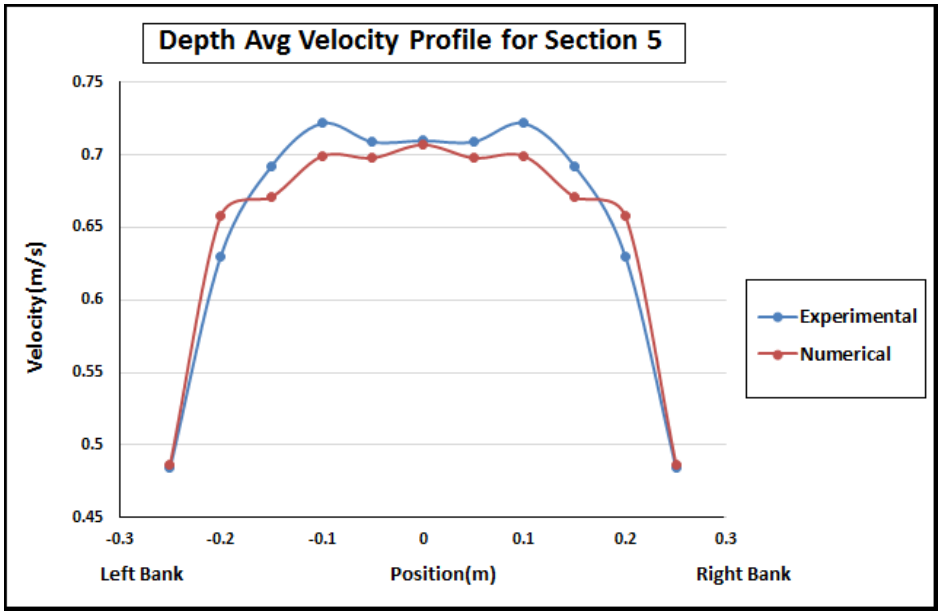

Figure 6.17. Comparison of Depth Average Velocity Profile of Section 5

It obvious that the depth-averaged velocity distributions show good symmetrical patterns in different measurement sections. The Figures show the following effects of the contractions on the velocity distributions, (a) the numerical simulation gives good agreement with the experimentation, (b) the depth average velocity increases along the converging part of the flume, (c) the velocity in the second half of the converging reach increases significantly, (d) for high relative depth, the effects of the lateral flow that comes into the main channel causes the velocity to increase locally near the main channel walls, especially in the second half of the convergence reach.

6.4 CONTOURS OF LONGITUDINAL VELOCITY

Figures 6.18 through 6.22 shows the longitudinal velocity contours at different sections along the convergence portion for 0.3 relative depth of flow and Figures 6.23 through 6.27 show the longitudinal velocity contours for relative depth (Dr)=0.2 at five different experimental sections. As section 1 is located before the convergence, the velocity distribution is symmetric (similar to straight compound channels). As previously mentioned, there is negligible secondary flow at the entrance of the convergence (section 2). However, at this section (section 2), under the influence of the convergence, there is a one-way radial flow directed towards the centre of the channel, making the velocity distribution asymmetric. So the high-velocity zone tends to the centre of the channel. This trend continues up to the section 3. Along the compression of the flood plain of the channel by the expansion of the major and minor secondary flows, it can be seen that at sections 3(middle of convergence) and 4(just before end of convergence) contours of the longitudinal velocity shift and the high velocity zone moves further towards the outer wall and the channel convergence. And at the section after the convergence (section 5), the high

velocity zone is completely separated from the centre and transferred to the outer wall and the channel bed. Comparison of velocity contour between experimental data and numerical analysis of different sections are shown in Figures 6.18 through 6.22 respectively for Dr 0.3. Similarly Figures 6.23 through 6.27 shows comparison of both results.

6.4.1 Comparison of Velocity Contours having Relative Depth of flow 0.3

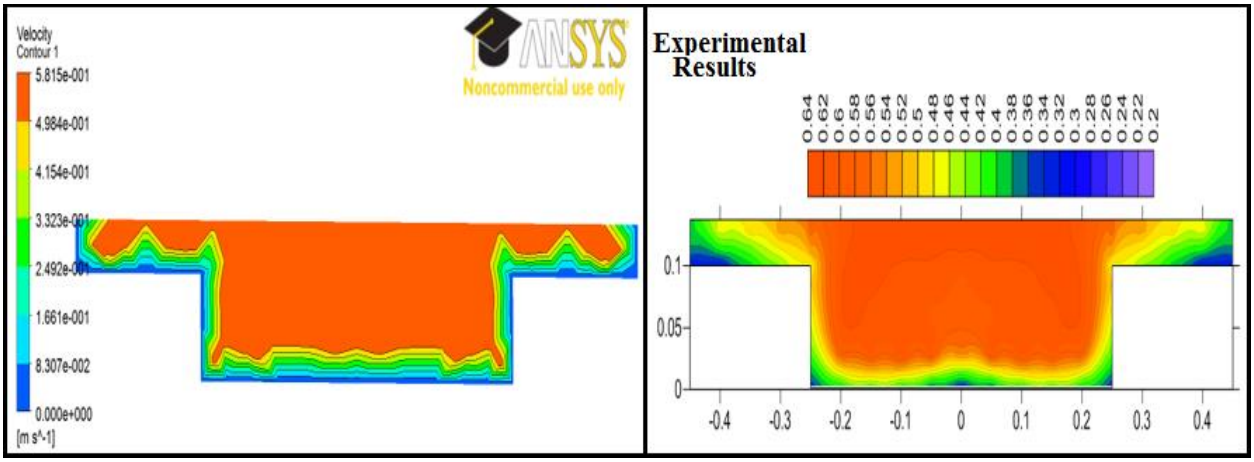

Figure 6.18. Comparison of Velocity Contour of Section 1

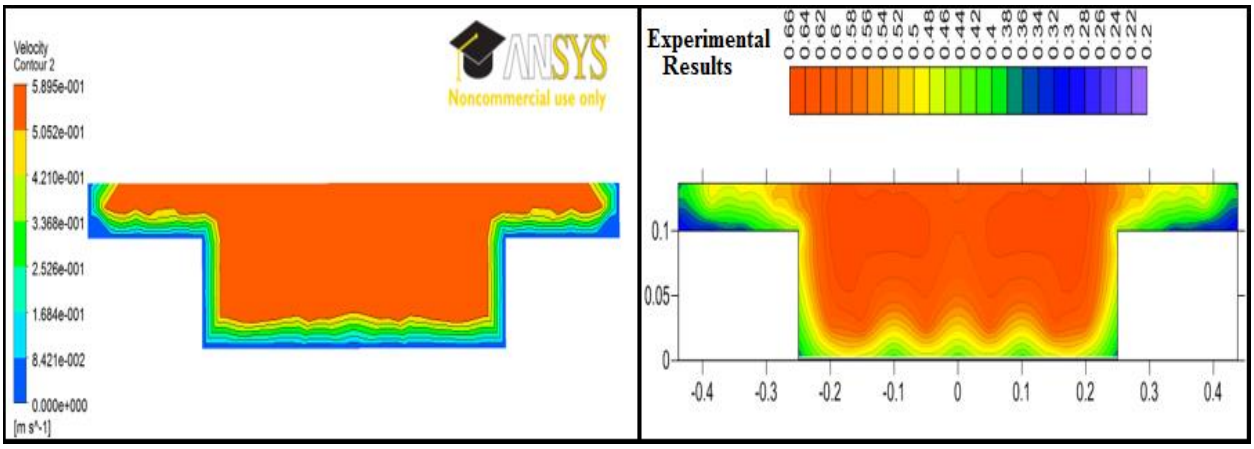

Figure 6.19. Comparison of Velocity Contour of Section 2

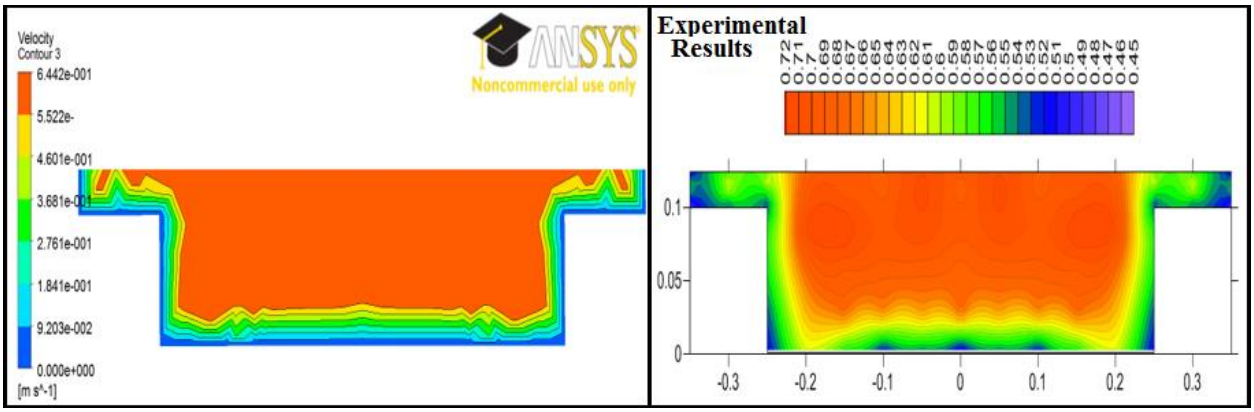

Figure 6.20. Comparison of Velocity Contour of Section 3

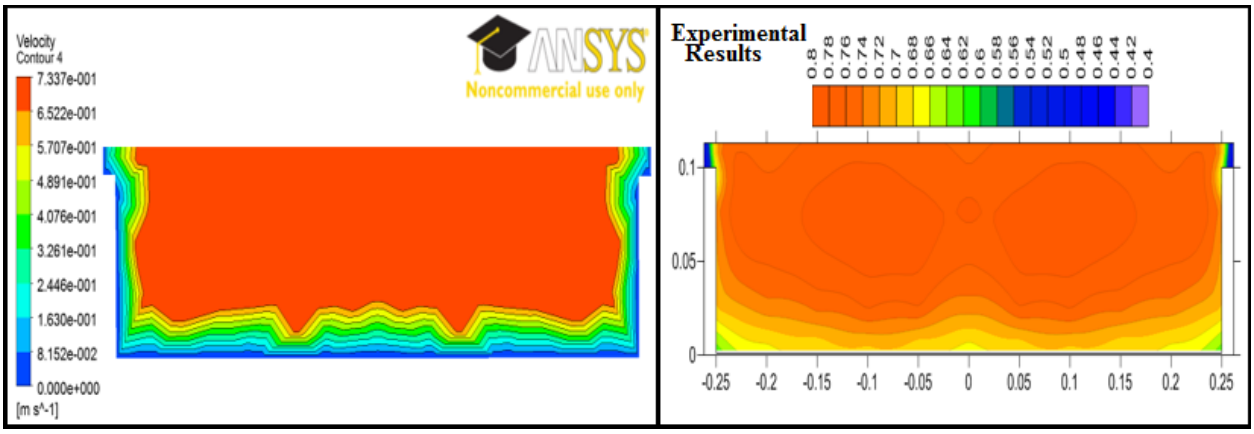

Figure 6.21. Comparison of Velocity Contour of Section 4

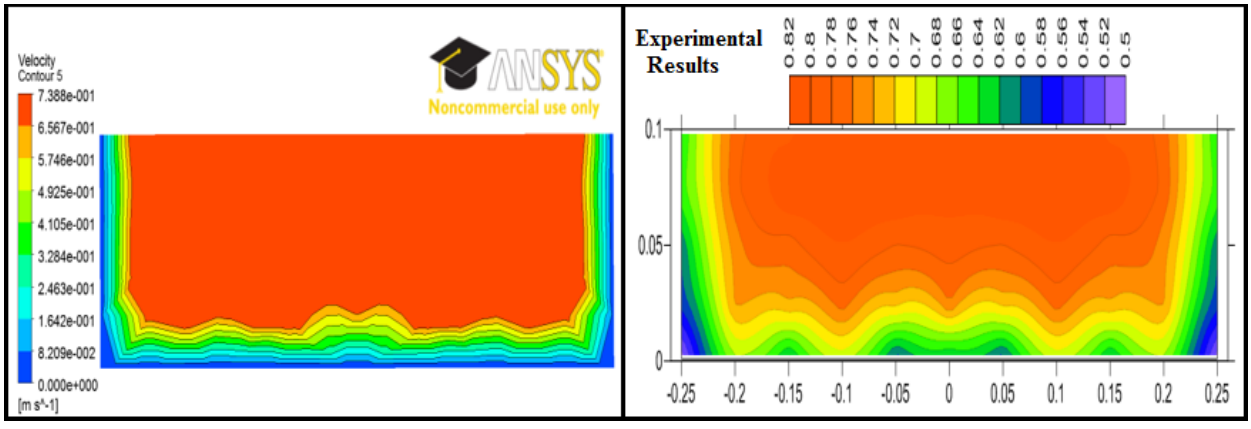

Figure 6.22. Comparison of Velocity Contour of Section 5

6.4.2. Comparison of Velocity Contours for relative depth of flow 0.2

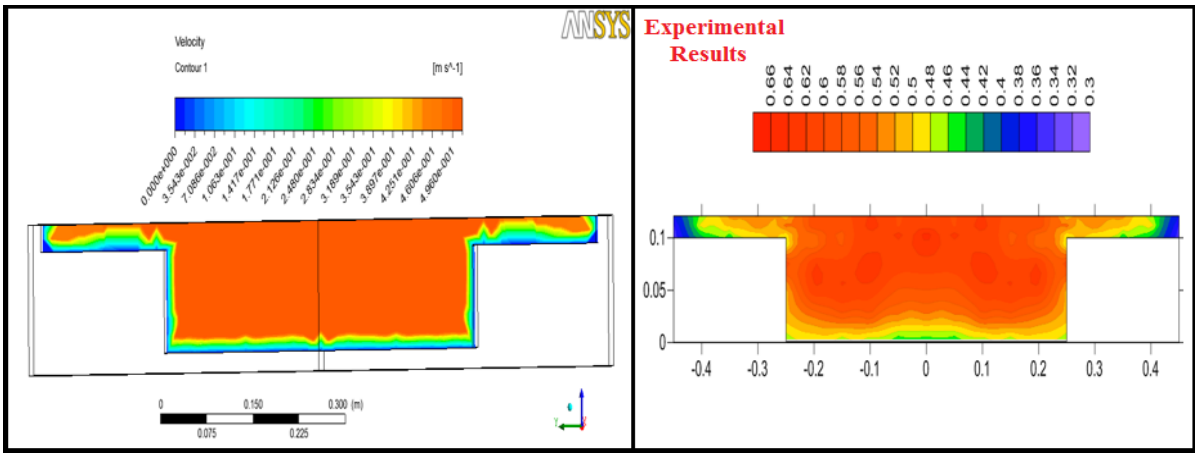

Figure 6.23. Comparison of Velocity Contour of Section 1

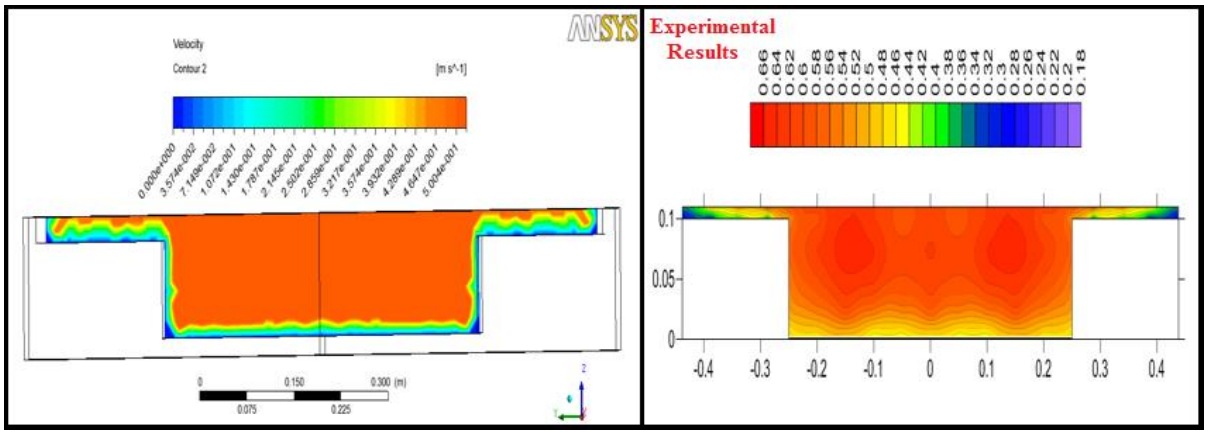

Figure 6.24. Comparison of Velocity Contour of Section 2

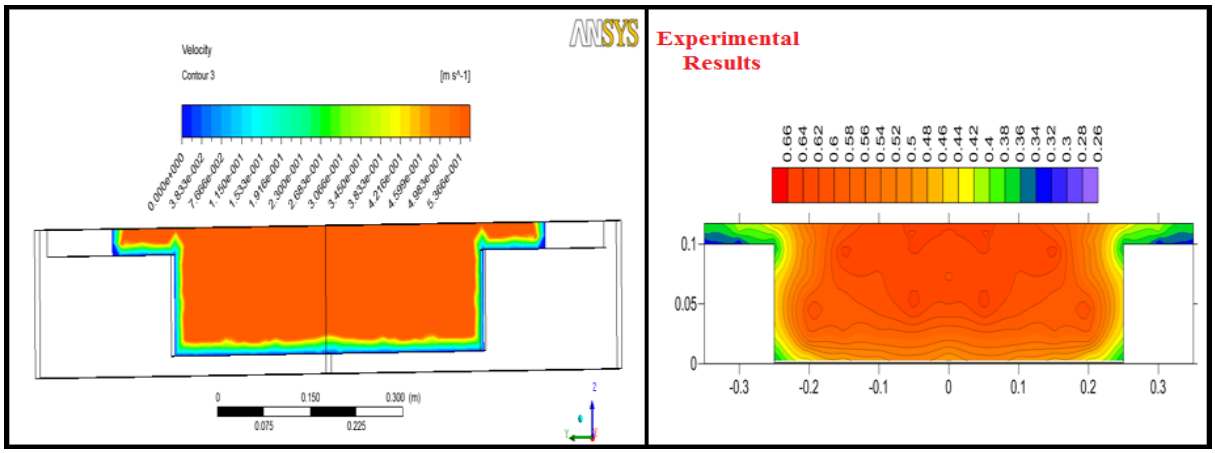

Figure 6.25. Comparison of Velocity Contour of Section 3

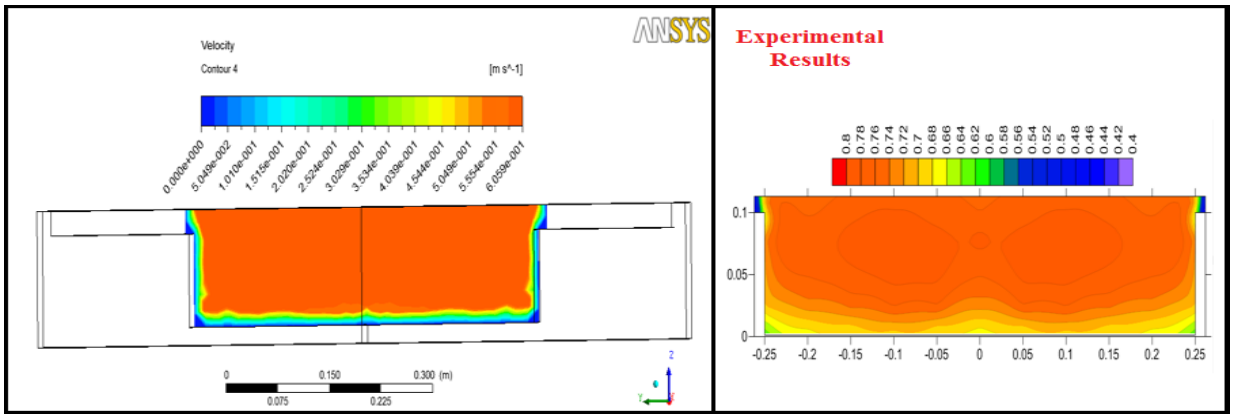

Figure 6.26. Comparison of Velocity Contour of Section 4

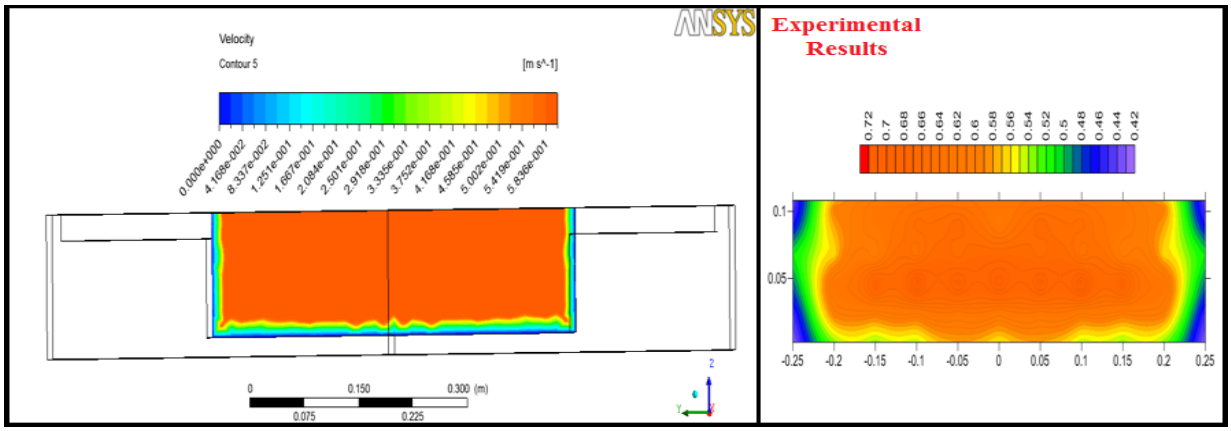

Figure 6.27. Comparison of Velocity Contour of Section 5

6.5. STREAMLINES ALONG THE CONVERGENCE

In Figure 6.28, the streamline of a non-prismatic compound channel with converging flood plain is shown by taking the 0.15 m water level or having depth average velocity 0.3 and Figure 6.29 shows the streamline of the non-prismatic converging compound channel for depth average velocity of 0.2. Figure 6.30 shows the streamline at free surface and axis symmetry of the channel half section having 0.2 relative depth of flow. As seen in Figures 6.28 and 6.29, the streamlines get close to each other at the water surface, due to the major and minor secondary flows at water surface. The flow direction on the floodplains is obviously forced by the convergence angle. This direction is also observed in the downstream cross-section, for the

velocities at the limit of the floodplain. The slight outwards component of the bottom velocity in the downstream section confirms this secondary flow. In this state, the direction of both secondary flows (major and minor ones) is towards the middle of the channel. At the middle of the channel the flow maintain streamlines almost follow the channel curvature. At the convergence of the channel, streamlines move inward direction, due to the convergence direction of the major secondary flow at the channel bed (with stronger flow) and the weakness of the minor secondary flow in this area. In this type of channels, the streamlines collide at the interface of main channel and flood plain.

6.5.1 Simulation Result for Relative Depth (Dr) 0.3

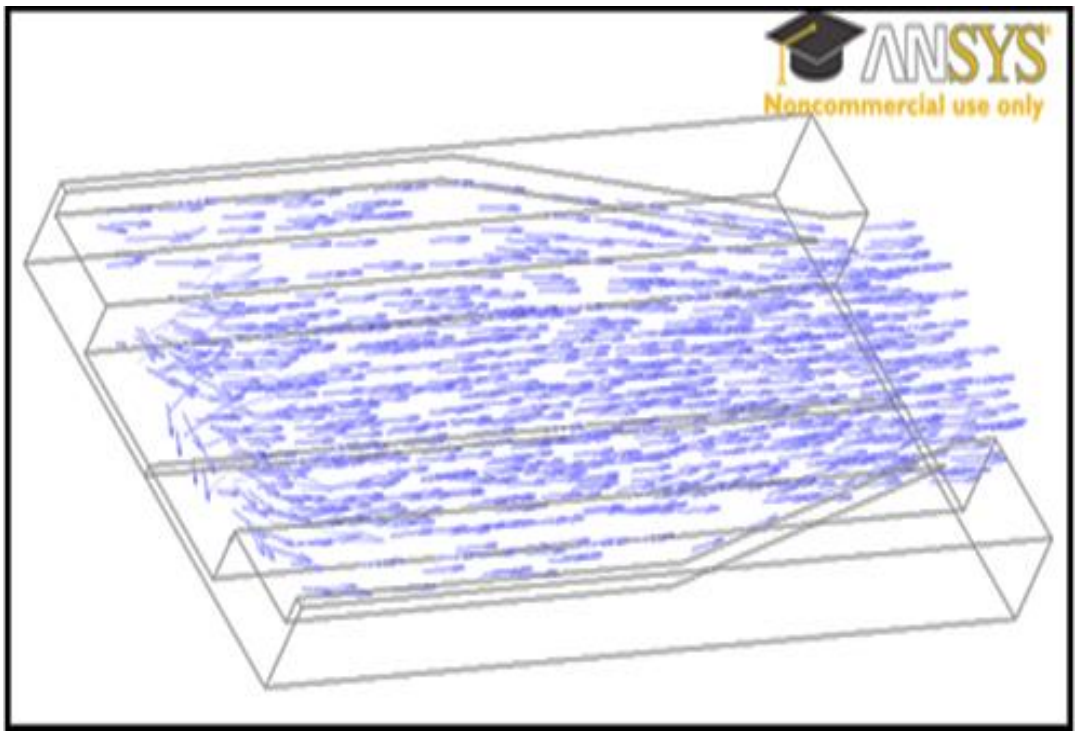

Figure 6.28. Streamline along the convergence for Dr=0.3

6.5.2 Simulation Result for Relative Depth (Dr) 0.2

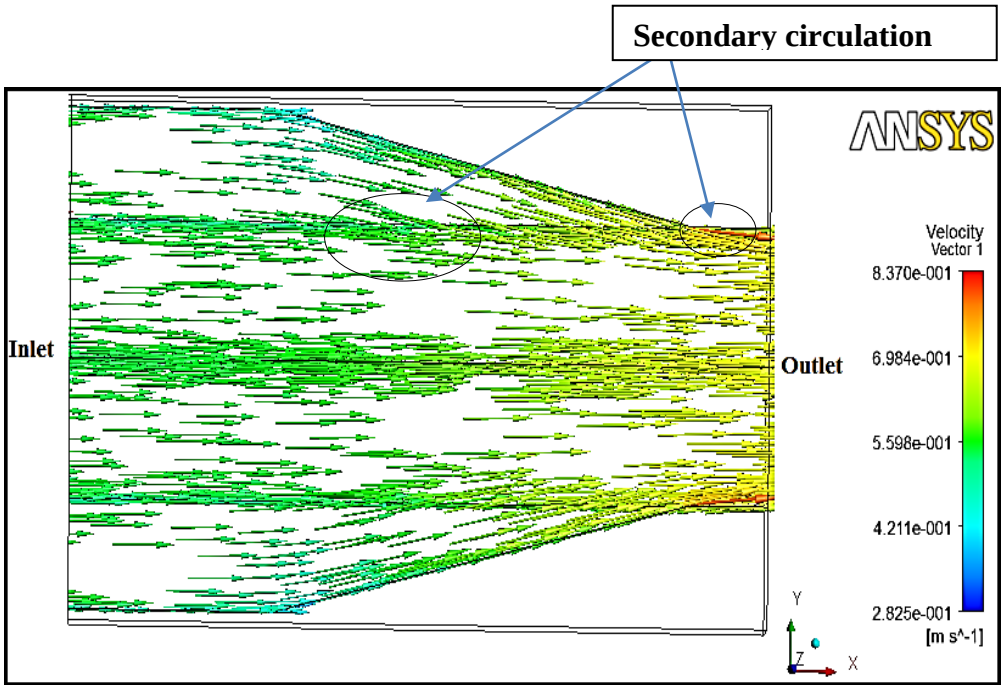

Figure 6.29. Streamline along the convergence for Dr=0.2

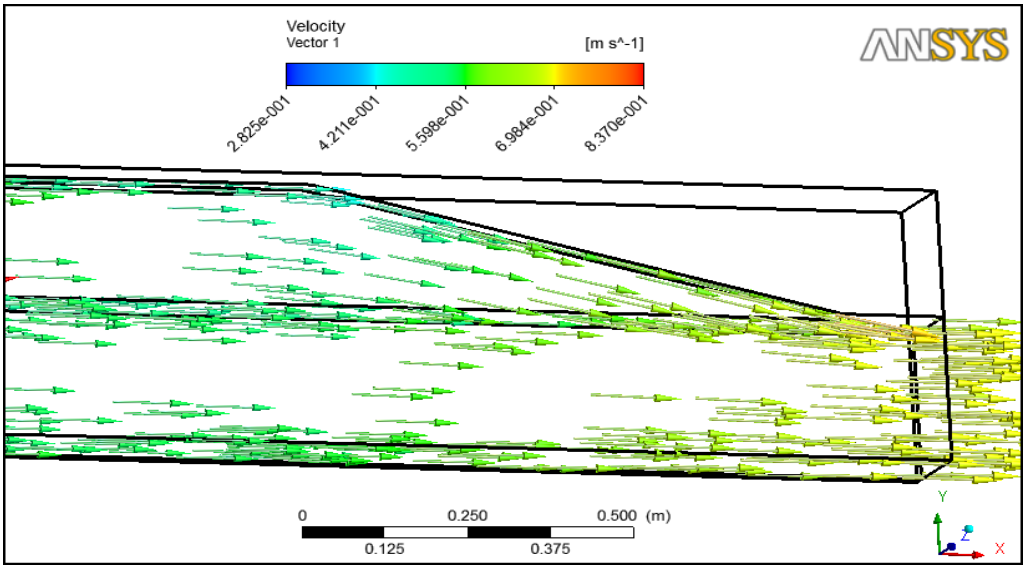

Figure 6.30. Streamline along the convergence of the channel half section

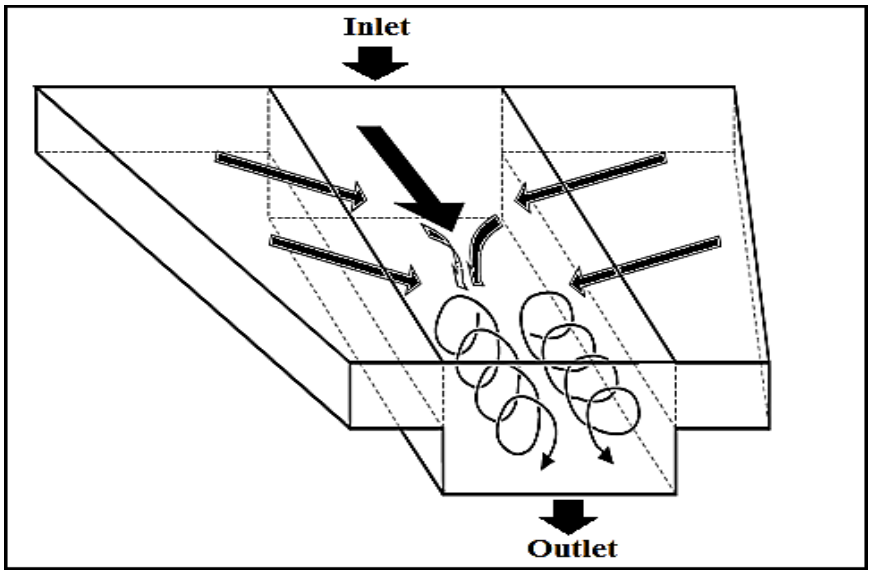

Figure 6.31. Schematic view of the flow structure in a compound channel with converging floodplains (Bousmar D,2004)

All these observations on the flow structure are generalized on Figure 6.31 as: (1) due to the symmetrically converging floodplains, the transverse flow currents are forced from the floodplain to the main-channel; (2) these currents enter the main-channel and plunges to the channel bottom around the centre-line as the experimental channel is symmetry

6.3. BOUNDARY SHEAR STRESS DISTRIBUTION

In hydraulic engineering, measuring of boundary shear stress distribution is very important for scour, bed and bank protection, sediment transport and the design of hydraulic structures in channel transition. There are various methods to determine boundary shear stress. Here, three methods will be employed to compare the results with each other. Chow (1959) used the average shear stress formula at the channel bottom.

$$\tau = \gamma RS \qquad \textbf{(6.2)}$$

Here, τ = boundary shear stress, γ= Unit weight of water, R= hydraulic radius, S =slope of the energy gradient line. Except for uniform wide open channel flow and closed pipe flow, the boundary shear stress is not uniformly distributed along the wetted perimeter. So, it is necessary to determine local boundary shear stress in open channel. Boundary shear stresses are generally small in magnitude and accurate measurements are difficult. The shear within the boundary layer thickness can be calculated using the formula, (Schlichting, 2000),

$$\tau = \mu \frac{du}{dy} \quad \textbf{(6.3)}$$

Here, τ = shear stress, μ = molecular viscosity, du =velocity and dy = distance of the point from the bed.

Later the logarithmic law was used to calculate shear velocity outside viscous sub-layer and from shear velocity relation, shear stress was calculated. The logarithmic equation can be written, irrespective of smooth, transitional or rough bed, in the form of, (Hollingshead, 1972)

$$\sqrt{\frac{\tau}{\rho}} = u_\tau = \frac{1}{A} \frac{u_2 - u_1}{log\left(\frac{y_2}{y_1}\right)} \quad \textbf{(6.4)}$$

Here, u_1 and u_2 are time averaged velocity measured at y_1 and y_2 distances from the bed, A =5.75 constant. Shear velocity u_τ is obtained by solving the right hand side of the above equation and by equating the LHS with RHS of equation (6.4) the shear stress τ is determined.

6.6.1. Discussion of Experimental Results:

Local boundary shear stress measurements were also made using a Pitot tube. These measurements were carried out at the particular five sections where distribution of velocity measurements were taken. Local boundary shear stress was measured around the wetted channel

perimeter 20 mm vertical intervals on the walls and 50 mm transverse intervals on the bed for 0.2 relative depth of flow(Dr= 0.2). Experimental local boundary shear stresses were numerically integrated over the wetted perimeter to calculate the boundary shear forces acting on each sections of the non-prismatic compound channel. Figures 6.32 through 6.36 show the Distribution of boundary shear stress at five different sections along the channel bed.

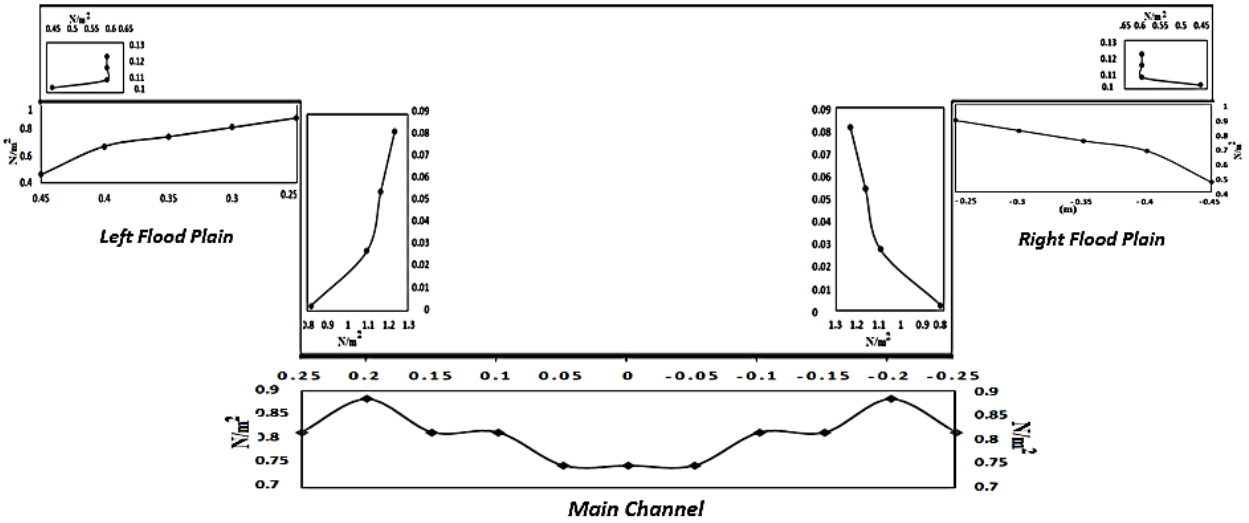

Figure 6.32. Boundary Shear Distribution at Section 1 for Dr 0.2

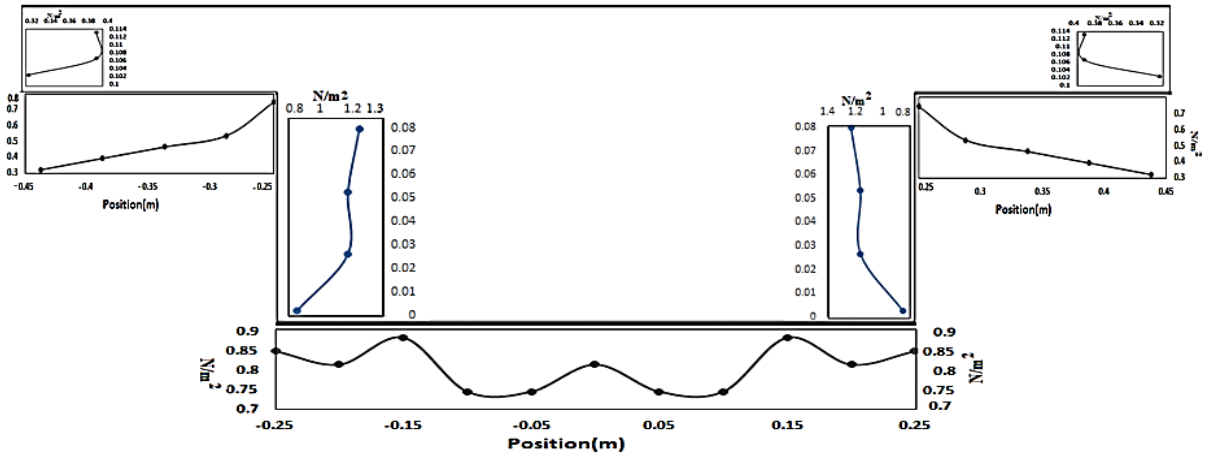

Figure 6.33. Boundary Shear Distribution at Section 2 for Dr 0.2

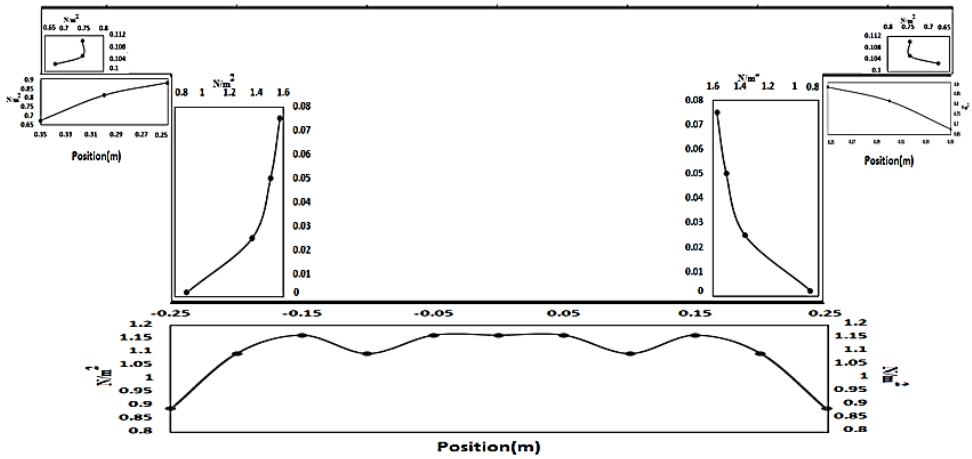

Figure 6.34. Boundary Shear Distribution at Section 3 for Dr 0.2

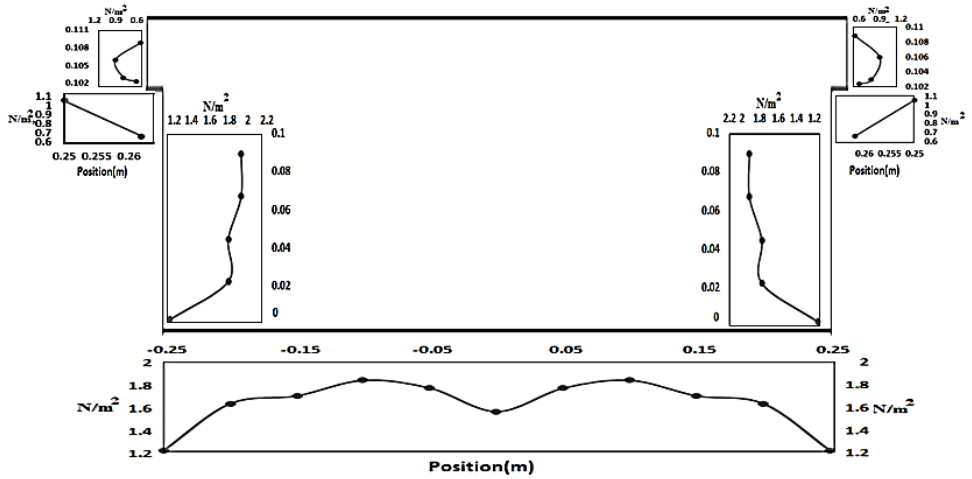

Figure 6.35. Boundary Shear Distribution at Section 4 for Dr 0.2

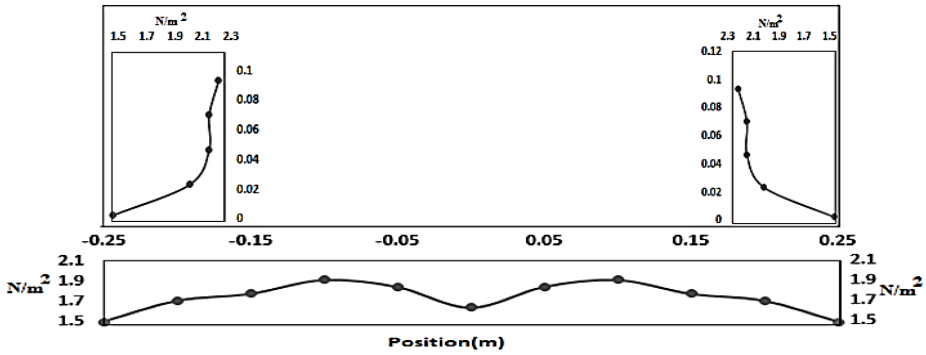

Figure 6.36. Boundary Shear Distribution at Section 5 for Dr 0.2

6.6.2. Analysis of Boundary Shear Distribution by Numerical (CFD) Simulation:

After CFD simulation, the distribution of the non-dimensional bed shear stress $\left(\frac{\tau}{\tau_{avg}}\right)$ is obtained and presented in Figure 6.37. The pattern of boundary shear distribution is found to be distributed evenly with the experimental results. The actual distribution of bed shear stress in experimental results attains two peak one at flood plain and other at the main channel and the simulation result has also attained the same pattern. The boundary shear stress distribution shows that the peaks can be observed both side of the junction of the main channel and flood plain. The average bed shear stress distribution in main channel is found to be lesser than the flood plain.

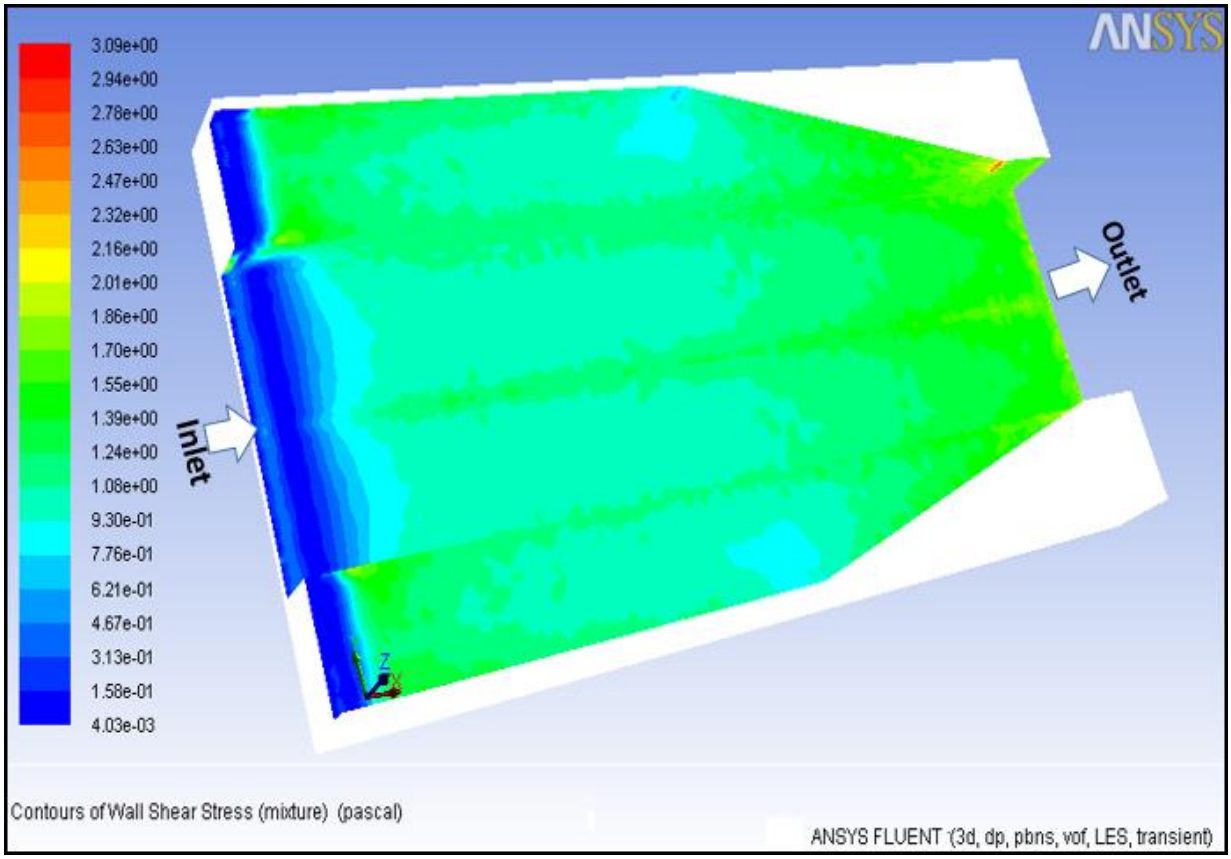

Figure 6.37. Boundary Shear Stress distribution along the channel bed

CONCLUSIONS AND FURTHER WORK

7.1 CONCLUSIONS

In the present study, the experimental and numerical modelling of the flow pattern at a non-prismatic compound channel with a converging flood plain has been carried out. On the basis of the investigations concerning flow, velocity distribution, depth average velocity distribution and boundary shear stress distribution along the channel bed for two different relative depth(0.2 Dr and 0.3 Dr) in a non-prismatic converging compound channel having 13.39° converging angle, the point to point observations are drawn for different experimental sections. Findings of the work are as follows:

- Three dimensional modelling of the free surface flow in non-prismatic compound channel having narrowing floodplains as relatively complex geometry have been successfully verified with a mesh refinement studies and validated with experiments.
- Experimental results related to longitudinal velocities are compared with the corresponding values obtained from Numerical analysis for 5 different sections i.e. sec-1, sec-2, sec-3, sec-4, sec-5 of the non-prismatic compound channel for two different relative depth of flow and concluded that the variation of longitudinal velocity in main channel region is found to be less as compared to that in the flood plain region.
- By experimental and numerical simulation it is clearly concluded that, in main channel region the velocity magnitude is nearly constant after the solid boundary however at flood plain region there is rapid variation found and maximum velocity occurs just below the

free surface of the converging compound channel because a boundary layer is formed due to interaction of air and top water surface which retards the flow velocity of the top layer.

- On the basis of velocity contour it is concluded that there is a good agreement between the results of the CFD analysis with that of experimental results.
- From velocity profiles of sec-1 to sec-5, it is observed that the velocity of flow goes on increasing with decrease in the channel width ratio.
- From the experiment it is found that for a given discharge the depth of flow is comparatively decreasing as the flow moves through the converging part resulting in increase of velocity at each section.
- From depth-average velocity profile, it clearly conclude that the numerical analysis give good results for five individual sections and are slightly underestimating the results drawn by experimentation with negative errors of more or less than 5%.
- From both experimentation and numerical analysis it is observed that there is difference in main channel and flood plain velocity at the junction due to formation of secondary circulation which retards the velocity at that section. The value and changes of velocity are larger in the convergent channel sections (section 2 through 5) than in the uniform channel section (section 1).
- Form the velocity contour it is shown that maximum velocity occurs at the central region of the compound channel and it gradually goes on decreasing towards the boundary.
- In the converging compound channel, a region with maximum bed shear stress is observed at the exit of converging channel, but at the end of the convergent region (at sec 5), boundary shear stress shows higher values than along the channel bed in the compound channel.

- From the numerical simulation it is detected that as compared to other turbulence model, LES turbulence model gives good agreement with the experimental data for a compound channel as it considers the near wall modelling.
- Using LES, the computed secondary flow pattern in the non-prismatic compound channel hardly deviates from the measured flow pattern and the turbulence is reproduced correctly.

7.2 SCOPE FOR FUTURE WORK

The present work leaves a wide scope for future investigators to explore many other aspects of a non-prismatic compound channel analysis. The future scope of the present work may be summarized as:

1. Modeling by conventional methods is not reliable due to its instinct one dimensional modeling of flow. Though the computational methods effectively capture intricate turbulent structures in flow but require huge computer resources. Thus analytical methods based on mechanism of energy transportation, momentum and continuity equations can be solved with least approximation.
2. The channel here is smooth and rigid. Further investigation for the distribution of boundary shear stress may also be carried out for mobile beds and by roughening the channel bed.
3. LES and other turbulence closure models like k-ε, k-ω, RSM etc. can be used to simulate various channel geometry with different hydraulic conditions.
4. LES modeling for other hydraulic and geometrical conditions can be carried out.
5. The result can be compared with data of straight channel and diverging channel and further the work can be extended to natural channels and other laboratory channels with different relative depths, convergence angle, channel geometry and surface conditions.

6. Further investigations can be done to study depth-averaged velocity in vertical and lateral directions and develop models using analytical and numerical approaches which are more convenient than conventional methods.
7. Proceedings on lateral velocity distribution can be done on mobile bed to represent real situation prevailing in natural rivers; so that sediment load transport and boundary shear distribution can be determined to its accuracy.
8. Distribution of boundary shear stress components in lateral and vertical directions can be evaluated which has implications for the sediment transport studies.

REFERENCES

- Ackers P. Hydraulic design of two-stage channels, In: Proceedings of the institution of civil engineers, water, maritime and energy, London: Thomas Telford, 4 (1992). pp. 247–57.
- Ackers P. Stage–discharge functions for two-stage channels: the impact of new researches, Inst Water Environ Manage, 7 (1993), pp. 52–61.
- Akhtari AA, Abrishami J. Effect of Non Submerged Vanes on Separation Zone at Strongly-curved Channel Bends, a Laboratory Scale Study, Water and Wastewater, 2009
- ANSYS, Ansys-CFX, version 13.0 Southpointe, Canonsburg PA, USA, 2011.
- Ansari K, Morvan HP, Hargreaves DM. Numerical investigation into secondary currents and wall shear in trapezoidal channels, Journal of Hydraulic Engineering, 137 (2011):pp. 432-440
- Beaman F. Large Eddy Simulation of open channel flows for conveyance estimation, Ph.D. thesis, University of Nottingham, 2010.
- Bodnar T, Prihoda. Numerical simulation of turbulent free-surface flow in curved channel Flow, turbulence and combustion, 76 (2006):pp. 429-442
- Booij R. Measurements and large eddy simulations of the flows in some curved flumes, J. Turbulence, 4 (2003):pp. 1-17
- Bousmar D, Zech Y. Momentum transfer for practical flow computation in compound channels, Journal of Hydraulic Engineering, 125 (1999):pp. 696-706
- Bousmar D, Zech Y. Periodical turbulent structures in compound channels, River Flow International Conference on Fluvial Hydraulics, Louvain-la-Neuve, Belgium, 2002:pp. 177-185

- Bousmar D, Wilkin N, Jacquemart J, Zech Y. Overbank Flow in Symmetrically Narrowing Floodplains, Journal of Hydraulic Engineering,130 (2004):pp. 305-312
- Bousmar D, Riviere N, Proust S, et al. Upstream discharge distribution in compound-channel flumes, Journal of Hydraulic Engineering,131 (2005):pp. 408-412
- Cater JE, Williams JJR. Large eddy simulation of a long asymmetric compound open channel, Journal of Hydraulic Research,46 (2008):pp. 445-453
- Chaturvedi RS. Expansive sub-critical flow in open channel transitions, J. Civil Engineering Division,43 (1962):pp. 447
- Chien K Y. Predictions of Channel and Boundary-Layer Flows with a Low-Reynolds-Number Turbulence Model, AIAA Journal, 20 (1982): pp. 33-38
- Chlebek J. Modelling of simple prismatic channels with varying roughness using the SKM and a study of flows in smooth non-prismatic channels with skewed floodplains, University of Birmingham, 2009
- Chlebek J, Bousmar D, Knight DW, Sterling M. A comparison of overbank flow conditions in skewed and converging/diverging channels, River flow international conference, 2010:pp. 503-511
- Cokljat D, Younis BA. Second-order closure study of open-channel flows, Journal of Hydraulic Engineering,121 (1995):pp. 94-107
- Cao Z, Meng J, Pender G, Wallis S. Flow Resistance and Momentum Flux in Compound Open Channels, Journal of Hydraulic Engineering,132 (2006): pp. 1272-1282
- Dixon AG, Walls G, Stanness H, Nijemeisland M, Stitt EH. Experimental validation of high Reynolds number CFD simulations of heat transfer in a pilot-scale fixed bed tube, J. Chemical Engineering, 200 (2012):pp. 344-356

- Elliott SCA, Sellin RHJ. SERC flood channel facility: skewed flow experiments, Journal of Hydraulic Research,28 (1990):pp. 197-214
- Ervine D.A, Jasem H.K. Observations on flows in skewed compound channels, J. Wat. Marit. En., ICE, 112 (1995): pp. 249-259.
- Ervine D, Willetts B, Sellin R, Lorena M. Factors Affecting Conveyance in Meandering Compound Flows, Journal of Hydraulic Engineering,119 (1993):pp. 1383-1399
- Gandhi BK, Verma HK, Abraham B. Investigation of Flow Profile in Open Channels using CFD, 8th Intl Conference on Hydraulic Efficiency Measurement, 2010:pp. 243-251
- Ghobadian R, Mohammadi K. Simulation of subcritical flow pattern in 180 uniform and convergent open-channel bends using SSIIM 3-D model, Water Science and Engineering, 4 (2011):pp. 270-283
- Han SS, Biron PM, Ramamurthy AS. Three-dimensional modelling of flow in sharp open-channel bends with vanes, Journal of Hydraulic Research, 49 (2013):pp. 64-72
- Hartel C, Meiburg E, Necker F. Analysis and direct numerical simulation of the flow at a gravity-current head. Part 1. Flow topology and front speed for slip and no-slip boundaries, Journal of Fluid Mechanics,418 (2000): pp. 3.1
- Hirt CW, Nichols BD. Volume of fluid (VOF) method for the dynamics of free boundaries, Journal of computational physics, 39 (1981): pp. 201-225
- http://www.cfd-online.com/
- Huthoff F, Roos PC, Augustijn DCM, Hulscher SJMH. Interacting Divided Channel Method for Compound Channel Flow, J. Hydraul. Engg., 134 (2008): 1158.

- Hosseini-Sargheyn T, Bazargan-Lari M, Nazari S. Effects of Convergence on Flow Pattern Characteristics in 90-Degree Converging Bends, World Environmental and Water Resources Congress, 2012: pp. 1341-1348
- Hsieh T, Yang J. Investigation on the Suitability of Two-Dimensional Depth-Averaged Models for Bend-Flow Simulation, Journal of Hydraulic Engineering, 129 (2003): pp. 597-612
- Issa RI. Solution of the implicitly discretised fluid flow equations by operator-splitting. Journal of computational physics,62 (1986):pp. 40-65
- James, M. & Brown, B.J. (1977). "Geometric parameters that influence floodplain flow." Report WES-RR-H, USACE, Vicksburg, USA, 77 (1977):pp. 1.
- Jasem HK. Flow in two-stage channels with the main channel skewed to the flood plain direction, University of Glasgow, 1990
- Jing H, Guo Y, Li C, Zhang J. Three dimensional numerical simulation of compound meandering open channel flow by the Reynolds stress model, International journal for numerical methods in fluids, 59 (2009):pp. 927-943
- Johnson T, Farrell G, Ellis C, Stefan H. Negatively Buoyant Flow in a Diverging Channel. I: Flow Regimes, Journal of Hydraulic Engineering,113 (1987):pp. 716-730
- Johnson TR, Ellis CR, Stefan HG. Negatively Buoyant Flow in Diverging Channel, IV: Entrainment and Dilution, Journal of Hydraulic Engineering,115 (1989):pp. 437-456
- Kang S, Sotiropoulos F. Numerical modeling of 3D turbulent free surface flow in natural waterways, Advances in water resources,40 (2012):pp. 23-36
- Kassem A, Imran J, Khan JA. Three-dimensional modeling of negatively buoyant flow in diverging channels, Journal of Hydraulic Engineering,129 (2003):pp. 936-947

- Khatua KK, Patra KC, Mohanty PK. Stage-Discharge prediction for straight and smooth compound channels with wide floodplains, Journal of Hydraulic Engineering, 138 (2011):pp. 93-99
- Khazaee I, Mohammadiun M. Effect of flow field on open channel flow properties using numerical investigation and experimental comparison, International Journal of Energy & Environment, 2012:pp. 3
- Knight DW, Stokes N. Refined calibration of a depth-averaged model for turbulent flow in a compound channel, J. ICE-Water Maritime and Energy, 118 (1996):pp. 151-159
- Larocque LA, Imran J, Chaudhry MH. 3D numerical simulation of partial breach dam-break flow using the LES and k-ε turbulence models, Journal of Hydraulic Research, 51 (2013):pp. 145-157
- Li CW, Zeng C. Flow division at a channel crossing with subcritical or supercritical flow, International journal for numerical methods in fluids, 62 (2010):pp.56-73
- Lin B, Shiono K. Numerical modelling of solute transport in compound channel flows, Journal of Hydraulic Research, 33 (1995):pp. 773-788
- Lien H, Hsieh T, Yang J, Yeh K. Bend-Flow Simulation Using 2D Depth-Averaged Model, Journal of Hydraulic Engineering, 125 (1999):pp. 1097-1108
- Lu WZ, Zhang WS, Cui CZ, Leung AYT. A numerical analysis of free-surface flow in curved open channel with velocity-pressure-free-surface correction, Computational Mechanics, 33 (2004):pp. 215-224
- Moncho-Esteve I, Palau-Salvador G, Shiono K, Muto Y. Turbulent structures in the flow through compound meandering channels, Proceedings of River Flow, 2010:pp. 1543-1550

- Myers WRC. Velocity and discharge in compound channels, Journal of Hydraulic Engineering, 113 (1987):pp. 753-766
- Nezu I. Open-channel flow turbulence and its research prospect in the 21st century, Journal of Hydraulic Engineering,131 (2005):pp. 229-246
- Nicholas AP. Computational fluid dynamics modelling of boundary roughness in gravel-bed rivers: an investigation of the effects of random variability in bed elevation, Earth Surface Processes and Landforms,26 (2001):pp. 345-362
- Prinos P, Townsend RD. Comparison of methods for predicting discharge in compound open channels, Advances in water resources,7 (1984):pp. 180-187
- Proust S, Riviere N, Bousmar D, et al. Flow in Compound Channel with Abrupt Floodplain Contraction, Journal of Hydraulic Engineering,132 (2006):pp. 958-970
- Proust S, Bousmar D, Riviere N, Paquier A, Zech Y. Energy losses in compound open channels, Advances in Water Resources, 33 (2010):pp. 1-16
- Ramamurthy AS, Han SS, Biron PM. Three-Dimensional Simulation Parameters for 90° Open Channel Bend Flows, Journal of Computing in Civil Engineering, 27 (2013):pp. 282-291
- Rameshwaran P, Naden PS. Three-dimensional numerical simulation of compound channel flows, Journal of Hydraulic Engineering, 129 (2003):pp. 645-652
- Rezaei B. Overbank flow in compound channels with prismatic and non-prismatic floodplains, University of Birmingham, 2006
- Rezaei B, Knight DW. Application of the Shiono and Knight Method in compound channels with non-prismatic floodplains, Journal of Hydraulic Research, 47 (2009):pp. 716-726

- Rezaei B, Knight DW. Overbank flow in compound channels with non-prismatic floodplains, Journal of Hydraulic Engineering,137 (2010):pp. 815-824
- Salami LA. On velocity-area methods for asymmetric profiles, University of Southampton Interim Report, 1972
- Salvetti M.V., Zang Y., Street R.L. and Banerjee S. Large-eddy simulation of free surface decaying turbulence with dynamic subgrid -scale models, Physics of Fluids, 9 (1997): pp.2405.
- Schlichting CD, Pigliucci M. Gene regulation, quantitative genetics and the evolution of reaction norms, Evolutionary Ecology, 9 (1995): pp.154-168
- Seyedashraf O, Akhtari AA, Shahidi MK. Numerical Study of Channel Convergence Effects on Flow Pattern in 90 Degree Bends, 9th International Congress, IUT, 2012
- Shiono K, Knight DW. Turbulent open-channel flows with variable depth across the channel, Journal of Fluid Mechanics,222 (1991): pp. 617-646
- Shiono K, Muto Y, Knight DW, Hyde AFL. Energy losses due to secondary flow and turbulence in meandering channels with overbank flows, Journal of Hydraulic Research, 37 (1999): pp. 641-664
- Song CG, Seo IW, Kim YD. Analysis of secondary current effect in the modeling of shallow flow in open channels, Advances in water resources, 41 (2012): pp. 29-48
- Sugiyama H, Hitomi D, Saito T. Numerical analysis of turbulent structure in compound meandering open channel by algebraic Reynolds stress model, International journal for numerical methods in fluids, 51 (2006): pp. 791-818
- Thomas TG, Williams JJR. Large eddy simulation of turbulent flow in an asymmetric compound open channel, Journal of Hydraulic Research,33 (1995): pp. 27-41

- Tominaga A, Nezu I. Turbulent structure in compound open-channel flows, Journal of Hydraulic Engineering, 117 (1991): pp. 21-41
- Van Balen W, Uijttewaal WSJ, Blanckaert K. Large-eddy simulation of a mildly curved open-channel flow, Journal of Fluid Mechanics, 630 (2009): pp. 413-442
- Van Balen W, Blanckaert K, Uijttewaal WSJ. Analysis of the role of turbulence in curved open-channel flow at different water depths by means of experiments, LES and RANS, Journal of Turbulence, 2010: pp. 12
- Van Balen W, Uijttewaal WSJ, Blanckaert K. Large-eddy simulation of a curved open-channel flow over topography, Physics of Fluids,22 (2010): pp. 075108
- Van Prooijen BC, Battjes JA, Uijttewaal WSJ. Momentum exchange in straight uniform compound channel flow, Journal of Hydraulic Engineering, 131 (2005): pp. 175-183
- Van Prooijen BC, Booij R, Uijttewaal WSJ. Measurement and analysis methods of large scale horizontal coherent structures in a wide shallow channel, 10th international symposium on applications of laser techniques to fluid mechanics Calouste Gulbenkian Foundation, Lisbon, 2000
- Willetts BB, Hardwick RI. Stage dependency for overbank flow in meandering channels, ICE-Water Maritime and Energy, 101 (1993): pp. 45-54
- Zheleznyakov GV. Relative deficit of mean velocity of instable river flow, kinematic effect in river beds with flood plains, 11th International congress of the Association for hydraulic research, Leningrad, USSR, 1965

Appendix A-I

Publications from the Work

A: Published

1. Mohanta A, Naik B, Patra KC, Khatua KK. Experimental and Numerical Study of Flow in Prismatic and Non-prismatic Section of a Converging Compound Channel, International Journal of Civil Engineering Research, 5 (2014): pp. 203-210
2. Mohanta A, Patra KC, Khatua KK. CFD Simulation And Two-Phase Modeling Of A Non-Prismatic Converging Compound Channel, International Journal of Engineering Research and Applications,2014

International Conference

1. A. Mohanta, B. Naik, K.C.Patra, K.K.Khatua, "Investigation of Flow Profile in Prismatic and Non prismatic compound channel using CFD." 2014 ANSYS Convergence Conference